

# BORDERED FLOER HOMOLOGY FOR MANIFOLDS WITH TORUS BOUNDARY VIA IMMERSED CURVES

JONATHAN HANSELMAN, JACOB RASMUSSEN, AND LIAM WATSON

ABSTRACT. We give a geometric interpretation of bordered Floer homology for a natural class of three-manifolds with torus boundary; namely, the loop-type manifolds defined by the first and third authors [10]. From this viewpoint, the invariant associated with a loop-type manifold is a collection of immersed curves in the punctured torus, and the pairing theorem of Lipshitz, Ozsváth and Thurston [21] amounts to taking the intersection Floer homology of the corresponding curves. Using these ideas, we are able to strengthen our results with S. Rasmussen [9, 10, 30] on when an L-space can contain an incompressible torus while simultaneously simplifying the proofs. Other applications include a dimension inequality for Heegaard Floer homology under pinching and a new description of the interval of L-space slopes of a Floer simple manifold.

## 1. INTRODUCTION

Bordered Floer homology is a suite of invariants, introduced by Lipshitz, Ozsváth and Thurston [21], assigned to three-manifolds with boundary. In recent work [10], the first and third authors studied a class of manifolds with torus boundary whose bordered invariants have a particularly nice form. Manifolds in this class are called loop-type, and the package developed for studying their bordered Floer homology is referred to as loop calculus. In this paper, we give a geometric interpretation of the loop calculus. This new perspective enables us to strengthen and simplify the proofs of many previous results [8, 10, 11, 30]. In particular, we strengthen the gluing results used in the proof that non-L-space graph manifolds admit coorientable taut foliations [9]. Other applications include a dimension inequality for  $\widehat{HF}$  under pinches and new constraints on satellite L-space knots.

We begin by describing the invariants. Let  $M$  be a closed compact oriented three-manifold with  $\partial M \cong S^1 \times S^1$ . To define the bordered Floer homology  $\widehat{CFD}(M, \alpha, \beta)$  we must fix a parametrization  $(\alpha, \beta)$  of  $\partial M$ . That is,  $\alpha$  and  $\beta$  are the cores of the one-handles in a handle decomposition of  $\partial M$ . If  $M$  is loop-type then we can describe  $\widehat{CFD}(M, \alpha, \beta)$  as a set of immersed closed curves  $\gamma(M) \subset T$ , where  $T = \partial M \setminus z$  and  $z$  is a marked point corresponding to the core of the zero-handle in the parametrization. Equivalently, we can think of  $\partial M$  as being identified with  $H_1(M, \mathbb{R})/H_1(M, \mathbb{Z})$ , with the marked point at the origin. Our first main result is that  $\gamma(M)$  is an invariant of  $M$ :

**Theorem 1.** *If  $M$  is loop-type then  $\gamma(M)$  is well-defined up to regular homotopy in  $T$ . In particular, the homotopy class of  $\gamma(M)$  does not depend on the choice of parametrization.*

As a very simple example, the invariant  $\gamma(D^2 \times S^1)$  consists of a single closed circle parallel to the longitude  $\lambda = \partial D^2 \times \{\text{pt}\}$ . More interesting examples are shown in Figure 1. When the curves are more complicated, it is generally easier to represent them by drawing some of their lifts to the cover  $\tilde{T} = H_1(M; \mathbb{R}) \setminus H_1(M; \mathbb{Z}) \cong \mathbb{R}^2 \setminus \mathbb{Z}^2$ . For example, if  $M$  is the complement of the figure-eight knot, the curve  $\gamma(M)$  has two components; one corresponding to the horizontal line in Figure 1, and one to the curves in the shape of the figure-eight.

---

*Date:* April 12, 2016.

JH was partially supported by NSF RTG grant DMS-1148490.

JR was partially supported by EPSRC grant EP/M000648/1.

LW was partially supported by a Marie Curie career integration grant and a CIRGET research fellowship.

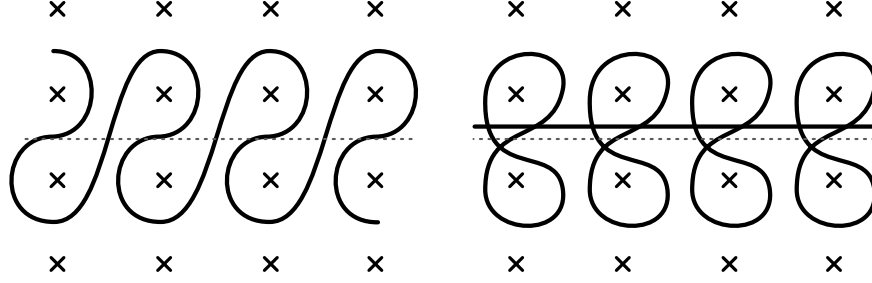


**Figure 1.** Two examples of curves: On the left  $M$  is the exterior of the right-hand trefoil and on the right  $M$  is the exterior of the figure eight knot. In both cases, the horizontal direction corresponds to the preferred longitude  $\lambda$ , and the vertical direction to the standard meridian of the knot.

Suppose  $Y = M_0 \cup_h M_1$ , where  $h: \partial M_1 \rightarrow \partial M_0$  is an orientation reversing diffeomorphism. The central result of bordered Floer homology is the pairing theorem, which expresses the Heegaard Floer homology  $\widehat{HF}(Y)$  in terms of  $\widehat{CFA}(M_0, h(\beta), h(\alpha))$  and  $\widehat{CFD}(M_1, \alpha, \beta)$ . If  $M_0$  and  $M_1$  are loop-type, the pairing theorem can be expressed very cleanly in terms of  $\gamma(M_0)$  and  $\gamma(M_1)$ .

**Theorem 2.** *Let  $M_0$  and  $M_1$  be loop-type manifolds with base points  $z_i \in \partial M_i$  and let  $Y = M_0 \cup_h M_1$ , where  $h: \partial M_1 \rightarrow \partial M_0$  is a diffeomorphism for which  $h(z_1) = z_0$ . Then*

$$\widehat{HF}(Y) \cong HF(\gamma_0, \gamma_1)$$

where  $HF(\gamma_0, \gamma_1)$  denotes immersed Lagrangian intersection Floer homology of  $\gamma_0 = \gamma(M_0)$  and  $\gamma_1 = \bar{h}(\gamma(M_1))$  in the punctured torus. Here  $\bar{h}$  is the composition of  $h$  with the elliptic involution, that is, the map  $T \rightarrow T$  induced by the map  $x \mapsto -x$  on  $H_1(M; \mathbb{R})$ .

In particular, if no component of  $\gamma_0$  is parallel to a component of  $\gamma_1$ , the dimension of  $\widehat{HF}(M_0 \cup_h M_1)$  is given by the minimal intersection number between  $\gamma_0$  and  $\gamma_1$ . For example, let  $Y_1$  be the manifold obtained by splicing the complements of the left-hand trefoil  $T_L$  and the right-hand trefoil  $T_R$ ; that is by taking  $M_0 = S^3 \setminus \nu(T_L)$ ,  $M_1 = S^3 \setminus \nu(T_R)$ , and  $h: \partial M_0 \rightarrow \partial M_1$  such that  $h(\mu) = \lambda$  and  $h(\lambda) = \mu$ , where  $\mu$  and  $\lambda$  are the preferred meridian and longitude of each trefoil in  $S^3$ . Similarly, let  $Y_2$  be the manifold obtained by splicing two copies of the complement of the right-hand trefoil. Consulting Figure 2, we see that  $\widehat{HF}(Y_1)$  has dimension 9, while  $\widehat{HF}(Y_2)$  has dimension 7, as calculated by Hedden and Levine [11].

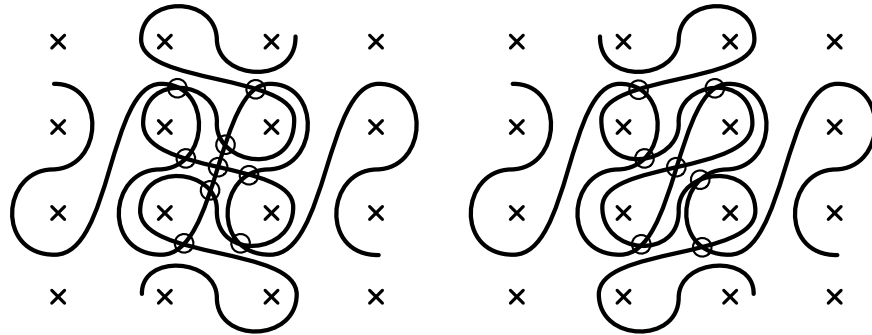


**Figure 2.** Splicing trefoils: The diagram on the left illustrates the intersection (carried out in  $\tilde{T}$ ) calculating  $\dim \widehat{HF}(Y_1) = 9$  where  $Y_1$  is the splice of a right-hand and left-hand trefoil, while the diagram on the right illustrates the intersection calculating  $\dim \widehat{HF}(Y_2) = 7$  where  $Y_2$  is the splice of two right-hand trefoils.

**1.1. Comparison with other invariants.** Although the invariant  $\gamma(M)$  contains no more information than  $\widehat{CFD}(M, \alpha, \beta)$ , it provides a very powerful way of encapsulating this information. For

this reason, we view  $\gamma(M)$  as the Heegaard Floer invariant associated with a loop type manifold  $M$ . We discuss its relation to other Floer-type invariants for manifolds with torus boundary.

First, Lekili and Perutz proposed that the Heegaard Floer invariant of a manifold with boundary  $\Sigma$  should be viewed as an element of the extended Fukaya category of the pair  $(\text{Sym}^g \Sigma, D_z)$  [20]. Here  $g$  is the genus of  $\Sigma$ , and  $D_z$  is the divisor consisting of unordered  $g$ -tuples of points in  $\Sigma$ , at least one of which is equal to a fixed basepoint  $z$ . Our construction can be viewed as a realization of Lekili and Perutz's proposal in a special case. Although it is much less general than the construction they suggest, it seems to be considerably easier to understand and compute.

Knot Floer homology is another construction giving rise to a Floer homological invariant for manifolds with torus boundary. To define it, we must specify a simple closed curve  $\alpha$  on  $\partial M$ . We view  $\alpha$  as the meridian of the knot  $K_\alpha$ , which is obtained as the core of the filling solid torus inside the Dehn filling  $M(\alpha)$ . Lipshitz, Ozsváth and Thurston show that knot Floer homology can be derived from bordered Floer homology [21]. Consequently, if  $M$  is loop-type, we can describe  $\widehat{HF\!K}(K_\alpha)$  in terms of  $\gamma(M)$ .

**Theorem 3.** *Let  $L_\alpha \subset \partial M$  be a line of slope  $\alpha$  passing through the marked point, and let  $w$  and  $z$  be two points on  $\partial M$  near the marked point and on either side of  $L_\alpha$ . If  $M$  is of loop type, then  $\widehat{HF\!K}(K_\alpha) \cong HF(\gamma(M), L_\alpha)$ , where the Lagrangian intersection homology is taken in  $\partial M \setminus \{w, z\}$ .*

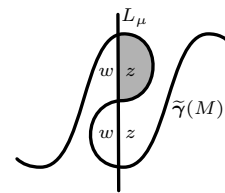


**Figure 3.** The three generators of  $\widehat{HF\!K}(T_R)$ .

For an example, consider Figure 3, which shows how to compute  $\widehat{HF\!K}$  of the right-hand trefoil. This process exhibits some interesting similarities with both the usual definition of knot Floer homology (which uses two basepoints on either side of the meridian) and with the instanton knot homology defined by Kronheimer and Mrowka [19]. Theorem 3 follows from a more general result recovering  $HF\!K^-(K_\alpha)$  from  $\gamma(M)$ ; see Theorem 45.

Another, somewhat older way of thinking about the relative invariant of a manifold with torus boundary is given by the Seiberg-Witten equations. If  $M$  is a manifold with torus boundary, we equip  $\text{int}(M)$  with a Riemannian metric which has a tubular end modeled on  $T^2 \times [0, \infty)$ , where the metric on  $T^2$  is flat. If  $\mathcal{M}$  is the moduli space of finite-energy Seiberg-Witten solutions on  $M$ , divided out by the action of the based gauge group, then there is a map  $j: \mathcal{M} \rightarrow H^1(\partial M; \mathbb{R})/H^1(\partial M; \mathbb{Z})$ . Here  $H^1(\partial M; \mathbb{R})/H^1(\partial M; \mathbb{Z})$  should be viewed as the space of flat  $S^1$  connections on  $\partial M$ . By Poincaré duality, it can be identified with the space  $T$  which contains  $\gamma(M)$ . Moreover, it contains a special point  $z$ , which corresponds to the unique flat connection whose associated Dirac operator has nontrivial kernel. We will not attempt to prove anything about  $\mathcal{M}$  here, but it seems plausible that an appropriately perturbed version of its image under  $j$  should be identified with  $\gamma(M)$ , as discussed in Section 6.

**1.2. Properties.** Many standard properties of Heegaard Floer homology are reflected in properties of  $\gamma(M)$ . We describe a few of these here.

**Spin<sup>c</sup> structures:** There is a decomposition  $\gamma(M) = \coprod_{\mathfrak{s} \in \text{Spin}^c(M)} \gamma(M, \mathfrak{s})$ . In the pairing theorem, the decomposition of  $\widehat{HF}(Y)$  into Spin<sup>c</sup> structures can be described in terms of the geometry of the curves  $\gamma(M_i)$  and their decomposition into Spin<sup>c</sup> structures.

**Orientations and the  $\mathbb{Z}/2\mathbb{Z}$  homological grading:** Petkova [28] defined a relative  $\mathbb{Z}/2\mathbb{Z}$  grading on bordered Floer homology. In our case, the presence of this grading amounts to saying that the curves in  $\gamma(M)$  are naturally oriented, and that this orientation is well-defined up to global orientation reversal. In the pairing theorem, the relative  $\mathbb{Z}/2\mathbb{Z}$  grading on  $\widehat{HF}$  is given by the sign of intersection of  $\gamma_0$  and  $\gamma_1$  at the corresponding generator.

**The lifted invariant:** It is often convenient to consider versions of  $\gamma(M)$  which live in covering spaces of  $T$ . Consider the map  $\pi_1(T) \rightarrow \pi_1(\partial M) \rightarrow H_1(\partial M) \rightarrow H_1(M)$ , and let  $\bar{T}$  be the corresponding covering space. Then for each  $\mathfrak{s} \in \text{Spin}^c(M)$ , there is a natural lift  $\bar{\gamma}(M, \mathfrak{s})$  of  $\gamma(M, \mathfrak{s})$  to  $\bar{T}$ .  $\bar{\gamma}(M, \mathfrak{s})$  is well-defined up to overall translation in  $\bar{T}$ . When drawing pictures, it is generally easier to consider the preimage of  $\bar{\gamma}(M, \mathfrak{s})$  in the covering space  $\tilde{T} = H_1(M; \mathbb{R}) \setminus H_1(M; \mathbb{Z})$ . We denote this by  $\tilde{\gamma}(M, \mathfrak{s})$ . For example the curves in Figure 1 are drawn according to this convention.

**Orientation reversal:** As curves in  $\partial M$ ,  $\gamma(-M) = \gamma(M)$ , however we must remember that the orientation of  $\partial M$  is different on the two sides of the equation. For example, the orientation reversing diffeomorphism of  $S^3$  which sends the right-hand trefoil to the left-hand trefoil sends the meridian of  $T_R$  to minus the meridian of  $T_L$ . Thus to get the analog of Figure 1 for the left-hand trefoil, we must reflect across the dotted line in the figure. As the figure-eight knot is amphichiral the corresponding curves are invariant (up to homotopy) under this operation.

**Alexander polynomial:** If  $H_1(M) \cong \mathbb{Z}$ , the Alexander polynomial of  $M$  can be read off from  $\bar{\gamma}(M)$ . There is a natural height function on  $\bar{T}$  given by intersection with the rational longitude  $\lambda$ . (In Figure 1, this coordinate is given by projection to a vertical line.) Let  $z_k$  be the preimage of  $z$  in  $\bar{T}$  at height  $k$ , and let  $\beta_k(t)$  be a path which starts at  $z_k$  and for which  $\beta_k \cdot \lambda \rightarrow -\infty$  as  $t \rightarrow \infty$ . If we define  $n_k$  to be the signed intersection number between  $\beta_k$  and  $\bar{\gamma}(M)$ , then

$$\sum n_k t^k \sim \frac{\Delta_M(t)}{1-t}$$

is the Milnor torsion of  $M$ . (As we have defined them, the  $n_k$  are defined up to an overall sign, depending on our choice of global orientation for  $\gamma(M)$ . Fixing a positive generator of  $H_1(M)$  picks out a preferred global orientation on  $\gamma(M)$ , namely, the one which makes the equation above correct.)

For example, if  $M$  is the complement of the right-hand trefoil, we see from Figure 1 that the  $n_k$ 's are  $\dots, 0, 1, 0, 1, \dots$  where the four values correspond to the four preimages of  $z$  in the figure. All the  $n_k$ 's corresponding to preimages below this region are 0, and those above this region are 1. Thus the Milnor torsion is  $1 + t^2 + t^3 + t^4 + \dots = (1 - t + t^2)/(1 - t)$ . More generally, the coefficients of the Turaev torsion of an arbitrary  $M$  can be read off from  $\tilde{\gamma}(M)$ , as described in Section 2.9.

**Thurston norm:** If  $H_1(M) \cong \mathbb{Z}$ , let  $k_+$  be the largest value of  $k$  such that  $z_k$  cannot be connected to  $+\infty$  by a path disjoint from  $\bar{\gamma}(M)$ . Similarly, let  $k_-$  be the smallest value of  $k$  such that  $z_k$  cannot be connected to  $-\infty$  by a path disjoint from  $\bar{\gamma}(M)$ . If  $\Sigma$  is a minimal genus surface generating  $H_2(M, \partial M)$ , then  $2g(\Sigma) - 1 = k_+ - k_-$ . (Note that if  $M = S^1 \times D^2$  then  $k_+ + 1 = k_-$ .) The Thurston norm of an arbitrary  $M$  with  $b_1(M) = 1$  can be determined similarly, as described in Section 7.4.

**1.3. Applications.** The set of L-space filling slopes of  $M$  can be easily determined from  $\tilde{\gamma}(M)$ . This enables us to give new, simplified (and in many cases strengthened) proofs of the results in [9, 10, 30]. Write  $M(\alpha)$  for the result of Dehn filling along a slope  $\alpha$  in the torus  $\partial M$ , and consider the set

$$\mathcal{L}_M = \{\alpha \mid M(\alpha) \text{ is an L-space}\}$$

(recall that  $M(\alpha)$  is an L-space whenever  $\dim \widehat{HF}(M(\alpha)) = |H_1(M(\alpha))|$ ). This is a (possibly empty) subset of the set of slopes on  $\partial M$ ; we identify the set of slopes with the extended rationals  $\hat{\mathbb{Q}}$ . Denote the interior of  $\mathcal{L}_M$  by  $\mathcal{L}_M^\circ$ .

Given a smooth curve  $\gamma \subset \tilde{T} \setminus p^{-1}(z)$ , let  $S(\gamma)$  be the set of slopes of tangent lines to  $\gamma$ . If  $\tilde{\gamma}(M)$  has one component for each  $\text{Spin}^c$  structure on  $M$ , we define  $S(M) = \cap_\gamma S(\gamma)$  where the intersection is taken over all smooth immersed curves homotopic to  $\tilde{\gamma}(M)$ ; otherwise, let  $S(M) = \hat{\mathbb{Q}}$ . We prove:

**Theorem 4.** *If  $M$  is a loop-type manifold then  $\mathcal{L}_M^\circ = \hat{\mathbb{Q}} \setminus S(M)$ .*

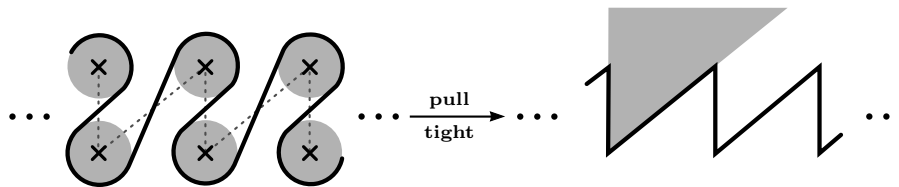


**Figure 4.** The pegboard diagram, obtained by taking the radius of each peg to zero, associated with the right-hand trefoil. The shaded region shows the set of L-space slopes.

In particular, this theorem applies to any manifold for which  $\mathcal{L}_M$  contains more than one element – such Floer simple manifolds are all of loop type [9]. If we imagine  $\tilde{\gamma}(M)$  as a rope lying in the plane  $H_1(M, \mathbb{R})$ , with a “peg” coming out of each point of  $H_1(M, \mathbb{Z})$ , then we can pull the rope tight, as illustrated in Figure 4; the set  $S(M)$  can be easily read off from the resulting “pegboard diagram”. This gives a new proof of the characterization of the set  $\mathcal{L}(M)$  in terms of the Turaev torsion of  $M$  given in [30]. Theorem 4 can be interpreted as giving an intrinsic definition of the notion of a non-L-space slope (compare [10]) that is well-defined for irrational slopes, namely, the subset  $S(M)$  in  $\hat{\mathbb{R}}$ . This provides a satisfying solution to a problem of Boyer and Clay [4, Problem 1.9].

Combining Theorem 2 and Theorem 4 gives rise to a gluing result for L-spaces which is considerably more general than those given in previous work.

**Theorem 5.** *If  $M_0$  and  $M_1$  are boundary incompressible loop-type manifolds and  $h: \partial M_1 \rightarrow \partial M_0$  is a diffeomorphism, then  $M_0 \cup_h M_1$  is an L-space if and only if  $\mathcal{L}_{M_0}^\circ \cup h(\mathcal{L}_{M_1}^\circ) = \hat{\mathcal{Q}}$ .*

Weaker versions of this theorem (with simple loop-type in place of loop-type) were established by the authors and S. Rasmussen in [9, 10, 30]. They are a key ingredient in the proof that every non-L-space graph manifold admits a coorientable taut foliation (see [9, Theorem 1]) and, more generally, that non-L-space, the existence of a coorientable taut foliation, and left-orderable fundamental group are equivalent conditions for graph manifolds (see [9, Theorem 2] and also [4]).

One is immediately led to the question of how general the loop-type condition is. Among complements of knots in  $S^3$ , there are far more manifolds which are loop-type than simple loop-type. The only knots in  $S^3$  whose complements are simple loop-type are L-space knots; in contrast, any knot in  $S^3$  whose knot Floer homology admits a basis which is simultaneously horizontally and vertically simplified (in the sense of [21, Section 11]) has a loop-type complement; compare Hom [13]. For example, any thin knot (in particular, any alternating knot) satisfies this hypothesis; see Petkova [29]. In fact, the authors are unaware of any knot in  $S^3$  whose knot Floer homology does not have this simple form (though this is likely a failure to look at sufficiently complicated examples, rather than any general pattern). For more general three-manifolds, the loop-type condition is satisfied surprisingly often. At present, we do not have a single example of a three-manifold which is certifiably not loop-type. Nevertheless we do not expect loop-type to be the generic condition – for instance, the class of manifolds for which  $\mathcal{L}_M$  is empty is virtually unstudied. We intend to return to this point in a subsequent paper.

Based on these observations and remarks we construct, among other examples, some explicit loop-type integer homology solid tori  $M$  with empty  $\mathcal{L}_M$  in Section 5. In particular, with this class of loop-type integer homology solid tori in hand, Theorem 5 allows us to extend a result due to Hedden and Levine [11]:

**Theorem 6.** *If  $Y \cong M_0 \cup M_1$  is a integer homology sphere L-space, and both  $M_0$  and  $M_1$  are loop-type manifolds, then at least one of  $M_0$  or  $M_1$  is boundary compressible.*

In place of the loop type assumption, Hedden and Levine assume that  $M_0$  and  $M_1$  have L-space integer homology sphere fillings [11]. There are many loop type manifolds which do not have such a

filling (such as the manifolds with no  $L$ -space fillings described above, as well as many Floer simple manifolds), so Theorem 6 covers many cases not addressed by the theorem of Hedden and Levine. The more general statement that an  $L$ -space homology sphere should not contain an incompressible torus was first formulated by Eftekhary, who has recently revised a proof of this general statement (without any additional hypothesis on  $M_0$  and  $M_1$ ) via different methods [5].

Theorem 6 is closely related to a more general statement pertaining to pinches. Recall that given  $M_0 \cup_h M_1$ , a pinch is the result of the Dehn surgery  $M_0(\alpha_h)$  where  $\alpha_h$  is the slope in  $\partial M_0$  determined by  $h(\lambda_1)$  and  $\lambda_1$  is the rational longitude of  $M_1$ .

**Theorem 7.** *For loop-type manifolds  $M_0$  and  $M_1$  there is an inequality*

$$\dim \widehat{HF}(M_0 \cup_h M_1) \geq nm \dim \widehat{HF}(M_0(\alpha_h))$$

where  $m$  is the order of  $\lambda_1$  and  $n$  is the order of the torsion in  $H_1(M_1)$ .

**Corollary 8.** *For loop-type  $M_0$  and  $M_1$  such that  $Y = M_0 \cup_h M_1$  is an integer homology sphere, there is an inequality  $\dim \widehat{HF}(M_0 \cup_h M_1) \geq \dim \widehat{HF}(M_0(\alpha_h))$ .*

*Proof.* If  $Y$  is an integer homology sphere then  $M_0$  and  $M_1$  are integer homology solid tori. Thus  $m = n = 1$  and the desired inequality follows from Theorem 7.  $\square$

Note that there is always a degree one map from  $M_0 \cup_h M_1$  to  $M_0(\alpha_h)$  under the hypothesis of Corollary 8, which, in turn, gives new information about the Heegaard Floer homology of integer homology spheres related by degree one maps. More generally, the following question seems natural:

**Question 9.** Given a degree one map  $Y \rightarrow Y'$  between integer homology spheres, is it the case that  $\dim \widehat{HF}(Y) \geq \dim \widehat{HF}(Y')$ ?

Closely related to this, we make the following observation: Restricting to loop type manifolds, given a satellite  $L$ -space knot both the companion knot and the pattern knot must be  $L$ -space knots; see Theorem 35. This shows that a conjecture of Hom, Lidman and Vafaee [14, Conjecture 1.7] holds for loop-type manifolds.

**1.4. Outline and further remarks.** The remainder of the paper is organized as follows. In Section 2 we review the essential aspects of loop calculus from [10]. This is used to define  $\gamma(M)$ , establish its key properties, and prove invariance (Theorem 1). Section 3 contains the proof of the pairing theorem for loop-type manifolds in terms of the Lagrangian intersection homology of immersed curves (Theorem 2). In Section 4, we give some applications, including detection and gluing results for  $L$ -spaces (Theorem 4 and Theorem 5), dimension inequalities concerning non-zero degree maps (Theorem 7), observations about toroidal  $L$ -spaces and satellite  $L$ -space knots. The loop-type condition is satisfied surprisingly often in practice, and Section 5 calculates some explicit examples including examples of loop-type integer homology solid tori for which no  $L$ -space fillings exist. Another interesting class of examples is given by surfaces with connected boundary times a circle. We compute the curves invariant for these manifolds explicitly and derive a formula for  $\dim \widehat{HF}(\Sigma_g \times S^1)$  as a consequence; see Corollary 41. This recovers calculations due to Jabuka and Mark [17] and Ozsváth and Szabó [26]. Section 6 contains a brief discussion of Seiberg-Witten theory, in which we compare the  $\gamma(M)$  to the moduli space of Seiberg-Witten solutions in the case  $M$  is a small Seifert-fibred space over the disk. Finally, Section 7 establishes the connection between the curves invariant and knot Floer homology, in particular, we describe how  $\gamma(M)$  determines  $HF^-$  (establishing, in turn, Theorem 3). We conclude by discussing some examples in which the pairing theorem can be enhanced to recover  $HF^\pm(M_0 \cup_h M_1)$ .

**Conventions and coefficients.** All three-manifolds arising in this work are compact, connected, smooth, and orientable. Consistent with the set-up in bordered Floer homology [21], all Floer invariants in this work take coefficients in the two element field  $\mathbb{F}$ . Unless explicitly stated otherwise, (singular) homology groups of manifolds should be assumed to take coefficients in  $\mathbb{Z}$ .

**Acknowledgements.** The authors would like to thank Peter Kronheimer, Yankı Lekili, Tye Lidman, Robert Lipshitz, Sarah Rasmussen and Ivan Smith for helpful discussions (some of them dating back a very long time). Part of this work was carried out while the third author was visiting Montréal as CIRGET research fellow.

## 2. BORDERED INVARIANTS AS IMMERSSED CURVES: THE PROOF OF THEOREM 1

This section contains the definition of the curves invariant. We begin with a brief review of the relevant notions from bordered Floer homology [21]. A less terse intro, with essentially the same notation used here, is given in [10].

**2.1. Modules over the torus algebra.** Let  $M$  be an orientable three-manifold with torus boundary, and choose oriented essential simple closed curves  $\alpha, \beta$  in  $\partial M$  with  $\beta \cdot \alpha = 1$ . The ordered triple  $(M, \alpha, \beta)$  is called a bordered three-manifold; the pair  $(\alpha, \beta)$  may be regarded as a parametrization of the torus boundary, in the sense that  $\langle \alpha, \beta \rangle$  generate the peripheral subgroup  $\pi_1(\partial M)$ .

We focus on two (equivalent) bordered invariants assigned to a bordered manifold  $(M, \alpha, \beta)$ . These will take the form of certain modules over the torus algebra  $\mathcal{A}$ . Various descriptions of this algebra are given by Lipshitz, Ozsváth and Thurston [21], but for our purposes, recall that  $\mathcal{A}$  is generated, as an algebra over the two-element field  $\mathbb{F}$ , by elements  $\rho_1, \rho_2$  and  $\rho_3$  and idempotents  $\iota_0$  and  $\iota_1$ . Multiplication in  $\mathcal{A}$  is described by the quiver depicted in Figure 5 together with the relations  $\rho_2\rho_1 = \rho_3\rho_2 = 0$ . The shorthand  $\rho_{12} = \rho_1\rho_2$ ,  $\rho_{23} = \rho_2\rho_3$ ,  $\rho_{123} = \rho_1\rho_2\rho_3$  is standard. Let  $\mathcal{I}$  denote the subring of idempotents, and write  $\mathbf{1} = \iota_0 + \iota_1$  for the unit in  $\mathcal{A}$ .

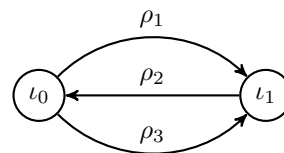


**Figure 5.** A quiver for the torus algebra, with relations  $\rho_2\rho_1 = \rho_3\rho_2 = 0$ .

The relevant bordered invariants are  $\widehat{CFA}(M, \alpha, \beta)$  and  $\widehat{CFD}(M, \alpha, \beta)$ ; both are invariants of the underlying bordered manifold up to homotopy [21]. The former is a type A structure, that is, a right  $A_\infty$ -module over  $\mathcal{A}$ . The latter is a type D structure, which consists of (1) a vector space  $V$  (over  $\mathbb{F}$ ) together with a splitting as a direct sum over a left action of the idempotents  $V \cong \iota_0 V \oplus \iota_1 V$ ; and (2) a map  $\delta^1: V \rightarrow \mathcal{A} \otimes_{\mathcal{I}} V$  satisfying a compatibility condition ensuring that  $\partial(a \otimes x) = a \cdot \delta(x)$  is a differential on  $\mathcal{A} \otimes_{\mathcal{I}} V$  (with left  $\mathcal{A}$ -action specified by  $a \cdot (b \otimes x) = ab \otimes x$ ). In particular,  $\mathcal{A} \otimes_{\mathcal{I}} V$  has the structure of a left differential module over  $\mathcal{A}$ . We will sometimes confuse the type D structure  $\widehat{CFD}(M, \alpha, \beta)$  (consisting of  $V$  and  $\delta^1$ ) and this associated differential module. Given any type D structure there is a collection of recursively defined maps  $\delta^k: V \rightarrow \mathcal{A}^{\otimes k} \otimes V$  where  $\delta^0: V \rightarrow V$  is the identity and  $\delta^k = (\text{id}_{\mathcal{A}^{\otimes k-1}} \otimes \delta^1) \circ \delta^{k-1}$ . The type D structure  $\widehat{CFD}(M, \alpha, \beta)$  is bounded if  $\delta^k$  vanishes for all sufficiently large integers  $k$ .

Given a bordered manifold  $(M, \alpha, \beta)$ , there is a duality relating the associated type A and type D structures. In particular, according to [22, Corollary 1.1],  $\widehat{CFA}(M, \alpha, \beta)$  is dual (in an appropriate sense) to  $\widehat{CFD}(M, \alpha, \beta)$ . However, the utility of the two structures, taken together, is a computable model for the  $A_\infty$  tensor product: Given bordered  $(M_0, \alpha_0, \beta_0)$  and  $(M_1, \alpha_1, \beta_1)$  consider the chain complex  $\widehat{CFA}(M_0, \alpha_0, \beta_0) \boxtimes \widehat{CFD}(M_1, \alpha_1, \beta_1)$  obtained from  $\widehat{CFA}(M_0, \alpha_0, \beta_0) \otimes_{\mathcal{I}} \widehat{CFD}(M_1, \alpha_1, \beta_1)$

with differential defined by

$$\partial^{\boxtimes}(x \otimes y) = \sum_{k=0}^{\infty} (m_{k+1} \otimes \text{id})(x \otimes \delta^k(y))$$

and the requirement that  $\widehat{CFD}(M_1, \alpha_1, \beta_1)$  is bounded (this ensures that the above sum is finite). Then the pairing theorem of Lipshitz, Ozsváth and Thurston asserts that the homology of  $\widehat{CFA}(M_0, \alpha_0, \beta_0) \boxtimes \widehat{CFD}(M_1, \alpha_1, \beta_1)$  is isomorphic to the Heegaard Floer homology  $\widehat{HF}(M_0 \cup_h M_1)$  of the closed manifold obtained from the homeomorphism  $h: \partial M_0 \rightarrow \partial M_1$  specified by  $h(\alpha_0) = \beta_1$  and  $h(\beta_0) = \alpha_1$  [21, Theorem 1.3].

**2.2. Conventions for bordered manifolds.** In the framework given by Lipshitz, Ozsváth and Thurston [21], the boundary parametrization of  $M$  is recorded by specifying a diffeomorphism  $\phi: F \rightarrow \partial M$  where  $F$  is a torus with a fixed handle decomposition. The image of the cores of the one-handles in  $F$  correspond to the pair of  $\alpha$ -arcs  $(\alpha_1^a, \alpha_2^a)$  in a bordered Heegaard diagram; completing this pair to curves in  $\partial M$  gives a pair corresponding to our parametrizing curves  $\alpha$  and  $\beta$ . To relate the two notations, we must specify which curve corresponds to each  $\alpha$ -arc in a bordered Heegaard diagram. We orient the arcs  $\alpha_1^a$  and  $\alpha_2^a$  so that, starting at the basepoint and following the boundary of the Heegaard surface, we pass the initial point of  $\alpha_1^a$ , the initial point of  $\alpha_2^a$ , the final point of  $\alpha_1^a$ , and the final point of  $\alpha_2^a$ . With this labelling,  $\alpha$  in our notation corresponds to  $\alpha_1^a$  and  $\beta$  corresponds to  $-\alpha_2^a$ . Note that when gluing two bordered manifolds together by an orientation reversing diffeomorphism taking basepoint to basepoint,  $\alpha_1^a$  must glue to  $-\alpha_2^a$  and  $\alpha_2^a$  must glue to  $-\alpha_1^a$ ; thus in our notation,  $\alpha$  glues to  $\beta$  and  $\beta$  glues to  $\alpha$ . Finally, the arcs defined above in a Heegaard diagram seem to satisfy  $\alpha_1 \cdot (-\alpha_2) = 1$ , which would imply that  $\alpha \cdot \beta = 1$ . However, the orientation of the Heegaard surface agrees with the opposite of the orientation on  $\partial M$ . Said another way, the surface in a bordered Heegaard diagram for  $M$  should be interpreted as being viewed from *inside*  $M$ , but we will generally look at  $\partial M$  from *outside*  $M$  so that  $\beta \cdot \alpha = 1$ .

**2.3. Gradings.** The bordered invariants described above decompose over  $\text{spin}^c$  structures. Recall that each generator  $x$  of  $\widehat{CFD}(M, \alpha, \beta)$  has an associated  $\text{spin}^c$  structure  $\mathfrak{s}(x) \in \text{Spin}^c(M)$ . The elements of  $\text{Spin}^c(M)$  are homology classes of nonvanishing vector fields on  $M$ , and  $\text{Spin}^c(M)$  has the structure of an affine set modeled on  $H^2(M) \cong H_1(M, \partial M)$ . The same decomposition holds for  $\widehat{CFA}(M, \alpha, \beta)$ , so that

$$\widehat{CFD}(M, \alpha, \beta) = \bigoplus_{\mathfrak{s} \in \text{Spin}^c(M)} \widehat{CFD}(M, \alpha, \beta; \mathfrak{s}) \quad \text{and} \quad \widehat{CFA}(M, \alpha, \beta) = \bigoplus_{\mathfrak{s} \in \text{Spin}^c(M)} \widehat{CFA}(M, \alpha, \beta; \mathfrak{s})$$

Restricting attention to the generators in a particular idempotent  $\iota$ , then we can also define a refined  $\text{spin}^c$  grading  $\mathfrak{s}_\iota(x) \in \text{Spin}^c(M, \iota)$ , which lives in an affine set modeled on  $H^2(M, \partial M) \cong H_1(M)$ . Elements of  $\text{Spin}^c(M, \iota)$  are homology classes of nonvanishing vector fields with prescribed behavior on  $\partial M$ , and  $\mathfrak{s}(x)$  is the image of  $\mathfrak{s}_\iota(x)$  in  $\text{Spin}^c(M)$ .

In order to compare the refined gradings of two generators, we adopt the following. Given  $\mathfrak{t} \in \text{Spin}^c(M)$ , let

$$\text{Spin}^c(M, \iota, \mathfrak{t}) = \{\mathfrak{s} \in \text{Spin}^c(M, \iota) \mid \mathfrak{s} = \mathfrak{t} \text{ in } \text{Spin}^c(M)\}.$$

If  $j_*: H_1(\partial M) \rightarrow H_1(M)$  is the map induced by inclusion,  $\text{Spin}^c(M, \iota, \mathfrak{t})$  is an affine set modeled on  $H_M = \text{im } j_* \cong H_1(\partial M) / \ker j_*$ . When  $\partial M$  is a torus we let  $\text{Spin}^c(M, \mathfrak{t}) = \text{Spin}^c(M, \iota_0, \mathfrak{t}) \cup \text{Spin}^c(M, \iota_0, \mathfrak{t})$  and define

$$\frac{1}{2}H_M = \{x \in H_1(\partial M, \mathbb{R}) \mid 2x \in H_1(\partial M, \mathbb{Z})\} / \ker j_*$$

Given two generators  $x$  and  $y$  in  $\widehat{CFD}(M, \alpha, \beta; \mathfrak{s})$  with idempotents  $\iota_x$  and  $\iota_y$ , respectively, we think of the grading difference  $\mathfrak{s}_{\iota_x}(x) - \mathfrak{s}_{\iota_y}(y)$  as an element of  $\frac{1}{2}H_M$ , which is in  $H_M$  if and only if  $\iota_x = \iota_y$ .

Let  $(M_0, \alpha_0, \beta_0)$  and  $(M_1, \alpha_1, \beta_1)$  be two bordered three-manifolds with torus boundary and consider the box tensor product  $\widehat{CFA}(M_0, \alpha_0, \beta_0) \boxtimes \widehat{CFD}(M_1, \alpha_1, \beta_1)$ . For  $x_0, y_0$  in  $\widehat{CFA}(M_0, \alpha_0, \beta_0; \mathfrak{s}_0)$  and



$x_1, y_1$  in  $\widehat{CFD}(M_1, \alpha_1, \beta_1; \mathfrak{s}_1)$ , the grading difference  $s_{\iota_{x_0}}(x_0) + s_{\iota_{x_1}}(x_1) - s_{\iota_{y_0}}(y_0) - s_{\iota_{y_1}}(y_1)$  between  $x_0 \otimes x_1$  and  $y_0 \otimes y_1$  is a well defined element of

$$H_1(\partial M_0) / (\ker(j_{0,*}) \oplus \ker(j_{1,*})) \cong H_1(M_0 \cup M_1),$$

where  $j_{i,*}$  is the map induced by the inclusion  $j_i: H_1(\partial M_i) \rightarrow H_1(M_i)$ . This recovers the  $\text{spin}^c$  decomposition of  $\widehat{CF}(M_0 \cup M_1)$ .

For each  $\text{spin}^c$  structure  $\mathfrak{s}$ ,  $\widehat{CFD}(M, \alpha, \beta; \mathfrak{s})$  admits a relative  $\mathbb{Z}/2\mathbb{Z}$  grading  $\text{gr}^D$  as defined by Petkova in [28]. (This grading may be identified with a specialization of the full grading package on the bordered invariants; see [15, Appendix A].) The relative  $\mathbb{Z}/2\mathbb{Z}$  grading satisfies  $\text{gr}^D(\partial x) = \text{gr}^D(x) - 1$  and  $\text{gr}^D(a \otimes x) = \text{gr}^D(a) + \text{gr}^D(x)$  for  $a \in \mathcal{A}$ , where  $\text{gr}^D(\rho_1) = \text{gr}^D(\rho_3) = 0$  and  $\text{gr}^D(\rho_2) = \text{gr}^D(\rho_{123}) = \text{gr}^D(\rho_{12}) = \text{gr}^D(\rho_{23}) = 1$ . Note that if  $\widehat{CFD}(M, \alpha, \beta; \mathfrak{s})$  is connected (see below), the relative  $\mathbb{Z}/2\mathbb{Z}$  grading is completely determined by this condition. The generators of  $\widehat{CFA}(M, \alpha, \beta; \mathfrak{s})$  inherit a grading  $\text{gr}^A$  from the corresponding generators in  $\widehat{CFD}(M, \alpha, \beta; \mathfrak{s})$ , where the grading of generators with idempotent  $\iota_0$  is reversed. A generator  $x_0 \otimes x_1$  in a box tensor product  $\widehat{CFA}(M_0, \alpha_0, \beta_0) \boxtimes \widehat{CFD}(M_1, \alpha_1, \beta_1)$  inherits the grading  $\text{gr}^A(x_0) + \text{gr}^D(x_1)$ , which recovers the relative  $\mathbb{Z}/2\mathbb{Z}$  grading on  $\widehat{CF}(M_0 \cup M_1)$ .

**2.4. Decorated graphs and loop-type manifolds.** There is a convenient graph-theoretic shorthand for describing these bordered invariants (see, for instance, [10, 11]). Let  $\Gamma$  be a directed graph with vertex set  $\mathcal{V}_\Gamma$  and edge set  $\mathcal{E}_\Gamma$ . A decorated graph has the property that every  $v \in \mathcal{V}_\Gamma$  is labelled with exactly one element from  $\{\bullet, \circ\}$  and every  $e \in \mathcal{E}_\Gamma$  is labelled with exactly one element from  $\{\emptyset, 1, 2, 3, 12, 23, 123\}$ .

A decorated graph  $\Gamma$  describes a type D structure as follows. The underlying vector space is generated by  $\mathcal{V}_\Gamma$ , with the idempotent splitting specified by  $\bullet$  labels identifying the  $\iota_0$  generators and  $\circ$  labels identifying the  $\iota_1$  generators. The map  $\delta^1$  is determined by the edge labels: Given  $e \in \mathcal{E}_\Gamma$  with label  $I \in \{\emptyset, 1, 2, 3, 12, 23, 123\}$  consider the source  $x$  and target  $y$  in  $\mathcal{V}_\Gamma$ . Then  $\rho_I \otimes y$  is a summand of  $\delta^1(x)$ , with the interpretation that  $\rho_\emptyset = \mathbf{1}$ . A decorated graph (and its associated type D structure) is reduced if none of the edges is labelled by  $\emptyset$ . An example is shown in Figure 6, describing the bordered invariant  $\widehat{CFD}(M, \mu, \lambda)$  when  $M$  is the complement of the right-hand trefoil,  $\mu$  is the knot meridian and  $\lambda$  is the Seifert longitude (see [21]). Notice that the higher  $\delta^k$  are determined by directed paths in  $\Gamma$ ; for the example shown, there exist generators  $x$  and  $y$  such that  $\delta^3(x) = \rho_3 \otimes \rho_2 \otimes \rho_1 \otimes y$  corresponding to the unique directed path of length 3. Clearly, the associated type D structure is bounded if and only if the decorated graph contains no directed cycles.

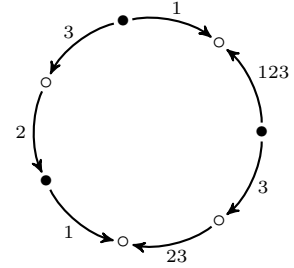


Figure 6. A decorated graph.

In the reduced case, the duality between type D and type A structures is encoded in the decorated graphs following an algorithm described by Hedden and Levine [11]. This takes the same interpretation for the underlying vector space (that is, the idempotent splitting according to vertex labels) but requires a different interpretation of the edge labels. First, one re-writes/re-interprets the edge labels according to the bijection  $1 \leftrightarrow 3$ ,  $2 \leftrightarrow 2$ ,  $3 \leftrightarrow 1$ . Next, given any length  $n$  directed path in  $\Gamma$  with source vertex  $x$  and target vertex  $y$  we construct a sequence  $I = I_1, \dots, I_k$  and assign a multiplication  $m_{k+1}(x \otimes \rho_{I_1} \otimes \dots \otimes \rho_{I_k}) = y$ . The sequence  $I$  is constructed by forming a word in  $\{1, 2, 3\}$  determined according to the labels of the directed edge read in order, and then regrouping to find the minimum  $k$  such that each  $I_j$  (for  $1 \leq j \leq k$ ) is an element

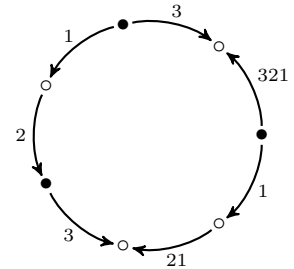


Figure 7. Relabelling by  $1 \leftrightarrow 3$ ,  $2 \leftrightarrow 2$ ,  $3 \leftrightarrow 1$  to extract a type A structure from a decorated graph.

of  $\{1, 2, 3, 12, 23, 123\}$ . Thus, in our example, to the length 3 directed path we assign the label sequence  $I = \{123\}$  so that  $m_2(x, \rho_{123}) = y$  while the edge label 321 (formerly 123 in the original decorated graph) gives rise to a sequence  $I = \{3, 2, 1\}$  and the product  $m_4(x', \rho_3, \rho_2, \rho_1) = y'$ .

Our focus will be on bordered invariants associated with a particular class of valence two graphs, as in the work of the first and third authors [10]. Specifically, we consider valence two decorated graphs satisfying an additional assumption: For any vertex labelled  $\bullet$ , exactly one incident edge is of the type  $\mathbf{I}_\bullet$  and exactly one incident edge is of the type  $\mathbf{II}_\bullet$ , as described in Figure 8. Similarly, for any vertex labelled  $\circ$  exactly one incident edge is of the type  $\mathbf{I}_\circ$  and exactly one incident edge is of the type  $\mathbf{II}_\circ$ . We will call the connected components of such a graph loops.

This requirement on  $\Gamma$  is, *a priori*, a strong restriction. However, if a valence two decorated graph represents  $\widehat{CFD}(M, \alpha, \beta)$ , then these conditions are forced by generalized coefficients maps [21]; see [10]. These coefficient maps were only defined for the type D structure computed from a bordered Heegaard diagram and, though we will not prove this, it seems likely that they are well defined for any homotopy equivalent type D structure.

In light of the relative  $\mathbb{Z}/2\mathbb{Z}$  grading on the bordered invariants, this is a natural class of decorated graphs to consider. Given a loop, fixing an orientation of the loop determines a  $\mathbb{Z}/2\mathbb{Z}$  grading on the vertices according to the following convention:

- A  $\bullet$ -vertex has grading 0 if it is followed by an arrow of type  $\mathbf{II}_\bullet$  and grading 1 if it is followed by an arrow of type  $\mathbf{I}_\bullet$ ; and
- a  $\circ$ -vertex has grading 0 if it is followed by an arrow of type  $\mathbf{I}_\circ$  and grading 1 if it is followed by an arrow of type  $\mathbf{II}_\circ$ .

Note that reversing the orientation of the loop switches the grading of every vertex. For consistency with the gradings on the relevant bordered invariants, if an orientation in a given loop is to be changed one must reverse orientations on every connected component (loop) corresponding to the relevant summand  $\widehat{CFD}(M, \alpha, \beta; \mathfrak{s})$ .

**Lemma 10.** *The grading on oriented loops, defined above, agrees with the relative  $\mathbb{Z}/2\mathbb{Z}$  grading  $\text{gr}^A$ .*

*Proof.* It is enough to check that edges labelled 2 and 123 change the grading and that all other labelings preserve the grading; we check this for 2-labelled edges and leave the rest to the reader. Suppose a vertex  $x$  is followed by a vertex  $y$ , according to the orientation on the loop. If the edge connecting  $x$  to  $y$  is a forward arrow labelled by 2 (so that the vertex  $x$  is type  $\mathbf{I}_\circ$ ), then  $x$  has grading 0 and  $y$  must be followed by an edge of type  $\mathbf{I}_\bullet$ . Thus  $y$  has grading 1. Similarly, if the edge connecting  $x$  and  $y$  is a backward arrow labelled by 2, then  $x$  has grading 0 and  $y$ , which must be followed by an edge of type  $\mathbf{II}_\circ$ , has grading 1.  $\square$

Now any loop with a choice of orientation admits a  $\mathbb{Z}/2\mathbb{Z}$  grading, which can be recorded (equivalently) as four types of vertices. Denote these by  $\bullet^+$ ,  $\bullet^-$ ,  $\circ^+$ , and  $\circ^-$ , where  $+$  designates grading 0 and  $-$  designates grading 1. Define the idempotent-specific Euler characteristics  $\chi_\bullet = \#(\bullet^+) - \#(\bullet^-)$  and  $\chi_\circ = \#(\circ^+) - \#(\circ^-)$ ; these are well defined up to multiplying both by  $-1$ . A loop is homologically trivial if  $\chi_\bullet$  and  $\chi_\circ$  are both 0.

The three-manifolds (and their bordered invariants) of interest in this work are specified as follows:

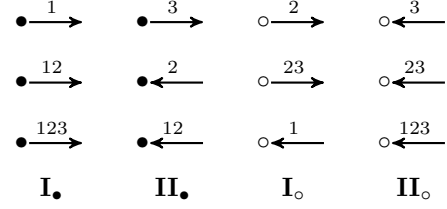


**Figure 8.** Vertex types for valence two decorated graphs.

**Definition 11.** An oriented three-manifold with torus boundary  $M$  is loop type if  $\widehat{CFD}(M, \alpha, \beta)$  can be represented by a directed graph  $\Gamma$  where each connected component of  $\Gamma$  is a loop.

This definition does not depend on the choice of parametrizing curves  $\alpha$  and  $\beta$ , as shown in [10].

There is a special class of loops, called solid torus-like, which for some choice of parametrization contain only 12-labelled arrows. These loops behave slightly differently with respect to the gluing results discussed later. As a result, a loop type manifold behaves differently if every loop in the collection of loops representing  $\widehat{CFD}$  is solid torus-like and there is one loop per  $\text{spin}^c$  structure; we say that such a manifold is solid torus-like. It is shown in [7] that a solid torus like manifold must be the solid torus connected sum with an L-space, and in particular is boundary compressible.

**2.5. Loops as immersed curves.** Consider a (reduced) loop  $\ell$  with a chosen orientation and chosen starting vertex. By appealing to the grading described above, this determines a word  $\mathbf{c}_{\alpha, \beta}(\ell)$  in  $\alpha^{\pm 1}$  and  $\beta^{\pm 1}$  defined via

$$\mathbf{c}_{\alpha, \beta}(x) = \begin{cases} \alpha^{\pm 1} & x \text{ is a vertex with label } \circ^{\pm} \\ \beta^{\pm 1} & x \text{ is a vertex with label } \bullet^{\pm} \end{cases}$$

when the vertices  $x$  in  $\ell$  are traversed in order according to the orientation starting at the specified vertex.

The resulting word may be interpreted as an element of  $F_2$ . Note that changing the starting vertex cyclically permutes the letters in the word; this corresponds to changing the element of  $F_2$  by conjugation. Reversing the orientation of the loop inverts each letter and reverses the order, giving the inverse element in  $F_2$ . In this way, any loop  $\ell$  determines a well defined element  $\mathbf{c}_{\alpha, \beta}(\ell)$  of  $F_2$  modulo conjugacy and inversion. The latter are in one-to-one correspondence with unoriented homotopy classes of closed curves in a punctured torus.

**Lemma 12.** *Given a choice of generators  $\alpha$  and  $\beta$  for  $F_2$ ,  $\mathbf{c}_{\alpha, \beta}$  is a bijection from the set of reduced loops to  $F_2$  modulo conjugacy and inversion.*

*Proof.* Note that the representative of  $\mathbf{c}_{\alpha, \beta}(\ell)$  constructed is automatically written as a reduced word, that is, there are no instances of  $\alpha\alpha^{-1}$ ,  $\alpha^{-1}\alpha$ ,  $\beta\beta^{-1}$  or  $\beta^{-1}\beta$ . This is because the pairs of consecutive vertex labels are determined by the arrows as in Table 1. The first and last letter in the word are also not inverses of each other; hence the word is cyclically reduced.

An element of  $F_2$  modulo conjugacy has a unique representation as a cyclically reduced word, up to cyclicly permutating the letters. Given a cyclically reduced word, a loop can be constructed by the reverse of the process above: Each consecutive pair of letters gives rise to an arrow according to Table 1. Cyclically permuting the letters in the word doesn't change the loop, only the starting vertex, and the inverse word gives rise to the same loop with the opposite orientation. Thus  $\mathbf{c}_{\alpha, \beta}$  is invertible.  $\square$

**2.6. The proof of Theorem 1.** Let  $M$  be a loop type manifold with torus boundary, and let  $z$  be a base point on  $\partial M$ . Fix a pair of oriented parametrizing curves  $\alpha$  and  $\beta$  in  $\partial M$  which are disjoint from the base point  $z$ . Note that  $\pi_1(\partial M \setminus z) \cong F_2$  with generators  $\alpha$  and  $\beta$  given by the parametrizing curves. It follows that the set of homotopy classes of closed curves in  $\partial M \setminus z$  can be identified with  $F_2$  modulo conjugacy and inversion (note that the particular identification depends on the choice of  $\alpha$  and  $\beta$ ). By Lemma 12, any reduced loop  $\ell$  determines an element of  $F_2$  modulo conjugacy and inversion,  $\mathbf{c}_{\alpha, \beta}(\ell)$ , which we now view as a homotopy class of curves. If  $\widehat{CFD}(M, \alpha, \beta)$  is determined by a collection of loops  $\{\ell_1, \dots, \ell_k\}$ , we will interpret the bordered Heegaard Floer invariant of  $M$  as the corresponding collection of curves  $\{\mathbf{c}_{\alpha, \beta}(\ell_1), \dots, \mathbf{c}_{\alpha, \beta}(\ell_k)\}$ . It remains to show that these curves do not depend on the choice of parametrizing curves  $\alpha$  and  $\beta$ .

Labeled edge	Subword	Labeled edge	Subword
$\xrightarrow{1}$	$\beta^{-1}\alpha^{-1}$	$\xleftarrow{1}$	$\alpha\beta$
$\xrightarrow{2}$	$\alpha\beta^{-1}$	$\xleftarrow{2}$	$\beta\alpha^{-1}$
$\xrightarrow{3}$	$\beta\alpha$	$\xleftarrow{3}$	$\alpha^{-1}\beta^{-1}$
$\xrightarrow{12}$	$\beta^{-1}\beta^{-1}$	$\xleftarrow{12}$	$\beta\beta$
$\xrightarrow{23}$	$\alpha\alpha$	$\xleftarrow{23}$	$\alpha^{-1}\alpha^{-1}$
$\xrightarrow{123}$	$\beta^{-1}\alpha$	$\xleftarrow{123}$	$\alpha^{-1}\beta$

**Table 1.** Instructions for passing between a loop and a word in  $F_2$ .

Consider a different choice of parametrizing curves (equivalently, basis for  $F_2$ ) given by  $\alpha' = \alpha$ ,  $\beta' = \beta\alpha$ . This parametrization is obtained from  $(\alpha, \beta)$  by performing a (positive) Dehn twist about  $\alpha$ , and  $\widehat{CFD}(M, \alpha', \beta')$  is obtained from  $\widehat{CFD}(M, \alpha, \beta)$  by taking the tensor product with the DA bimodule associated with the Dehn twist. The effect of this bimodule is easy to describe for loops; see [10, Section 3.3]. Given a loop  $\ell$  (representing a type D module), tensoring with the Dehn twist bimodule produces another loop, which we denote  $\tau(\ell)$ . Following the notation of [10], let  $d_k$  denote the segment

$$\bullet \xrightarrow{123} \circ \xrightarrow{23} \circ \xrightarrow{23} \dots \xrightarrow{23} \circ \xrightarrow{2} \bullet$$

with  $k \geq 1$   $\circ$ -generators, let  $d_{-k}$  denote the segment

$$\bullet \xrightarrow{1} \circ \xleftarrow{23} \circ \xleftarrow{23} \dots \xleftarrow{23} \circ \xleftarrow{3} \bullet$$

with  $k \geq 1$   $\circ$ -generators, and let  $d_0$  denote the segment

$$\bullet \xrightarrow{12} \bullet$$

Note that if we are reading the loop with a fixed orientation, these segments may appear backwards; we use  $\bar{d}_k$  to denote the corresponding segment read backwards. Now  $\tau(\ell)$  is obtained from  $\ell$  by replacing each instance of  $d_k$  with  $d_{k+1}$  and each instance of  $\bar{d}_k$  with  $\bar{d}_{k+1}$  (for all integers  $k$ ). Segments of any other form in  $\ell$  are preserved by the operation  $\tau$ .

The collection of curves determined by  $\widehat{CFD}(M, \alpha', \beta')$  is given by  $\mathbf{c}_{\alpha', \beta'}(\tau(\ell_1)), \dots, \mathbf{c}_{\alpha', \beta'}(\tau(\ell_k))$ . The following lemma implies that this is in fact the same collection of curves (up to homotopy) that is determined by  $\widehat{CFD}(M, \alpha, \beta)$ .

**Lemma 13.** *For  $\alpha' = \alpha$ ,  $\beta' = \beta\alpha$  (as above) and any loop  $\ell$ ,  $\mathbf{c}_{\alpha', \beta'}(\tau(\ell)) = \mathbf{c}_{\alpha, \beta}(\ell)$  as elements of the free group  $F_2$ .*

*Proof.* Recall that  $\mathbf{c}_{\alpha, \beta}$  gives a well defined cyclic word in  $\alpha^{\pm 1}$  and  $\beta^{\pm 1}$  once an orientation is chosen for the loop  $\ell$ . An instance of  $d_k$  in  $\ell$  is equivalent to an instance of the subword  $\beta^{-1}\alpha^k\beta^{-1}$  in  $\mathbf{c}_{\alpha, \beta}(\ell)$ , and an instance of  $\bar{d}_k$  in  $\ell$  is equivalent to an instance of the subword  $\beta\alpha^{-k}\beta$  in  $\mathbf{c}_{\alpha, \beta}(\ell)$ . It follows that  $\mathbf{c}_{\alpha, \beta}(\tau(\ell))$  is obtained from  $\mathbf{c}_{\alpha, \beta}(\ell)$  by inserting an  $\alpha$  after any occurrence of  $\beta^{-1}$  that is followed by  $\alpha^k\beta^{-1}$  for some  $k \in \mathbb{Z}$  and by inserting an  $\alpha^{-1}$  after each  $\beta$  that is followed by  $\alpha^k\beta$  for some  $k$ . Now  $\mathbf{c}_{\alpha', \beta'}(\tau(\ell))$  is obtained from  $\mathbf{c}_{\alpha, \beta}(\tau(\ell))$  by replacing  $\alpha$  with  $\alpha'$  and  $\beta$  with  $\beta'$ .

Since  $\alpha' = \alpha$  and  $\beta' = \beta\alpha$ , the curve  $\mathbf{c}_{\alpha', \beta'}(\tau(\ell))$ , written in terms of the basis  $(\alpha, \beta)$ , is obtained from  $\mathbf{c}_{\alpha, \beta}(\tau(\ell))$  by adding an  $\alpha$  after each  $\beta$  and adding an  $\alpha^{-1}$  before each  $\beta^{-1}$ . If a  $\beta$  is followed by  $\alpha^k\beta^{-1}$ , the  $\alpha$  added after the  $\beta$  cancels with the  $\alpha^{-1}$  added before the  $\beta^{-1}$ . For each instance of  $\beta^{-1}\alpha^k\beta^{-1}$ , adding an  $\alpha^{-1}$  before the second  $\beta^{-1}$  is equivalent to adding an  $\alpha^{-1}$  after the first  $\beta^{-1}$ . It follows that  $\mathbf{c}_{\alpha', \beta'}(\tau(\ell))$  is obtained from  $\mathbf{c}_{\alpha, \beta}(\tau(\ell))$  by inserting an  $\alpha$  after any  $\beta$  that is followed by  $\alpha^k\beta$  for some  $k$  and by inserting an  $\alpha^{-1}$  after each  $\beta^{-1}$  that is followed by  $\alpha^k\beta^{-1}$  for

some  $k$ . This is the inverse of process for obtaining  $\mathbf{c}_{\alpha,\beta}(\mathbb{T}(\ell))$  from  $\mathbf{c}_{\alpha,\beta}(\ell)$ , so  $\mathbf{c}_{\alpha',\beta'}(\mathbb{T}(\ell)) = \mathbf{c}_{\alpha,\beta}(\ell)$  as claimed.  $\square$

A similar proof shows that the collection of curves is invariant under the Dehn twist around  $\beta$ . Since any reparametrization is a composition of these Dehn twists, it follows that the collection of homotopy classes of curves in  $\partial M \setminus z$  determined by  $\widehat{CFD}(M, \alpha, \beta)$  does not depend on the choice of bordered structure  $\alpha$  and  $\beta$ , it is an invariant of the underlying manifold  $M$ . To complete the proof of Theorem 1 then, we need the following observation extracted from [10]:

**Lemma 14.** *A reduced valence two decorated graph representing the bordered invariants of a loop type manifold is unique.*  $\square$

We now define the central object in this paper:

**Definition 15.** If  $M$  is a loop-type manifold, denote the marked boundary  $\partial M \setminus z$  by  $T$  and let  $\gamma(M)$  denote the collection of homotopy classes of closed curves in  $T$  determined by the map  $\mathbf{c}_{\alpha,\beta}$ .

**2.7. Orientation reversal.** The curves  $\gamma(M)$  are unchanged by reversing orientation of  $M$ . More precisely,  $\gamma(-M) = \gamma(M)$ , but note that the orientation of the boundary also reverses, so the diagram for  $\gamma(M)$  changes by a reflection. This follows from the fact that reversing the orientation of a bordered Heegaard diagram for  $(M, \alpha, \beta)$  gives a bordered Heegaard diagram for  $(-M, \beta, \alpha)$ . The corresponding change to the (directed graphs representing)  $\widehat{CFD}$  is to interchange the idempotents, reverse the direction of every arrow, and interchange  $\rho_1$  and  $\rho_3$  arrow labels. Applying this change to a loop, the effect on the corresponding curve is to interchange  $\alpha$  and  $\beta$ , or equivalently to reflect across the diagonal  $y = x$ . When comparing the curves  $\tilde{\gamma}(M)$  and  $\tilde{\gamma}(-M)$  in the plane, by convention we will rotate  $\tilde{\gamma}(-M)$  so that  $\beta$  parametrizes the (positive) horizontal direction for both curves; with this convention,  $\tilde{\gamma}(-M)$  is obtained from  $\tilde{\gamma}(M)$  by reflecting across a horizontal line.

**2.8. The lifted invariant.** When  $M$  is loop type, we have shown that each loop in  $\widehat{CFD}(M, \alpha, \beta)$  determines a class of curves in  $T = \partial M \setminus z$ ; given a basis  $\{\alpha, \beta\}$  for  $F_2 \cong \pi_1(T)$ , this class can be represented as a word in  $\alpha^{\pm 1}$  and  $\beta^{\pm 1}$  by the map  $\mathbf{c}_{\alpha,\beta}$ . In fact, this curve can be naturally lifted to a certain covering space of  $T$  in a way which allows us to recover/encode more of the graded information from  $\widehat{CFD}(M, \alpha, \beta)$ .

We consider two covers of  $T$ . Let  $i_*: \pi_1(\partial M \setminus z) \rightarrow \pi_1(\partial M)$  be the map induced by inclusion and let  $p: \tilde{T} \rightarrow T$  be the covering map corresponding to  $\ker i_*$ . The group of deck transformations of  $\tilde{T}$  is isomorphic to  $\text{im } i_*$ , and  $\tilde{T}$  may be identified with  $\mathbb{R}^2 \setminus \mathbb{Z}^2$ . We will also use the intermediate cover  $\bar{T}$  corresponding to the kernel of the composition  $\pi_1(\partial M \setminus z) \rightarrow \pi_1(\partial M) \rightarrow H_1(M)$ .  $\bar{T}$  is always homeomorphic to  $S^1 \times \mathbb{R}$ ; its fundamental group is generated by the homological longitude  $\lambda$ . The preimage of  $z$  in  $\bar{T}$  can be identified with an affine copy of  $\mathbb{Z} \oplus \mathbb{Z}/n$ , where  $n$  is the order of the rational homological longitude  $l$  in  $H_1(M)$ . (So  $\lambda = nl$ .)

For each  $\mathfrak{s} \in \text{Spin}^c(M)$ , we will define a collection of closed curves  $\bar{\gamma}(M, \mathfrak{s})$  which is a lift of  $\gamma(M, \mathfrak{s})$  to  $\bar{T}$ . When drawing pictures, it is often easier to think about  $\tilde{\gamma}(M, \mathfrak{s})$ , which we define to be the preimage of  $\bar{\gamma}(M, \mathfrak{s})$  in  $\tilde{T}$ . Although the curves  $\bar{\gamma}(M, \mathfrak{s})$  for different values of  $\mathfrak{s}$  are all subsets of  $\bar{T}$ , there is no natural way to think of them all together in the same copy of  $\bar{T}$ . When we want to emphasize this fact, we will use  $\bar{T}_{\mathfrak{s}}$  to denote the copy of  $\bar{T}$  containing  $\bar{\gamma}(M, \mathfrak{s})$ .

To define  $\bar{\gamma}(M, \mathfrak{s})$ , we recall how the differentials in  $\widehat{CFD}$  relate to the  $\text{spin}^c$  grading.

**Lemma 16.** *We can identify  $\text{Spin}^c(M, \mathfrak{t})$  with a subset of  $\frac{1}{2}H_M$  in such a way that arrows in  $\widehat{CFD}(M, \alpha, \beta)$  shift the  $\text{Spin}^c$  grading as shown in Table 2.*

Labeled edge	$\mathfrak{s}(y) - \mathfrak{s}(x)$	Labeled edge	$\mathfrak{s}(y) - \mathfrak{s}(x)$
$x \xrightarrow{1} y$	$-(\alpha + \beta)/2$	$x \xrightarrow{12} y$	$-\beta$
$x \xrightarrow{2} y$	$(\alpha - \beta)/2$	$x \xrightarrow{23} y$	$\alpha$
$x \xrightarrow{3} y$	$(\alpha + \beta)/2$	$x \xrightarrow{123} y$	$(\alpha - \beta)/2$

**Table 2.** Grading shifts in  $\widehat{CFD}(M, \alpha, \beta)$  associated with labelled edges when  $M$  is loop type.

*Proof.* This is just a rephrasing of [30, Lemma 3.8]; compare [21, Lemma 11.42]. Specifically, choose some identification  $f: \text{Spin}^c(M, \iota_0, \mathfrak{t}) \rightarrow H_M$ . For  $\mathfrak{s} \in \text{Spin}^c(M, \iota_0, \mathfrak{t})$ , we identify  $\mathfrak{s}$  with  $f(\mathfrak{s})$ , and for  $\mathfrak{s} \in \text{Spin}^c(M, \iota_1, \mathfrak{t})$  we identify  $\mathfrak{s}$  with  $f(j^{-1}(\mathfrak{s})) - (\alpha + \beta)/2$ , where  $j: \text{Spin}^c(M, \iota_0, \mathfrak{t}) \rightarrow \text{Spin}^c(M, \iota_1, \mathfrak{t})$  is the map defined in [30, Lemma 3.8].  $\square$

As in the previous section, we let  $\alpha$  and  $\beta$  be cells in the 1-skeleton on  $T$ . The set of lifts of  $\alpha$  to  $\overline{T}$  is an  $H_M$  torsor; fix identification of this set with  $\text{Spin}^c(M, \iota_1, \mathfrak{t})$ . The set of lifts of  $\beta$  is also an  $H_M$  torsor; identify it with  $\text{Spin}^c(M, \iota_0, \mathfrak{t})$  in such a way that if  $p_1$  is the midpoint of  $\alpha_{\bar{\mathfrak{s}}_1}$  and  $p_2$  is the midpoint of  $\beta_{\bar{\mathfrak{s}}_2}$ , then  $p_1 - p_2 = \bar{\mathfrak{s}}_1 - \bar{\mathfrak{s}}_2$ , where the difference on the right-hand side is the one given by Lemma 16.

**Lemma 17.** *If  $\gamma$  is a loop of  $\gamma(M, \mathfrak{s})$  corresponding to a loop  $\ell$  in  $\widehat{CFD}(M, \alpha, \beta)$ , then  $\gamma$  lifts to a closed loop  $\bar{\gamma}$  in  $\overline{T}$ .*

*Proof.* Let  $x$  be a generator of  $\widehat{CFD}(M, \alpha, \beta)$  belonging to  $\ell$ . Lift  $\gamma$  to  $\overline{T}$  starting at the segment corresponding to  $x$ . Suppose that  $y$  and  $z$  are two generators of  $\widehat{CFD}(M, \alpha, \beta)$  which belong to  $\ell$ , and  $p_x$  and  $p_y$  are midpoints of the corresponding lifts. We claim that  $p_x - p_y = \mathfrak{s}(x) - \mathfrak{s}(y)$ . If  $y$  and  $z$  are consecutive vertices of  $\ell$ , the claim is easily verified by comparing Table 1 and Table 2. Since both sides of the equation are additive, the general case follows. If  $p'_x$  be the midpoint of lift of  $x$  we arrive at once we have gone once around  $\gamma$ . Then  $p'_x - p_x = \mathfrak{s}(x) - \mathfrak{s}(x) = 0$ , so  $\gamma$  lifts to a closed loop in  $\overline{T}$ .  $\square$

More generally, if  $\gamma(M, \mathfrak{s}) = \{\gamma_1, \dots, \gamma_n\}$  is the set of curves associated with all the loops in  $\widehat{CFD}(M, \alpha, \beta; \mathfrak{s})$ , we define  $\bar{\gamma}(M, \mathfrak{s})$  to be the union of the lifts  $\bar{\gamma}_1, \dots, \bar{\gamma}_n$ , where the relative position of the various lifts is chosen so that the relation  $p_x - p_y = \mathfrak{s}(x) - \mathfrak{s}(y)$  still holds. Finally, we define  $\tilde{\gamma}(M, \mathfrak{s})$  to be the preimage of  $\bar{\gamma}(M, \mathfrak{s})$  in  $\overline{T}$ .

To summarise the discussion to this point, consider the construction of the curves for an explicit example. Let  $M$  be the complement of the right-hand trefoil, with the boundary parametrized by the meridian  $\mu$  and the Seifert longitude  $\lambda$ . Then  $\widehat{CFD}(M, \mu, \lambda)$  is given by the loop in Figure 9, shown together with the construction of the corresponding path  $\gamma(M)$  in  $T$  and cover  $\tilde{\gamma}(M)$ .

**2.9. Relation with the Turaev torsion.** We now explain how to derive the Turaev torsion of  $M$  from  $\tilde{\gamma}(M)$ . The torsion can be thought of as a function  $\tau_M: \text{Spin}^c(M, \partial M) \rightarrow \mathbb{Z}$ . If  $b_1(M) > 1$ ,  $\tau(\bar{\mathfrak{s}}) = 0$  for all but finitely many values of  $\bar{\mathfrak{s}}$ . If  $b_1(M) = 1$ , we must first choose a generator  $[\Sigma]$  of  $H_2(M, \partial M)$ . Once this choice has been made, the torsion function is defined so that  $\tau_M(\bar{\mathfrak{s}}) = 1$  if  $\langle c_1(\bar{\mathfrak{s}}), [\Sigma] \rangle \gg 0$ , and  $\tau_M(\bar{\mathfrak{s}}) = 0$  if  $\langle c_1(\bar{\mathfrak{s}}), [\Sigma] \rangle \ll 0$ .

Next, we fix some notation for  $\tilde{\gamma}(M, \mathfrak{s})$ . Recall that the set of preimages of  $\beta$  in  $\overline{T}$  is an  $H_M$  torsor, which we identified with  $\text{Spin}^c(M, \iota_0, \mathfrak{s})$ . The set of preimages of  $z$  in  $\overline{T}$  is also an  $H_M$  torsor. We identify it with  $\text{Spin}^c(M, \partial M)$  in the following way: if  $p_{\bar{\mathfrak{s}}}$  is the midpoint of  $\beta_{\bar{\mathfrak{s}}}$ , then  $z_{\bar{\mathfrak{s}}}$  is the midpoint of the segment between  $p_{\bar{\mathfrak{s}}}$  and  $p_{\bar{\mathfrak{s}}+\alpha}$ .

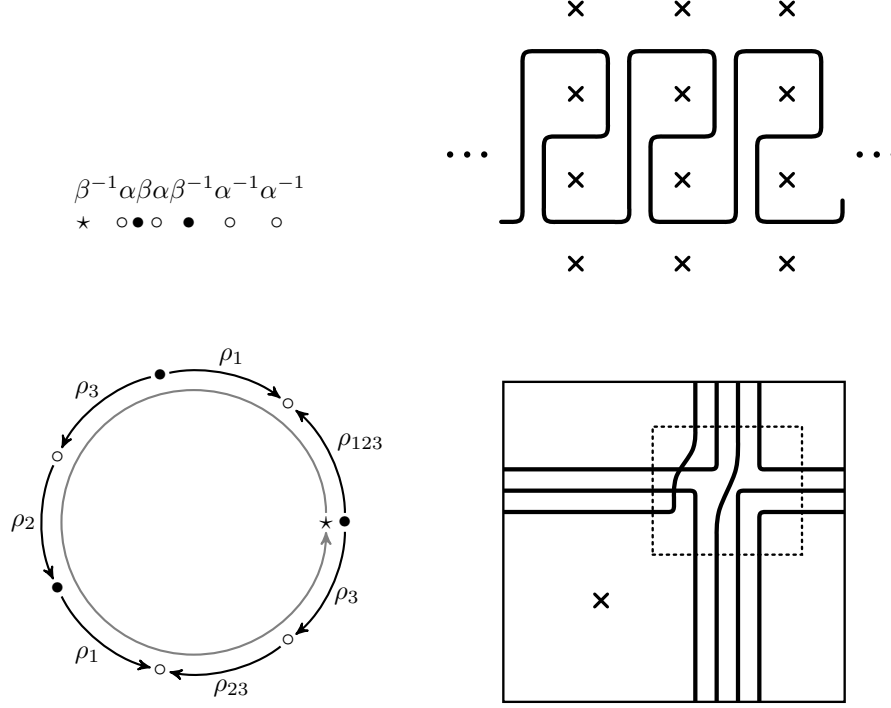


**Figure 9.** Constructing the immersed curve  $\gamma(M)$ , together with the lift  $\tilde{\gamma}(M)$  compatible with the preferred framing  $\{\mu, \lambda\}$ , associated with the right-hand trefoil.

The cover  $\bar{T}$  is homeomorphic to  $S^1 \times \mathbb{R}$ , so it has two ends. Recall that in defining the torsion function, we had to choose a generator  $[\Sigma]$  for  $H_2(M, \partial M)$ . We use  $\Sigma$  to identify these ends as *positive* and *negative*, according to the convention that for  $p \in \bar{T}$  and  $h \in H_M$ ,  $p + nh$  converges to the positive end if  $h \cdot [\Sigma] > 0$ , and to the negative end if  $h \cdot [\Sigma] < 0$ .

**Proposition 18.**  $\tau_M(\bar{s}) = n_{\bar{s}}$ , where  $n_{\bar{s}}$  is the signed intersection number of  $\bar{\gamma}(M, \bar{s})$  with a path from the negative end of  $\bar{T}$  to  $z_{\bar{s}}$ .

*Proof.* We first observe that  $n_{\bar{s}}$  is well-defined, since it can be realized as an intersection number between a class in  $H_1(S, \partial S)$  and the image of  $\bar{\gamma}(M, \bar{s})$  in  $H_1(S)$ , where  $S$  is the manifold with boundary obtained by removing small open neighborhoods of  $z_{\bar{s}}$  and truncating the positive and negative ends of  $\bar{T}$ .

Next, we choose a parametrization  $\alpha, \beta$  of  $\partial M$  with the property that  $\alpha \cdot [\Sigma] > 0$ . Consider the 1-cell  $\beta_{\bar{s}}$  in  $\bar{T}$ . Each segment of  $\bar{\gamma}(M, \bar{s})$  which runs along  $\beta_{\bar{s}}$  corresponds to a generator of  $\widehat{CFD}(M, \alpha, \beta, \bar{s})$  in the  $\iota_0$  idempotent, or equivalently, to a generator of  $SFH(M, \gamma_\alpha, \bar{s})$ , where  $\gamma$  is a set of two sutures parallel to the curve  $\alpha$ . Since the  $\mathbb{Z}/2\mathbb{Z}$  grading of  $x$  determines the orientation of the corresponding segment, the signed number of segments of  $\bar{\gamma}(M, \bar{s})$  which run along  $\beta_{\bar{s}}$  is given by  $\chi(SFH(M, \gamma_\alpha, \bar{s}))$ . It follows that

$$n_{\bar{s}} - n_{\bar{s} - \alpha} = \chi(SFH(M, \gamma_\alpha, \bar{s})) = \tau_M(\bar{s}) - \tau_M(\bar{s} - \alpha)$$

Both  $n_{\bar{s} - k\alpha}$  and  $\tau_M(\bar{s} - k\alpha)$  vanish for  $k \gg 0$  — the former because  $\gamma(M, \bar{s})$  is compactly supported, and the latter by the definition of the torsion function. It follows that  $n_{\bar{s}} = \tau_M(\bar{s})$  for all  $\bar{s} \in \text{Spin}^c(M, \partial M)$ .  $\square$

**Remark 19.** The fact that  $\tau_M(\bar{s} + k\alpha) = 1$  for all  $k \gg 0$  means that the homology class of  $\bar{\gamma}(M, \bar{s})$  is always the positive generator of  $H_1(\bar{T})$ . This is also a handy way of pinning down the global orientation on  $\gamma(M)$ .

We conclude this section by explaining our earlier statement that there is no natural way to embed all of the curves  $\overline{\gamma}(M, \mathfrak{s})$  in the same copy of  $\overline{T}$ . When  $b_1(M) = 1$ , there is a natural “height function”  $\pi_\ell: \overline{T}_\mathfrak{s} \rightarrow \mathbb{R}$  given by defining  $\pi_\ell(z_{\overline{\mathfrak{s}}}) = \langle c_1(\overline{\mathfrak{s}}), [\Sigma] \rangle$ , and extending to all of  $\overline{T}$  by the relation  $\pi_\ell(x) - \pi_\ell(y) = 2(x - y) \cdot \ell$ , where  $\ell$  is the positive generator of  $\ker i_*$ . This height function plays an important role when we consider conjugation symmetry or the relation with the Thurston norm. When  $\ell$  is not a primitive element of  $H_1(\partial M)$ , the images of the lattice points  $z_{\overline{\mathfrak{s}}}$  will appear at different heights depending on the  $\text{Spin}^c$  structure  $\mathfrak{s}$  that we consider. Thus, there is no natural way to put all of the  $\overline{\gamma}(M, \mathfrak{s})$  into the same picture.

### 3. PAIRING VIA INTERSECTION: THE PROOF OF THEOREM 2

In this section, we show that the pairing theorem in bordered Floer homology can be described using Lagrangian Floer homology of curves in the punctured torus. Since the torus is two dimensional, this Floer homology can be defined in a purely combinatorial way, as we describe below.

**3.1. Immersed curves in the punctured torus.** We consider immersed, essential, closed curves  $\gamma: S^1 \rightarrow T$ , subject to two additional constraints:

- (1) All points of self intersection are transverse and double; and
- (2) there exists a cover of  $T$  with a lift of  $\gamma$  that is embedded.

The second requirement rules out points of self intersection that form a cusp bounding a disk in  $T$  (that is, local pictures as illustrated in Figure 10). Immersed curves with this property are called unobstructed; see Abouzaid [1]. Note that the cover required in (2) may be taken to be the universal cover, that is, a subset of hyperbolic space that retracts to the Caley graph of  $\pi_1 T \cong F_2$ . We will abuse notation and write  $\gamma$  for the image  $\gamma(S^1)$  in  $T$ . Immersions subject to (1) and (2) will be referred to as nice immersions. Our interest will be in pairs of nice immersions  $(\gamma_0, \gamma_1)$  such that all intersections between  $\gamma_0$  and  $\gamma_1$  are transverse and double. We will restrict attention to admissible pairs, in the following sense:



**Figure 10.** Local pictures of a cusp (left) and a bigon (right).

The pair  $(\gamma_0, \gamma_1)$  is admissible if it does not bound an immersed annulus in  $T$ .

An immersed annulus is an immersion  $A: S^1 \times [0, 1] \rightarrow T$  such that  $A(S^1 \times \{i\})$  is contained in  $\gamma_i$ , for  $i = 0, 1$ . Given an pair of nice immersions  $(\gamma_0, \gamma_1)$ , there are two regular homotopies that we will consider. The first is regular homotopy of either one of the  $\gamma_i$  that does not alter the intersections between the two curves. These are referred to as local homotopies. The second is the addition and removal of bigons formed between  $\gamma_0$  and  $\gamma_1$ . These are referred to as bigon moves; a local picture of such a bigon is shown in Figure 10.

**Proposition 20.** *Let  $(\gamma_0, \gamma_1)$  and  $(\gamma'_0, \gamma'_1)$  be two pairs of nice, admissible immersed curves in  $T$ . Then  $(\gamma_0, \gamma_1)$  is regular homotopic to  $(\gamma'_0, \gamma'_1)$  if and only if there is a sequence of local homotopies and bigon moves taking  $(\gamma_0, \gamma_1)$  to  $(\gamma'_0, \gamma'_1)$ . Moreover, this homotopy may be realized through admissible pairs of immersed curves.*

*Proof.* Both statements follow from standard arguments. In particular, since the immersed curves lift to embedded curves in the universal cover, we may appeal to the material of [6, Chapter 1], for example, to study the homotopies in question via isotopy in the cover.  $\square$

Given a pair of nice immersed curves  $(\gamma_0, \gamma_1)$  denote by  $\mathbf{i}(\gamma_0, \gamma_1)$  their minimal geometric intersection number. Note that when  $\gamma_0$  and  $\gamma_1$  are essential simple closed curves,  $\mathbf{i}(\gamma_0, \gamma_1)$  coincides with the



distance between slopes representing  $\gamma_0$  and  $\gamma_1$ . Similarly, let  $\mathbf{a}(\gamma_0, \gamma_1)$  denote the maximum number of immersed annuli bounded by isotopy classes of  $\gamma_0$  and  $\gamma_1$ . Given a pair  $(\gamma_0, \gamma_1)$ , we will consider the adjusted count defined by:

$$\mathbf{i}^a(\gamma_0, \gamma_1) = \mathbf{i}(\gamma_0, \gamma_1) + 2\mathbf{a}(\gamma_0, \gamma_1)$$

Of particular interest will be this count applied to admissible pairs. Note that admissibility may be violated in order to compute  $\mathbf{i}^a(\gamma_0, \gamma_1)$ .

**3.2. Minimal intersection in terms of Floer homology in the punctured torus.** We now turn to a variant of intersection Floer homology for immersed curves. This may be viewed as a specialization to  $T$  of the more general setup given by Akaho [2] (see also Abouzaid [1]).

Given an admissible pair of immersed curves  $(\gamma_0, \gamma_1)$ , let  $CF(\gamma_0, \gamma_1)$  denote the vector space (over  $\mathbb{F} = \mathbb{Z}/2\mathbb{Z}$ ) generated by intersections between  $\gamma_0$  and  $\gamma_1$ . (Self intersections in  $\gamma_0$  or  $\gamma_1$  are ignored.) This vector space is promoted to a chain complex by counting immersed bigons in  $T$ . To be precise, given intersection points  $x, y$ , let  $f: D^2 \rightarrow T$  denote a Whitney disk, where  $D^2 \subset \mathbb{C}$  is the standard unit disk in the complex plane and  $f(x) = -i, f(y) = i, f(\partial D^2_+) \subset \gamma_0$ , and  $f(\partial D^2_-) \subset \gamma_1$ . (Here  $\partial D^2_+$  is the part of the boundary with positive real part, and  $\partial D^2_-$  is the part of the boundary with negative real part). We will regard two Whitney disks as equivalent if they differ only by reparametrization of the natural  $\mathbb{R}$ -action on  $D^2$ . Note that, by construction, the image of a Whitney disk is an immersed bigon in  $T$  with boundary on the pair  $(\gamma_0, \gamma_1)$ . Let  $N_0(x, y)$  denote the number of Whitney disks (up to equivalence and modulo 2) connecting  $x$  to  $y$  and consider the linear map defined on generators of  $CF(\gamma_0, \gamma_1)$  via  $d(x) = \sum_{y \in \gamma_0 \cap \gamma_1} N_0(x, y) \cdot y$ .

**Proposition 21.** *The pair  $(CF(\gamma_0, \gamma_1), d)$  is a chain complex.*

*Proof.* This generalises the construction in the case of embedded curves in the torus; see Ozsváth and Szabó [26, Section 6], for example. We need to verify that  $d^2(x) = 0$  for any generator  $x \in CF(\gamma_0, \gamma_1)$ . Suppose that there is a generator  $y$  in the image of  $x$  under the map  $d$ , and that  $d(y) = z$ . Then there are two possible configurations of bigons that give rise to these maps, as illustrated in Figure 11: Either there is a  $y'$  so that  $d(x) = y + y'$  and  $d^2(x) = 0$ , or  $d^2(x) = z$ . However, in the latter case a cusp must be present, and this is ruled out since we have restricted to nice immersions.  $\square$

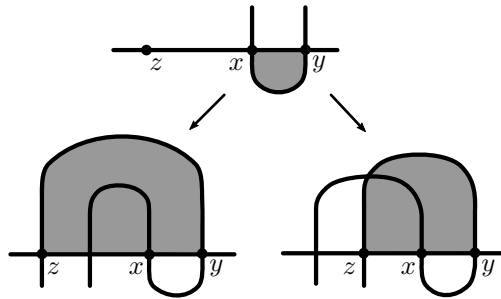


**Figure 11.** Local pictures certifying that  $d^2 = 0$ : Either  $d^2(x) = 0$  owing to the fact that 4 bigons must be present (as illustrated on the left), or there must be a cusp in one of the  $\gamma_i$  (as illustrated on the right) that is ruled out by restricting to nice immersions. Note that, while bigons need not be embedded, it is always possible to pass to an appropriate cover to obtain these local pictures.

**Proposition 22.** *The homology group  $HF(\gamma_0, \gamma_1)$  is an invariant of the admissible homotopy class of the pair  $(\gamma_0, \gamma_1)$ .*

*Proof.* By Proposition 20, we need to check the effect on  $CF(\gamma_0, \gamma_1)$  when a bigon between  $(\gamma_0, \gamma_1)$  is removed. In particular, suppose there is a configuration of immersed bigons giving rise to intersection points  $x, y, z, w$  such that  $d(x) = y + z$  and  $y$  is in the image of  $d$  applied to  $w$ ; see Figure 12. We now appeal to a standard argument: Consider the change of basis realized by  $y \mapsto y + z = y'$  and  $w \mapsto x + w = w'$ . Now  $d(x) = y'$  and  $z$  is in the image of  $d$  applied to  $w'$ . Cancelling the former by Gaussian elimination produces a new chain complex with the same homology. The effect of an isotopy adding a bigon is similar.  $\square$

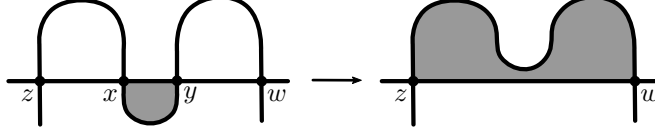


**Figure 12.** Local pictures arising in the proof of homotopy invariance.

**Corollary 23.** *For any admissible pair  $(\gamma_0, \gamma_1)$ ,  $\dim HF(\gamma_0, \gamma_1) = \mathbf{i}^a(\gamma_0, \gamma_1)$ .*

*Proof.* This is immediate on observing that a pair of nice immersions bounding an immersed annulus may be promoted to an admissible pair by a homotopy introducing a two new generators and a pair of bigons.  $\square$

An important special case of this construction arises when each curve in the admissible pair  $(\gamma_0, \gamma_1)$  is embedded. In this case, the pair of curves is naturally associated to a genus one Heegaard splitting for some  $Y$  (either a lens space or  $S^2 \times S^1$ ) and  $\widehat{HF}(Y) \cong HF(\gamma_0, \gamma_1)$ , as in [27, Section 3]. In this way, we might regard the setup in this section as a generalization of a genus one splitting.

**3.3. Refinements.** There are a few refinements of this setup that will be used in the sequel. The first is to consider finite collections of nice immersed curves  $\gamma = \{\gamma^i\}_{i=1}^n$ . Pairs of such collections  $(\gamma_0, \gamma_1)$  are admissible if for each  $i$  and each  $j$  the pair  $(\gamma_0^i, \gamma_1^j)$  is admissible. Then we define  $HF(\gamma_0, \gamma_1) = \bigoplus_{i,j} HF(\gamma_0^i, \gamma_1^j)$ .

Another refinement is the addition of a relative  $\mathbb{Z}/2\mathbb{Z}$  grading. To define such a grading, we must fix orientations on  $\gamma_0$  and  $\gamma_1$ . The generator associated to an intersection point  $p$  has even grading if  $\gamma_0$  and  $\gamma_1$  intersect positively at  $p$ , and odd grading if they intersect negatively.

The third refinement corresponds to a relative  $\text{spin}^c$  grading on  $HF(\gamma_0^i, \gamma_1^j)$ . Given two intersection points  $x$  and  $y$  in  $\gamma_0^i \cap \gamma_1^j$ , let  $c_0$  be a curve from  $x$  to  $y$  in  $\gamma_0^i$  and let  $c_1$  be a curve from  $y$  to  $x$  in  $\gamma_1^j$ . The grading difference between  $x$  and  $y$  is the homology class  $[c_0 \cup c_1]$  in  $H_1(T)/\langle [\gamma_0^i], [\gamma_1^j] \rangle$ . Note that  $x$  and  $y$  are in the same  $\text{spin}^c$  structure when this class is zero, or equivalently, when  $c_0 \cup c_1$  in  $T$  lifts to a closed curve in the cover  $\tilde{T}$ . More generally, if  $\gamma_0$  and  $\gamma_1$  are collections of curves, we can define a  $\text{spin}^c$  grading on  $HF(\gamma_0, \gamma_1)$  using additional grading information on each collection of curves. Recall that the grading data for each collection  $\gamma_i$  takes the form of a choice of lift  $\tilde{\gamma}_i$  to  $\tilde{T}$  up to an overall translation of every curve in  $\tilde{\gamma}_i$ . A point  $x$  in  $\gamma_0 \cap \gamma_1$  lifts to an intersection  $\tilde{x}$  in  $\tilde{\gamma}_0 \cap \tilde{\gamma}_1$  for some shift of  $\tilde{\gamma}_1$ ; similarly  $y$  lifts to an intersection  $\tilde{y}$  in  $\tilde{\gamma}_0 \cap \tilde{\gamma}_1$  for a shift of  $\tilde{\gamma}_1$ . As before,  $x$  and  $y$  have the same  $\text{spin}^c$  grading if and only if the shifts for these two lifts are the same.

**3.4. The proof of Theorem 2.** We can now interpret the chain complex arising from a box tensor product in terms of the intersection homology developed above.

Let  $M_0$  and  $M_1$  be manifolds with torus boundary. Fix any parametrization  $(\alpha_1, \beta_1)$  for  $\partial M_1$  and set  $\alpha_0 = h(\beta_1)$  and  $\beta_0 = h(\alpha_1)$ . By the pairing for bordered Heegaard Floer homology [21],  $\widehat{CF}(Y) \cong \widehat{CFA}(M_0, \alpha_0, \beta_0) \boxtimes \widehat{CFD}(M_1, \alpha_1, \beta_1)$  provided that one of the bordered invariants involved

in the pairing is bounded. We will show that, whenever  $M_0$  and  $M_1$  are loop type manifolds, there exist particular (admissible) representatives of the regular homotopy classes of  $\gamma(M_0)$  and  $\gamma(M_1)$  such that  $\widehat{CFA}(M_0, \alpha_0, \beta_0) \boxtimes \widehat{CFD}(M_1, \alpha_1, \beta_1)$  is isomorphic to  $CF(\gamma(M_0), \bar{h}(\gamma(M_1)))$ , where  $\bar{h}$  is the composition of  $h$  with the elliptic involution on  $\partial M_0$  taking  $\alpha_0$  to  $-\alpha_0$  and  $\beta_0$  to  $-\beta_0$ .

First consider  $\gamma_0 = \gamma(M_0)$  associated with the loop type manifold  $M_0$  and thought of as immersed in  $T = \partial M_0 \setminus z_0$ . Represent  $T$  as the square  $[0, 1] \times [0, 1]$  with opposite sides identified, such that the base point  $z_0$  is identified with  $(0, 0)$ ,  $\alpha_0$  is identified with the curve  $\{\frac{3}{4}\} \times [0, 1]$  and  $\beta_0$  is identified with the curve  $[0, 1] \times \{\frac{3}{4}\}$ . We will require the curves  $\gamma_0$  to lie in a small  $\epsilon$  neighborhood of  $\alpha_0 \cup \beta_0$ . The curves naturally decompose into small segments in the box  $[\frac{3}{4} - \epsilon, \frac{3}{4} + \epsilon] \times [\frac{3}{4} - \epsilon, \frac{3}{4} + \epsilon]$ , which we will call corners, together with vertical segments parallel to  $\alpha_0$ , and horizontal segments parallel to  $\beta_0$ . By construction, vertical segments correspond to generators for the associated bordered invariant with idempotent  $\iota_1$ , while horizontal segments correspond to generators with idempotent  $\iota_0$ . There are exactly 6 possibilities for these corners, as illustrated in Figure 14, which can be decorated in order to agree with the type A conventions associated with the loop description of  $\widehat{CFA}(M_0, \alpha_0, \beta_0)$ .

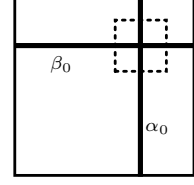


**Figure 13.** Conventions for corners.

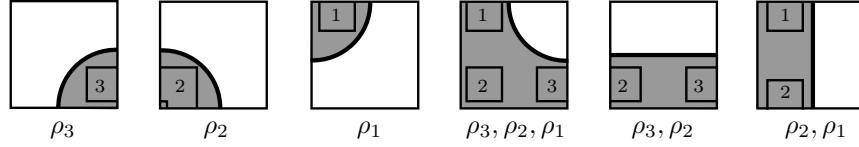


**Figure 14.** Corner labels for  $\gamma_0$ , consistent with the a type A structure for  $(M_0, \alpha_0, \beta_0)$ .

Following exactly the same procedure, we arrive at a choice of representative for  $\gamma(M_1)$  immersed, this time, in the marked torus  $\partial M_1 \setminus z_1$ . In order to compare  $\gamma(M_1)$  with  $\gamma(M_0)$ , we push the curves and corner data forward by  $h$ . We also must apply the elliptic involution on the torus  $\partial M_0$ , which takes  $\alpha_0$  to  $-\alpha_0$  and  $\beta_0$  to  $-\beta_0$ ; the resulting curve is  $\gamma_1 = \bar{h}(\gamma(M_1))$  in  $T$ .

**Remark 24.** The need for  $\bar{h}$  instead of  $h$  here was surprising to us, although in all examples we are aware of  $\bar{h}(\gamma(M_1))$  and  $h(\gamma(M_1))$  are homotopic. This symmetry should correspond to the conjugation symmetry on Floer homology. It is known to hold when  $M_1$  is a knot complement in  $S^3$  by a result of Xiu [33], when  $M_1$  is a graph manifold as discussed in [10], or when  $M_1$  is Floer simple (in which case it follows from the symmetry of the Turaev torsion). We expect this symmetry should hold for all three-manifolds with torus boundary.

Graphically,  $\gamma_1$  is obtained from  $\gamma(M_1)$  by reflecting across the anti-diagonal  $y = -x$ ; it follows that  $\gamma_1$  lies in an epsilon neighborhood of  $\{\frac{1}{4}\} \times [0, 1]$  and  $[1, 0] \times \{\frac{1}{4}\}$ , so that the corners lie in the box  $[\frac{1}{4} - \epsilon, \frac{1}{4} + \epsilon] \times [\frac{1}{4} - \epsilon, \frac{1}{4} + \epsilon]$ . We give these corners labels, as in Figure 15, this time consistent with the type D structure associated with the loop type description of  $\widehat{CFD}(M_1, \alpha_1, \beta_1)$ . Horizontal segments of  $\gamma_1$  correspond to  $\iota_1$  generators of  $\widehat{CFD}(M_1, \alpha_1, \beta_1)$ , while vertical segments correspond to  $\iota_0$  generators.

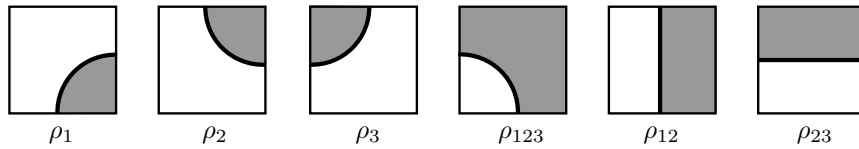


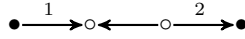
**Figure 15.** Corner labels for  $\gamma_1$ , consistent with the a type D structure for  $(M_1, \alpha_1, \beta_1)$ .

Notice that  $\widehat{CFA}(M_0, \alpha_0, \beta_0)$  and  $\widehat{CFD}(M_1, \alpha_1, \beta_1)$  can now be recovered directly from  $\gamma_0$  and  $\gamma_1$ , respectively, as immersed curves in  $T$ . Each corner in  $\gamma_1$  is decorated by some  $I$  giving rise to the

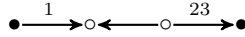
appropriate label on the edge of the decorated graph for  $\widehat{CFD}(M_1, \alpha_1, \beta_1)$ . Recall that the decorated graph for  $\widehat{CFD}(M_0, \alpha_0, \beta_0)$  determines a graph for  $\widehat{CFA}(M_0, \alpha_0, \beta_0)$ , which is obtained by replacing the arrow labels: Each algebra element for a type D arrow corresponds to a sequence of algebra elements labeling a type A arrow. We decorate the corners of  $\gamma_0$  by these sequences of algebra elements (see Figure 14). In particular, reflection in the anti-diagonal together with this relabeling on corners (compare Figure 14 and Figure 15) precisely encodes the observation of Hedden and Levine [11] described in Section 2.1. Note that this all uses the fact that loops, as decorated graphs describing bordered invariants, are reduced.

As a result, we can now consider the chain complex  $CF(\gamma_0, \gamma_1)$ , provided the pair  $(\gamma_0, \gamma_1)$  is admissible.

Without loss of generality, assume that for  $i = 0, 1$  we have chosen a bordered structure for which  $\widehat{CFD}(M_i, \alpha_i, \beta_i)$  has generators with idempotent  $\iota_0$ . If both associated decorated graphs give rise to unbounded bordered invariants, we modify the graph representing  $\widehat{CFD}(M_1, \alpha_1, \beta_1)$  by replacing a 12 labelled edge with



or by replacing a 123 labelled edge with



Note that at least one edge of either form exists when a loop associated with  $\widehat{CFD}(M_1, \alpha_1, \beta_1)$  (corresponding to some component of  $\gamma(M_1)$ ) is unbounded. The local effect on the relevant component of  $\gamma_1$  (in  $T$ ) is shown in Figure 16. This modification ensures that the bordered invariants for  $(M_1, \alpha_1, \beta_1)$  are bounded, and hence the pairing theorem applies. Moreover:

**Lemma 25.** *Under the assumptions above, the pair  $(\gamma_0, \gamma_1)$  is admissible.*

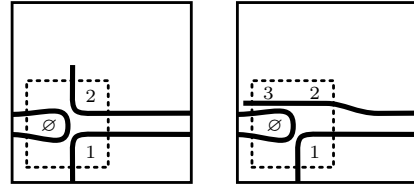


**Figure 16.** Homotopy in a component of  $\gamma_1$  associated with an unbounded loop.

*Proof.* Suppose that  $(\gamma_0, \gamma_1)$  bounds an immersed annulus in  $T$ . Consulting Figure 19, this annulus can be decomposed into copies of the the four connecting pieces (shown in the bottom row of Figure 19). In particular, the relevant component of the curve  $\gamma_1$  would have only corners labeled by  $\{2, 12, 23, 123\}$  (with the same orientation), which would imply that  $\widehat{CFD}(M_1, \alpha_1, \beta_1)$  contains an unbounded loop. (Similarly, the corners of the  $\gamma_0$  boundary would imply that  $\widehat{CFA}(M_0, \alpha_0, \beta_0)$  is unbounded.)  $\square$

Now observe that, with all of the foregoing in place, each vertical (respectively horizontal) segment in  $\gamma_0$  intersects each horizontal (respectively vertical) segment of  $\gamma_1$ ; there are no other intersection points. It follows immediately that  $CF(\gamma_0, \gamma_1)$  and  $\widehat{CFA}(M_0, \alpha_0, \beta_0) \boxtimes \widehat{CFD}(M_1, \alpha_1, \beta_1)$  are isomorphic as vector spaces.

We now turn to the differential. First, consider a bigon that contains a corner of  $\gamma_1$  with the label  $\emptyset$ . This corner (there is at most one such corner for any given component of  $\gamma_1$ ) connects the right ends of two parallel horizontal segments; let the upper (respectively lower) segment correspond to a generator  $x$  (respectively  $y$ ) in  $\iota_1 \widehat{CFD}(M_1, \alpha_1, \beta_1)$ . Moreover, the left end of the segment corresponding to  $y$  is attached to a 1 labelled corner. There is a bigon that fills in the space between the two horizontal segments, but it must not extend to contain the whole horizontal segment since then the bigon would cover the base point; see Figure 17. Thus there must be a vertical segment in  $\gamma_0$ , corresponding to some generator  $w$  in  $\widehat{CFA}(M_0, \alpha_0, \beta_0)$ , and the bigon does not extend to the left of this vertical segment. A bigon of this form gives a differential between (the intersection point corresponding to)  $w \otimes x$  and (the intersection point corresponding to)  $w \otimes y$ . The  $\emptyset$ -labeled corner in  $\gamma_1$  arises from a differential from  $x$  to  $y$  in  $\widehat{CFD}(M_1, \alpha_1, \beta_1)$ , so the corresponding differential is counted in the box tensor product as well.

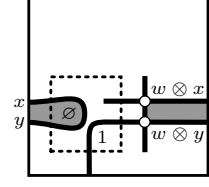


**Figure 17.** The bigon for  $\delta^1(x) = 1 \otimes y$ .

We may assume that any other bigon does not involve a corner with a  $\emptyset$  label. The only bigon that does not intersect the boundary of  $[0, 1] \times [0, 1]$  is shown in Figure 18. Let  $\tilde{x}_0$  denote the relevant vertical segment in  $\gamma_0$  corresponding to some  $x_0 \in \iota_1 \widehat{CFA}(M_0, \alpha_0, \beta_0)$ . Let  $\tilde{x}_1$  denote the relevant horizontal segment in  $\gamma_1$  corresponding to some generator  $x_1 \in \iota_1 \widehat{CFD}(M_1, \alpha_1, \beta_1)$ . Similarly, let  $\tilde{y}_0$  and  $\tilde{y}_1$  denote the relevant horizontal segment in  $\gamma_0$  and vertical segment in  $\gamma_1$ , respectively, and let  $y_0$  and  $y_1$  denote the corresponding generators in  $\widehat{CFA}(M_0, \alpha_0, \beta_0)$  and  $\widehat{CFD}(M_1, \alpha_1, \beta_1)$ . A bigon of this form gives a differential from  $\tilde{x}_0 \cap \tilde{x}_1$  to  $\tilde{y}_0 \cap \tilde{y}_1$ . The left side of the bigon is a path in  $\gamma_1$  from  $\tilde{x}_1$  to  $\tilde{y}_1$  with a single corner labeled 2. This corresponds to a path of arrows (of length one) from  $x_2$  to  $y_2$  labeled by 2, which, in turn, encodes the operation  $\delta^1(x_1) = \rho_2 \otimes y_1$  in  $\widehat{CFD}(M_1, \alpha_1, \beta_1)$ . The right edge of the bigon is a path in  $\gamma_0$  with a corner labeled by the sequence 2; this in turn corresponds to a map  $m_2(x_0, \rho_2) = y_0$  in  $\widehat{CFA}(M_0, \alpha_0, \beta_0)$ . These operations pair in the box tensor product, so there is a differential from  $x_0 \otimes x_1$  to  $y_0 \otimes y_1$  in the complex  $\widehat{CFA}(M_0, \alpha_0, \beta_0) \boxtimes \widehat{CFD}(M_1, \alpha_1, \beta_1)$ .

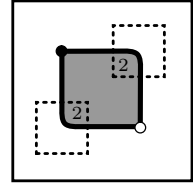
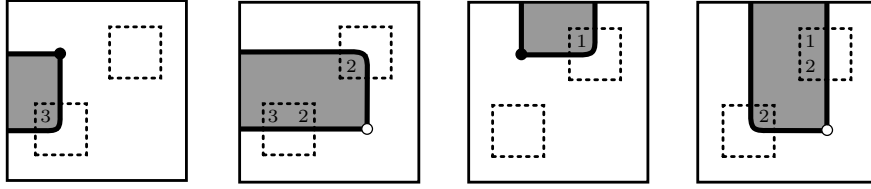


**Figure 18.** Bigon compatible with  $m_2(x_0, \rho_2) = y_0$  and  $\delta^1(x_1) = \rho_2 \otimes y_1$ .

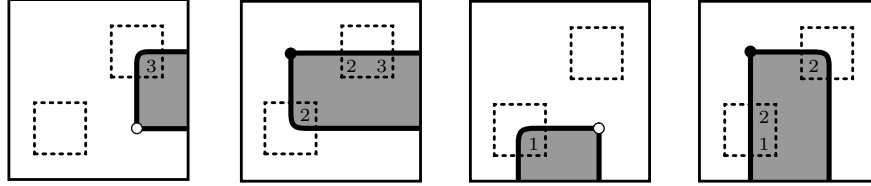
More generally, consider any immersed bigon  $D$  which gives rise to a differential between  $\tilde{x}_0 \cap \tilde{x}_1$  and  $\tilde{y}_0 \cap \tilde{y}_1$  in  $CF(\gamma_0, \gamma_1)$ . The boundary of  $D$  determines a path from  $\tilde{x}_0$  to  $\tilde{y}_0$  in  $\gamma_0$ , and the corner decorations along this path determines an  $\mathcal{A}_\infty$  operation from  $x_0$  to  $y_0$  in  $\widehat{CFA}(M_0, \alpha_0, \beta_0)$ . The boundary of  $D$  also determines a path  $\tilde{x}_1$  to  $\tilde{y}_1$  in  $\gamma_1$  and the corner decorations along this path determines a sequence of operations from  $x_1$  to  $y_1$  in  $\widehat{CFD}(M_1, \alpha_1, \beta_1)$ . We will show that these operations always pair in the box tensor product, producing a differential from  $x_0 \otimes x_1$  to  $y_0 \otimes y_1$ . If  $D$  is not one of the bigons considered in the preceding paragraphs, then it can be cut along the lattice curves  $\{0\} \times [0, 1]$  and  $[0, 1] \times \{0\}$  into pieces of the form listed in Figure 19. As illustrated, the corner decorations can be recorded with sequences of the integers 1, 2, and 3; with this notation, each path from  $\tilde{x}_0 \cap \tilde{x}_1$  to  $\tilde{y}_0 \cap \tilde{y}_1$  determines a sequence in  $\{1, 2, 3\}$ . To recover a sequence of type D operations from the path in  $\gamma_1$ , we break this sequence of integers into increasing subsequences (this is how the integers are already grouped by the division of the bigon into pieces) and interpret, say, the increasing sequence 23 as a  $\rho_{23}$  operation. To recover a type A operation from the path in  $\gamma_0$ , we also divide the sequence in  $\{1, 2, 3\}$  into increasing subsequences which determine the inputs to the type A operation. Consider, for example, the bigon pictured in Figure 20: Both paths determine the sequence 123. The path in  $\gamma_1$  corresponds to the map  $\delta^1(x_1) = \rho_{123} \otimes y_1$  while the path in  $\gamma_0$  corresponds to the operation  $m_2(x_0, \rho_{123}) = y_0$ .

To see that the type A operation determined by a bigon always pairs with the sequence of type D operations determined by that bigon, we simply need to check that the two sequences determined by the corner decorations agree. To see this, start with bigon pieces labeled as in Figure 19. We then slide any 3 label on the  $\gamma_0$  portion of the boundary to the right into the adjacent piece of the bigon,

Starting pieces:



Ending pieces:



Connecting pieces:

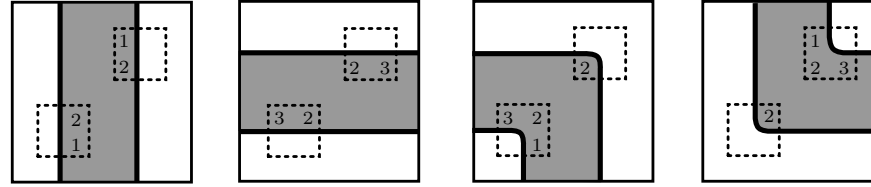


**Figure 19.** Decomposing a bigon into tiles: Any bigon bounded by  $(\gamma_0, \gamma_1)$  consists of one starting piece, some number of connecting pieces, and one ending piece. Note that any immersed annulus consists of a collection of connecting pieces only (compare the proof of Lemma 25), but these have been ruled out to achieve admissibility.

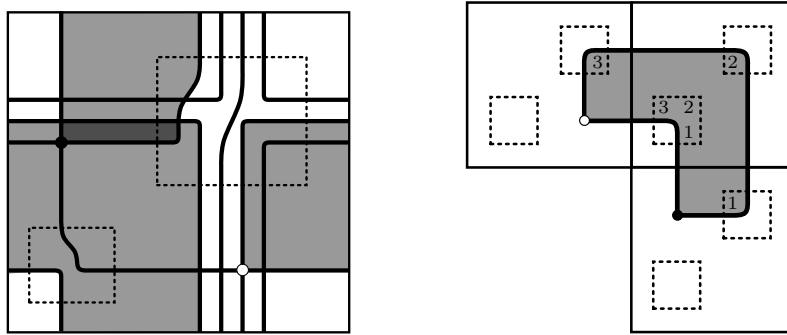


**Figure 20.** The chain complex arising from  $-1$  surgery on the right-hand trefoil. The shaded region highlights a bigon with edges corresponding to  $m_2(x_0, \rho_{123}) = y_0$  and  $\delta^1(x_1) = \rho_{123} \otimes y_1$  so that  $y_0 \otimes y_1$  is a summand of  $\partial^{\boxtimes}(x_0 \otimes x_1)$ .

and we slide any 1 label on  $\gamma_0$  upward into the adjacent piece of the bigon. It is clear from Figure 19 that, after this modification in a given bigon, the labeling on both curves is the same within each piece.

This establishes a bijection between bigons contributing to the differential in  $CF(\gamma_0, \gamma_1)$  and differentials in  $\widehat{CFA}(M_0, \alpha_0, \beta_0) \boxtimes \widehat{CFD}(M_1, \alpha_1, \beta_1)$ , completing the proof of Theorem 2.

**3.5. Grading refinements of Theorem 2.** It remains to show that the gradings of  $\widehat{HF}(M_0 \cup_h M_1)$  and  $HF(\gamma_0, \gamma_1)$  agree.

Consider first the relative  $\mathbb{Z}/2\mathbb{Z}$  grading. Recall that fixing the  $\mathbb{Z}/2\mathbb{Z}$  grading on  $\widehat{CFA}(M_0, \alpha_0, \beta_0)$  corresponds to choosing an orientation of each curve in  $\gamma_0$ . In particular, upward (respectively downward) oriented  $\alpha_0$  segments in  $\gamma_0$  correspond to  $\circ^+$  (respectively  $\circ^-$ ) generators of  $\widehat{CFA}(M_0, \alpha_0, \beta_0)$ , and rightward (respectively leftward) oriented  $\beta_0$  segments in  $\gamma_0$  correspond to  $\bullet^+$  (respectively  $\bullet^-$ ) generators of  $\widehat{CFA}(M_0, \alpha_0, \beta_0)$ . Fixing the  $\mathbb{Z}/2\mathbb{Z}$  grading on  $\widehat{CFD}(M_1, \alpha_1, \beta_1)$  corresponds to choosing orientations on  $\gamma(M_1)$  with similar identification except that the grading is reversed on  $\bullet$  generators. Reflecting across the anti-diagonal, it follows that upward (respectively downward) oriented segments in  $\gamma_1$  correspond to  $\bullet^+$  (respectively  $\bullet^-$ ) generators of  $\widehat{CFD}(M_1, \alpha_1, \beta_1)$  and rightward (respectively leftward) oriented segments in  $\gamma_1$  correspond to  $\circ^-$  (respectively  $\circ^+$ ) generators of  $\widehat{CFD}(M_1, \alpha_1, \beta_1)$ . The (relative)  $\mathbb{Z}/2\mathbb{Z}$  grading on  $\widehat{HF}(M_0 \cup_h M_1)$  is given by  $\text{gr}(x \otimes y) = \text{gr}^A(x) + \text{gr}^D(y)$ , while the grading of  $HF(\gamma_0, \gamma_1)$  is given by intersection signs. It is straightforward to check that generators of  $\widehat{HF}(M_0 \cup_h M_1)$  of the form  $\circ^+ \otimes \circ^+$ ,  $\circ^- \otimes \circ^-$ ,  $\bullet^+ \otimes \bullet^+$ , and  $\bullet^- \otimes \bullet^-$ , which all have the same  $\mathbb{Z}/2\mathbb{Z}$  grading, correspond exactly to positive intersection points and the remaining generators correspond to negative intersection points.

Finally, to see that the  $\text{spin}^c$  decomposition of both invariants coincide, it is sufficient to check this within fixed  $\text{spin}^c$  structures  $\mathfrak{s}_0$  on  $M_0$  and  $\mathfrak{s}_1$  on  $M_1$ . Consider the collections of curves  $\tilde{\gamma}(M_0, \mathfrak{s}_0)$  and  $\bar{h}(\tilde{\gamma}(M_1, \mathfrak{s}_1))$  in the cover  $\tilde{T}$ , with  $x, y \in \gamma(M_0, \mathfrak{s}_0) \cap \bar{h}(\gamma(M_1, \mathfrak{s}_1))$ . If these curves are lifts of representatives defined in the proof of Theorem 2, the reader can verify that the  $\text{spin}^c$  grading agrees with the conventions in bordered Floer homology on comparing Section 2.8 and Section 3.3.

## 4. APPLICATIONS

Throughout this section, all manifolds with torus boundary are assumed to be loop type. In Section 5 we will discuss this restriction in further detail by establishing many broad classes of examples.

**4.1. Characterizing L-space slopes.** Given a manifold with torus boundary  $M$ , let  $\mathcal{L}_M$  denote the set of L-space slopes, that is, the subset of slopes giving rise to L-spaces on Dehn filling, and let  $\mathcal{L}_M^\circ$  denote the interior of  $\mathcal{L}_M$ . This section gives a characterization of the set  $\mathcal{L}_M^\circ$  in terms of the collection of curves  $\gamma(M)$ .

Given an immersed curve  $\gamma$  in  $T$  and a slope  $r$  in  $\hat{\mathbb{R}}$ , we say that  $r$  is a tangent slope of  $T$  if every smooth immersed curve homotopic to  $T$  has a tangent line with slope  $r$ . For a  $\text{spin}^c$  structure  $\mathfrak{s}$  on  $M$ , consider the curve(s)  $\gamma(M; \mathfrak{s})$ . Let  $S(M; \mathfrak{s}) \subset \hat{\mathbb{R}}$  denote the set of tangent slopes to  $\gamma(M; \mathfrak{s})$  if  $\gamma(M; \mathfrak{s})$  consists of a single immersed curve, with the convention that  $S(M; \mathfrak{s}) = \hat{\mathbb{R}}$  if  $\gamma(M; \mathfrak{s})$  is disconnected. We define  $S(M)$  to be the union of  $S(M; \mathfrak{s})$  over all  $\text{spin}^c$  structures.

To visualize the set of tangent slopes  $S(M)$ , it is helpful to consider particular minimal representatives of  $\gamma(M)$  defined as follows: Fix a metric on the torus  $T$  and a sufficiently small  $\epsilon > 0$ . Consider the minimal length representative of the homotopy class of  $\gamma(M)$ , subject to the requirement that the resulting curve is distance at least  $\epsilon$  from the marked point. We call the result a peg-board representative for  $\gamma(M)$ , imagining that there is a *peg* of radius  $\epsilon$  centered at the marked point. We can also discuss peg-board representatives for the lift  $\tilde{\gamma}(M)$  of  $\gamma(M)$  to  $\mathbb{R}^2 \setminus \mathbb{Z}^2$ , imagining a peg of radius  $\epsilon$  centered at each lattice point; see Figure 21, for example. For a given  $\epsilon$ , let  $S_\epsilon(M)$  be the set of tangent slopes of the  $\epsilon$  radius peg-board representative of  $\tilde{\gamma}(M)$ , or  $\hat{\mathbb{R}}$  if there are multiple curves in any one  $\text{spin}^c$  structure.  $S(M)$  can be realized by taking  $\epsilon \rightarrow 0$ , in the sense that  $S(M) = \bigcap_{n=N}^{\infty} S_{\frac{1}{n}}(M)$ .



**Figure 21.** The peg board diagram (left) and singular peg board diagram (right) associated with the curve of the right hand trefoil, lifted to  $\mathbb{R}^2 \setminus \mathbb{Z}^2$ .

In practice,  $S(M)$  can be computed from the piecewise linear curve which results from shrinking the peg radius to 0 in a peg-board diagram for  $\tilde{\gamma}(M)$ . This curve, which we call the *singular peg-board representative* of  $\tilde{\gamma}(M)$ , consists of line segments connecting lattice points in  $\mathbb{R}^2$ ; see Figure 21, for example. If  $\gamma(M)$  has one loop per per spin<sup>c</sup> structure, we define  $S^{sing}(M)$  to be the set of slopes of tangent lines to the singular peg-board representative of  $\tilde{\gamma}(M)$ , where we say a line  $L$  through a corner is a tangent line if  $L$  coincides with one of the two segments at that corner or if both segments lie on the same side of  $L$ . Equivalently,  $S^{sing}(M)$  is the set of tangent slopes after smoothing the corners in a singular peg-board diagram. Each corner determines a closed interval of tangent slopes, bounded by the slopes of the incoming and outgoing segments, and  $S^{sing}(M)$  is the union of these intervals. The singular peg-board representative may contain a degenerate corner, where the incoming and outgoing segments coincide; any slope is a tangent slope at such a corner. If there are no corners, then the singular peg-board representative for  $\tilde{\gamma}(M)$  is a straight line of some rational slope  $\alpha$ , and  $S^{sing}(M) = \{\alpha\}$ . As with  $S(M)$ , we set  $S^{sing}(M) = \hat{\mathbb{R}}$  if  $\gamma(M)$  has more than one curve in any spin<sup>c</sup> structure.

Note that passing from a peg-board diagram to a singular peg-board diagram loses some information. In particular, in a peg-board diagram a curve may wrap entirely around a peg (that is, it changes direction by an angle of at least  $\pi$ ); we call this *peg wrapping*. A singular peg-board diagram only records the slopes of the incoming and outgoing segments each time the curve passes a peg; it can not determine if peg-wrapping occurs. It is clear that the two sets of slopes  $S(M)$  and  $S^{sing}(M)$  are the same unless there is peg-wrapping in  $\tilde{\gamma}(M)$ , in which case  $S(M) = \hat{\mathbb{R}}$ . For arbitrary curves in  $\mathbb{R}^2 \setminus \mathbb{Z}^2$ , these two intervals of tangent slopes need not be the same, but in fact we will see that they agree for any collection of curves  $\tilde{\gamma}(M)$  for a loop type manifold  $M$ . That is,  $S(M) = S^{sing}(M)$ .

Peg-board diagrams are a simple way to put curves in minimal intersection position. If  $\gamma_1$  and  $\gamma_2$  are peg-board representatives for two curves relative to some peg radius  $\epsilon$  and  $\gamma_1$  intersects  $\gamma_2$  transversally, then it is not difficult to see that  $\gamma_1$  and  $\gamma_2$  are in minimal position. Suppose, to the contrary, that there is some bigon in  $T$  connecting intersection points  $x$  and  $y$ . The corresponding segments from  $x$  to  $y$  in  $\gamma_1$  and in  $\gamma_2$  are homotopic to each other in  $T$ . They are not equal to each other, since  $\gamma_1$  and  $\gamma_2$  intersect transversally, so at most one of them can be the (unique) minimal length path connecting  $x$  to  $y$  in  $T$  with distance at least  $\epsilon$  from the marked point; this contradicts the fact that both  $\gamma_1$  and  $\gamma_2$  have minimal length. In general, peg-board representatives for two curves relative to the same radius will not have transverse intersection, but the same principle applies after perturbing the curves slightly, as we now describe.

By a corner we will mean any time a curve passes through a lattice point in a singular peg-board diagram (even if there is no change in direction), or equivalently any time the curve touches a peg in a peg-board diagram. To ensure transverse intersection, we will think of each corner as wrapping around a peg of a different radius. More precisely, let  $k$  be the total number of corners in  $\gamma_1$  and  $\gamma_2$ , and let  $\epsilon_1, \dots, \epsilon_k$  be  $k$  different peg radii between  $\epsilon$  and  $\frac{3\epsilon}{2}$ . Starting with (radius  $\epsilon$ ) peg-board representatives for  $\gamma_1$  and  $\gamma_2$ , we perturb the  $i$ th corner by pushing the curve away from the marked point to a minimum distance of  $\epsilon_i$  for  $1 \leq i \leq k$ , and we minimize the length of each curve subject to this new constraint. After this modification,  $\gamma_1$  and  $\gamma_2$  have transverse intersection; whether or not the intersection is minimal depends on relative sizes of the peg radii  $\epsilon_i$ . Note that each corner in a peg-board includes a path in the boundary of the peg, the circle of radius  $\epsilon$ ; this in turn determines



an interval in  $\mathbb{R}$ , by mapping  $(\epsilon \cos \theta, \epsilon \sin \theta)$  to  $\theta$ , well defined up to shifting by  $2\pi$ . We define a partial order on corners by saying  $c_1 < c_2$  if the interval in  $\mathbb{R}$  corresponding to  $c_2$  is strictly contained in the interval corresponding to  $c_1$ , possibly after shifting by a multiple of  $2\pi$ . We will require that  $\epsilon_1, \dots, \epsilon_k$  above are chosen to be consistent with this partial order, in the sense that if  $c_i < c_j$  then  $\epsilon_i < \epsilon_j$ , for any two corners  $c_i$  and  $c_j$  on opposite curves.

Moreover, if the intervals in  $\mathbb{R}$  determined by  $c_i$  and  $c_j$  are equal, the relative size of  $\epsilon_i$  and  $\epsilon_j$  is determined by neighboring corners. Given an orientation of  $\gamma_1$  and  $\gamma_2$  such that  $c_i$  and  $c_j$  wrap in the same direction, consider the corners  $c'_i$  and  $c'_j$  following  $c_i$  and  $c_j$  on  $\gamma_1$  and  $\gamma_2$ ; we require that the line segment connecting  $c_i$  to  $c'_i$  does not cross the segment connecting  $c_j$  to  $c'_j$ .

If two curves, or collections of curves, in a radius  $\epsilon$  peg-board diagram are perturbed as described above, we say that they are in *transverse peg-board position*. The following lemma states that transverse peg-board position realizes the minimal intersection number for two homotopy classes of curves.

**Lemma 26.** *Suppose  $\gamma_1$  and  $\gamma_2$  are two curves in transverse peg-board position. Then, for sufficiently small  $\epsilon$ ,  $\gamma_1$  intersects  $\gamma_2$  transversally and  $\gamma_1$  and  $\gamma_2$  are in minimal position.*

*Proof.* It is clear that the intersection of  $\gamma_1$  and  $\gamma_2$  is transverse locally near each peg, since any intersection is between two line segments tangent to different concentric circles or between a circle and a line segment tangent to a different circle with the same center. As long as  $\epsilon$  is sufficiently small so that line segments in the singular diagram are a minimum distance of  $2\epsilon$  from any lattice point they do not hit, the only other intersection points are between line segments connecting different pairs of lattice points, which must not be parallel.

If  $\gamma_1$  and  $\gamma_2$  are not in minimal position, then there is some bigon in  $T$  connecting intersection points  $x$  and  $y$ . The corresponding segments from  $x$  to  $y$  in  $\gamma_1$  and in  $\gamma_2$  are homotopic to each other in  $T$ . Each are perturbations of the minimal length path from  $x$  to  $y$  (given by the  $\epsilon$  peg-board representative) by at most  $\epsilon/2$ . Thus the bigon is contained in a thin strip, an  $\epsilon/2$ -neighborhood of the minimal length path. From this it is clear that  $x$  and  $y$  must be intersections between a line segment and an arc at some corner, or between two line segments coming from the same segment in an unperturbed peg-board diagram. Consider the subcurves of  $\gamma_1$  and  $\gamma_2$ , starting from  $x$ , forming the bigon. Both must approach the same corner (since otherwise the bigon would not be contained in a strip of width  $\epsilon$ ). In fact, both segments must meet the corner on the same side. Each curve traverses an arc along concentric circles before leaving the corner on a line segment. If a greater angle is covered on the inner arc, then the curves will separate by more than  $\epsilon$  before intersecting at  $y$ , which contradicts that the bigon lies in a strip of width  $\epsilon$ . By our choice of ordering, the outer arc does not cover a greater angle, so both arcs must have the same angle. In this case the curves approach the next corner along parallel segments, but repeating the reasoning above implies that these curves will never cross.  $\square$

Using tangent slopes in peg-board diagrams, we can give a new interpretation of L-space slopes for a loop type manifold.

**Theorem 27.** *If  $M$  is a manifold with torus boundary with associated curves  $\gamma(M)$  then  $\mathcal{L}_M^\circ$  is the complement of the set  $S_{\mathbb{Q}}^{\text{sing}}(M) = S^{\text{sing}}(M) \cap \hat{\mathbb{Q}}$ .*

*Proof.* By the pairing theorem,  $\widehat{HF}(M(\alpha))$  is equivalent to the intersection Floer homology of  $\gamma(M)$  and a straight line with slope  $\alpha$ , which we denote  $L_\alpha$ . Suppose first that  $\alpha$  is a non-L-space slope, so that the Dehn filling  $M(\alpha)$  is not an L-space and there is some  $\text{spin}^c$ -structure  $\mathfrak{s}$  so that  $\dim \widehat{HF}(M(\alpha); \mathfrak{s}) > 1$ . It follows that (for any homotopy representative of  $\gamma(M)$ ) there are two intersection points  $x$  and  $y$  between  $\gamma(M)$  and the line  $L_\alpha$  with the same  $\text{spin}^c$ -grading. This means that  $x$  and  $y$  are intersections of  $L_\alpha$  with  $\gamma(M; \mathfrak{s})$  and that the lifts  $\tilde{x}$  and  $\tilde{y}$  of  $x$  and  $y$  on  $\tilde{\gamma}(M; \mathfrak{s})$

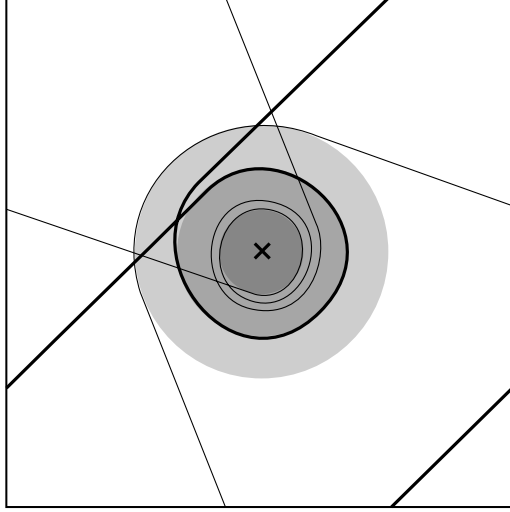


**Figure 22.** Two curves in  $T$  in transverse peg-board position.

in  $\mathbb{R}^2 \setminus \mathbb{Z}^2$  lie on the same lift of  $L_\alpha$ . If  $\tilde{\gamma}(M; \mathfrak{s})$  contains more than one curve then  $S^{\text{sing}}(M) = \hat{\mathbb{R}}$  by definition and  $\alpha \in S_{\mathbb{Q}}^{\text{sing}}(M)$ , so suppose that  $\tilde{\gamma}(M)$  contains a single curve. The intersection points  $\tilde{x}$  and  $\tilde{y}$  exist for any homotopy representative of  $\tilde{\gamma}(M)$  (in particular the peg-board representatives for arbitrarily small  $\epsilon$ ) and since  $L_\alpha$  can be taken to be some finite distance away from every peg, we can in fact take  $\tilde{x}$  and  $\tilde{y}$  to be intersections of the singular peg-board representative for  $\tilde{\gamma}(M)$  with a lift of  $L_\alpha$ . Note that the corners of the singular representative for  $\tilde{\gamma}(M)$  can be smoothed without affecting intersections with  $L_\alpha$  and that  $S^{\text{sing}}(M)$  is precisely the set of tangent slopes after this smoothing. By the (extended) mean value theorem, there is a point on the smoothing of the singular representative of  $\tilde{\gamma}(M)$  for which the tangent line has slope  $\alpha$ . We conclude that  $\alpha \in S_{\mathbb{Q}}^{\text{sing}}(M)$  as claimed. We have proved that  $\mathcal{L}_M^c \subset S_{\mathbb{Q}}^{\text{sing}}(M)$ ; in fact, since  $S_{\mathbb{Q}}^{\text{sing}}(M)$  is closed (as a subset of  $\hat{\mathbb{Q}}$ ), we have  $\overline{\mathcal{L}_M^c} = (\mathcal{L}_M^\circ)^c \subset S_{\mathbb{Q}}^{\text{sing}}(M)$ .

Conversely consider a slope  $\alpha$  in  $S_{\mathbb{Q}}^{\text{sing}}(M) = S^{\text{sing}}(M) \cap \hat{\mathbb{Q}}$ . We will work with the singular peg-board representative of  $\tilde{\gamma}(M)$ . If  $S^{\text{sing}}(M) = \{\alpha\}$ , then  $\alpha$  is the rational longitude of  $M$  and thus not an L-space slope. Otherwise,  $\alpha$  is in the interval of tangent slopes determined by some corner  $c$ ; let  $s_1$  and  $s_2$  denote the two line segments meeting at  $c$ . First suppose  $\alpha$  is in the interior of the interval for the corner  $c$ . Let  $L_\alpha$  be the line of slope  $\alpha$  through  $c$ ; since  $L_\alpha$  is a tangent line,  $s_1$  and  $s_2$  both lie on one side of line  $L_\alpha$ . Let  $L'_\alpha$  be a small pushoff of  $L_\alpha$  that intersects the segments  $s_1$  and  $s_2$  and is disjoint from all lattice points. For sufficiently small  $\epsilon$  (smaller than the minimum distance between  $L'_\alpha$  and any lattice point), replacing the singular representative for  $\gamma(M)$  with the radius  $\epsilon$  peg-board representative preserves these two intersection points. These points give two generators with the same  $\text{spin}^c$  grading in the intersection Floer chain complex of  $\gamma(M)$  with  $L'$ . Since both  $L'_\alpha$  and  $\gamma(M)$  are peg-board representatives relative to the radius  $\epsilon$  and they have transverse intersection, they are in minimal position and both generators survive in homology. It follows that  $M(\alpha)$  is not an L-space, that is,  $\alpha \notin \mathcal{L}_M$ . Now suppose  $\alpha$  is a boundary of the interval of slopes determined by the corner  $c$ ; there are slopes arbitrarily close to  $\alpha$  in the interior of this interval, and these slopes are not in  $\mathcal{L}_M$ , so  $\alpha \notin \mathcal{L}_M^\circ$ .  $\square$

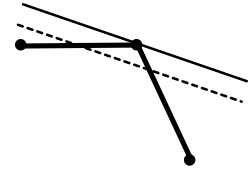


**Figure 23.** Intersection points for a slope in  $S^{\text{sing}}(M)$ .

Theorem 27 is in fact true for arbitrary immersed curves in  $T$  (using an appropriate definition of the set of L-space slopes for a curve), not just for the collections of curves associated to loop type

manifolds. For curves arising from loop type manifolds, however, we can replace  $S^{sing}(M)$  with  $S(M)$ . To prove this, we first make the following observation about Floer simple manifolds:

**Lemma 28.** *If  $M$  is Floer simple, then  $S(M) \neq \hat{\mathbb{R}}$ .*

*Proof.* If  $M$  is Floer simple, then by [9, Proposition 6]  $M$  has simple loop type, that is, for some parametrization  $(\alpha, \beta)$  of  $\partial M$ ,  $\widehat{CFD}(M, \alpha, \beta)$  is a collection of loops (one for each  $Spin^c$  structure on  $M$ ) consisting only of  $\rho_1$ ,  $\rho_3$  and  $\rho_{23}$  arrows. It follows that the corresponding curves in the plane travel only up and right. Clearly  $S(M)$  contains only positive slopes (relative to the chosen parametrization), and so  $S(M) \neq \hat{\mathbb{R}}$ . Note that reparametrizing the boundary changes this interval but does not change whether or not it is all of  $\hat{\mathbb{R}}$ .  $\square$

**Corollary 29.** *For any loop type manifold  $M$ ,  $S(M) = S^{sing}(M)$ .*

*Proof.* In the absence of peg-wrapping  $S(M) = S^{sing}(M)$ . If there is peg-wrapping, then  $S(M) = \hat{\mathbb{R}}$ , and by Lemma 28,  $M$  is not Floer simple. It follows that  $\mathcal{L}_M^\circ = \emptyset$ , and by Theorem 27  $S^{sing}(M) = \hat{\mathbb{R}}$ .  $\square$

Taken together, this completes the proof of Theorem 4.

**Corollary 30.** *With respect to the coordinates above, the pegboard diagram for  $\tilde{\gamma}(M, \mathfrak{s})$  is a graph of the form  $y = f(x)$ .*

*Proof.* Consider the vertical line  $L_c$  given by the equation  $x = c$ , where  $c$  is chosen so that  $L_c$  does not pass through any pegs. Since both  $L_c$  and  $\tilde{\gamma}(M, \mathfrak{s})$  are pulled tight, they are in minimal position. Since  $M(\alpha)$  is an L-space,  $L_c \cap \tilde{\gamma}(M, \mathfrak{s})$  contains a single point. It follows that  $\tilde{\gamma}(M, \mathfrak{s})$  is a graph, except possibly for some vertical segments joining lattice points. If such a segment exists, then  $\alpha \in S^{sing}(M)$ , which contradicts  $\alpha \in \mathcal{L}_M^\circ$ .  $\square$

**4.2. L-space slopes and torsion.** As an application, we give a short proof of Theorem 1 of [30], which characterizes the set  $\mathcal{L}(M)$  in terms of the Turaev torsion of  $M$ . Suppose  $\alpha \in \mathcal{L}_M^\circ$ , and identify  $H^1(\partial M; \mathbb{R})$  with  $\mathbb{R}^2$  by the map  $\beta \mapsto (\beta \cdot \alpha, \beta \cdot l)$ , where  $l$  is the rational homological longitude. For  $\mathfrak{s} \in Spin^c(M)$ , we let  $S^{sing}(M, \mathfrak{s})$  be the set of slopes in a singular peg-board diagram of  $\tilde{\gamma}(M, \mathfrak{s})$ . Clearly

$$S^{sing}(M) = \bigcup_{\mathfrak{s} \in Spin^c(M)} S^{sing}(M, \mathfrak{s}).$$

If  $M$  is Floer simple, Corollary 30 implies that  $\tilde{\gamma}(M, \mathfrak{s})$  is an embedded curve which divides the plane into two connected components. One of these components contains all points  $h \in H_1(M, \mathbb{R})$  with  $h \cdot l \ll 0$  and the other contains all points with  $h \cdot l \gg 0$ . We call points in the first component *black*, and those in the second component *white*. Equivalently, if we identify pegs with relative  $Spin^c$  structures, as in Section 2.9, black pegs have  $n_{\bar{\mathfrak{s}}} = 0$ , while white pegs have  $n_{\bar{\mathfrak{s}}} = 1$ .

If  $\mathbf{p}$  and  $\mathbf{q}$  are two distinct pegs, let  $[\mathbf{p} - \mathbf{q}] \in \hat{\mathbb{R}}$  be the slope of the line joining them. We define

$$X_{\mathfrak{s}} = \{[\mathbf{p} - \mathbf{q}] \mid \mathbf{p} \text{ is black, } \mathbf{q} \text{ is white and } (\mathbf{p} - \mathbf{q}) \cdot l \geq 0\}$$

to be the set of slopes of lines joining a black peg to a white peg which is no higher than it is.

**Proposition 31.** *Suppose  $M$  is Floer simple and not solid-torus-like, and let  $\alpha \in \mathcal{L}(M)$ . Then  $S^{sing}(M, \mathfrak{s})$  is the smallest interval in  $\hat{\mathbb{R}} \setminus \{\alpha\}$  which contains the set  $X_{\mathfrak{s}}$ .*

*Proof.* The set  $S^{sing}(M, \mathfrak{s})$  is an interval which does not contain  $\alpha$ . We first show that  $X_{\mathfrak{s}} \subset S^{sing}(M, \mathfrak{s})$ . Suppose that  $\mathbf{p}$  is a black peg,  $\mathbf{q}$  is a white peg, and that  $(\mathbf{p} - \mathbf{q}) \cdot l > 0$ . Let  $\gamma$  be a curve representing  $\tilde{\gamma}(M, \mathfrak{s})$ , and consider the ray from  $\mathbf{p}$  to  $\mathbf{q}$ . Since  $\mathbf{p}$  is black and  $\mathbf{q}$  is white, there

must be some point  $x$  on the segment from  $\mathbf{p}$  to  $\mathbf{q}$  which lies on  $\gamma$ . The ray from  $\mathbf{p}$  to  $\mathbf{q}$  points down, so it must eventually reenter the black region. Thus there is some other point  $y$  on the ray past  $\mathbf{q}$  which lies on  $\gamma$ . Applying the (extended) mean value theorem to  $x$  and  $y$ , we see that  $[\mathbf{p} - \mathbf{q}] \in S(\gamma)$ . It follows that  $[\mathbf{p} - \mathbf{q}] \in S^{sing}(M, \mathfrak{s})$ .

To show that  $S^{sing}(M, \mathfrak{s})$  is the smallest interval containing  $X_{\mathfrak{s}}$ , it suffices to show that the endpoints of  $S^{sing}(M, \mathfrak{s})$  lie in  $X_{\mathfrak{s}}$ . If  $M$  is not solid-torus-like, then  $S^{sing}(M, \mathfrak{s})$  is a union of intervals whose endpoints are slopes of the pegboard diagram for  $\tilde{\gamma}(M, \mathfrak{s})$ . Thus its endpoints are slopes of the pegboard diagram.

We now identify  $H_1(\partial M, \mathbb{R})$  with  $\mathbb{R}^2$  via the map  $\beta \rightarrow (\beta \cdot \alpha, \beta \cdot l)$ . By Corollary 30, the pegboard diagram is the graph of a piecewise linear curve  $y = f(x)$  in this coordinate system. The slope  $\alpha$  corresponds to a vertical line, which has infinite slope. Thus the endpoints of  $S^{sing}(M, \mathfrak{s})$  will be the maximum and minimum values of  $f'(x)$ .

At each corner of the graph, either the curve is concave up ( $f''(x) \geq 0$ ), and the curve lies just below a white peg, or the curve is concave down ( $f''(x) \leq 0$ ) and the curve lies just above a black peg. Clearly the maximal value of the slope  $f'(x)$  is attained on an interval where we transition from having  $f''(x) \geq 0$  to having  $f''(x) \leq 0$ . The left endpoint of the corresponding segment lies below a white peg, while the right endpoint is above a black peg. Thus the slope is an element of  $X_{\mathfrak{s}}$ . Similarly, the minimal value of the slope must occur on a segment where the left endpoint lies above a black peg, and the right endpoint lies above a white one. This slope is also in  $X_{\mathfrak{s}}$ .  $\square$

In [30],  $\mathcal{L}(M)$  was characterized in terms of the set

$$D^\tau(M) = \{\bar{\mathfrak{s}}_0 - \bar{\mathfrak{s}}_1 \mid \bar{\mathfrak{s}}_0, \bar{\mathfrak{s}}_1 \in Spin^c(M, \partial M), \tau(M, \bar{\mathfrak{s}}_i) = i, (\bar{\mathfrak{s}}_0 - \bar{\mathfrak{s}}_1) \cdot [\Sigma] \geq 0\} \subset H_1(M)$$

where  $\Sigma \in H_2(M, \partial M)$  satisfies  $\partial \Sigma = nl$  with  $n > 0$ . Let  $j_* : H_1(\partial M) \rightarrow H_1(M)$  be the inclusion, and denote by  $[j_*^{-1}(D^\tau(M))] \subset Sl(\partial M)$  the projectivization of the set  $j_*^{-1}(D^\tau(M))$ .

**Lemma 32.**  $[j_*^{-1}(D^\tau(M))] = \bigcup_{\mathfrak{s} \in Spin^c(M)} X_{\mathfrak{s}}$ .

*Proof.* If  $\bar{\mathfrak{s}}_0, \bar{\mathfrak{s}}_1 \in Spin^c(M, \partial M)$ , then  $\bar{\mathfrak{s}}_0 - \bar{\mathfrak{s}}_1 \in \text{im } j_*$  if and only if  $\bar{\mathfrak{s}}_0$  and  $\bar{\mathfrak{s}}_1$  induce the same  $Spin^c$  structure  $\mathfrak{s} \in Spin^c(M)$ . If this is the case, then  $j_*^{-1}(\bar{\mathfrak{s}}_0 - \bar{\mathfrak{s}}_1)$  is the set of differences of the form  $\mathbf{p}_0 - \mathbf{p}_1$ , where  $\mathbf{p}_i$  is a lattice point in  $H_1(\partial M, \mathbb{R})$  whose image in  $\bar{T} = H_1(M, \mathbb{R}) / \ker j_*$  is  $z_{\bar{\mathfrak{s}}_i}$ . The condition that  $\tau(M, \bar{\mathfrak{s}}_i) = i$  is equivalent to saying that  $n_{\bar{\mathfrak{s}}_i} = i$  in other words, that  $\mathbf{p}_0$  is black and  $\mathbf{p}_1$  is white. Finally, the condition that  $(\bar{\mathfrak{s}}_0 - \bar{\mathfrak{s}}_1) \cdot [\Sigma] \geq 0$  is equivalent to saying that  $(\mathbf{p}_0 - \mathbf{p}_1) \cdot l \geq 0$ .  $\square$

Combining Proposition 31 with Lemma 32, we arrive at

**Theorem 33.** (Theorem 1 of [30]) *Suppose  $M$  is Floer simple and not solid torus like, and that  $\alpha \in \mathcal{L}^\circ(M)$ . Then  $\mathcal{L}^\circ(M)$  is the largest interval of  $Sl(\partial M)$  which contains  $\alpha$  and does not contain any element of  $[j_*^{-1}(D^\tau(M))]$ .*

**4.3. A gluing result for L-spaces.** We now turn to the proof of Theorem 5. In previous works [10, 30, 9] the authors and S. Rasmussen prove this L-space gluing criterion when the manifolds have simple loop type. Using the immersed curves pairing theorem for bordered Floer homology, we now give an elegant reproof of this gluing theorem and in fact generalize it to all loop type manifolds.

*Proof of Theorem 5.* By the pairing theorem,  $M_0 \cup_h M_1$  is equivalent to the intersection Floer homology of  $\gamma_0 = \gamma(M_0)$  and  $\gamma_1 = \bar{h}(\gamma(M_1))$ . Suppose first that  $M_0 \cup_h M_1$  is not an L-space, implying that there is some  $\mathfrak{s}$  so that  $\dim \widehat{HF}(M_0 \cup_h M_1, \mathfrak{s}) > 1$ . In other words, there are two intersection points  $x$  and  $y$  between  $\gamma_0$  and  $\gamma_1$  with the same  $spin^c$  grading. This means, in particular, that  $x$

and  $y$  are intersection points of  $\gamma_{0, \mathfrak{s}_0} = \gamma(M_0; \mathfrak{s}_0)$  and  $\gamma_{1, \mathfrak{s}_1} = \bar{h}(\gamma(M_1; \mathfrak{s}_1))$  for some  $\mathfrak{s}_0 \in \text{Spin}^c(M_0)$  and  $\mathfrak{s}_1 \in \text{Spin}^c(M_1)$ . We will assume for  $i \in \{0, 1\}$  that  $\gamma_{i, \mathfrak{s}_i}$  contains only one curve, since otherwise  $\mathcal{L}_{M_i}^\circ$  is empty and  $\mathcal{L}_{M_0}^\circ \cup h(\mathcal{L}_{M_1}^\circ) \neq \hat{\mathbb{Q}}$ . Let  $c_0$  be the path from  $x$  to  $y$  in  $\gamma_{0, \mathfrak{s}_0}$  and let  $c_1$  be the path from  $x$  to  $y$  in  $\gamma_{1, \mathfrak{s}_1}$ . The fact that  $x$  and  $y$  have the same  $\text{spin}^c$  grading implies that  $[c_0 - c_1] = 0 \in H_1(T)$ , or equivalently that the paths lift to form a bigon in  $\mathbb{R}^2$ , the corners of which are lifts  $\tilde{x}$  and  $\tilde{y}$  of  $x$  and  $y$ . Let  $\alpha$  be the slope of the line segment connecting  $\tilde{x}$  and  $\tilde{y}$ . By the (extended) mean value theorem,  $\tilde{c}_0$  and  $\tilde{c}_1$  each contain a point with slope  $\alpha$ .

This argument applies for any homotopy representative of  $\gamma_0$  and  $\gamma_1$ . In particular, if we take peg-board representatives relative to some peg radius  $\frac{1}{n}$  we find a slope  $\alpha_n$  that is a tangent slope to both curves. It follows that  $\alpha_n \in S_{\frac{1}{n}}(M_0) \cap h(S_{\frac{1}{n}}(M_1))$ . Here, by abuse of notation,  $h$  refers to the map on slopes induced by  $h$ ; note that, as maps on slopes,  $\bar{h}$  and  $h$  agree since the elliptic involution preserves slopes. Since  $S_{\frac{1}{n}}(M_0) \cap h(S_{\frac{1}{n}}(M_1))$  for positive integers  $n$  gives a nested sequence of nonempty closed sets there is some slope  $\alpha$  in the total intersection, which is simply  $S(M_0) \cap h(S(M_1))$ . Moreover, we can take this  $\alpha$  to be rational, since  $S(M_0)$  and  $h(S(M_1))$  have rational endpoints. By Theorem 27 and Corollary 29,  $S_{\mathbb{Q}}(M_0) = (\mathcal{L}_{M_0}^\circ)^c$  and  $S_{\mathbb{Q}}(M_1) = (\mathcal{L}_{M_1}^\circ)^c$ . Thus  $\alpha$  is not in  $\mathcal{L}_{M_0}^\circ \cup h(\mathcal{L}_{M_1}^\circ)$ .

Conversely, suppose that there is a slope  $\alpha$  not in  $\mathcal{L}_{M_0}^\circ \cup h(\mathcal{L}_{M_1}^\circ)$ . Equivalently,  $\alpha$  is in both  $S_{\mathbb{Q}}^{\text{sing}}(M_0)$  and  $h(S_{\mathbb{Q}}^{\text{sing}}(M_1))$ , so  $\alpha$  is a tangent slope of both  $\gamma_0$  and  $\gamma_1$  in a singular peg-board diagram. Let  $c_0$  and  $c_1$  be components of  $\gamma_0$  and  $\gamma_1$ , respectively, for which  $\alpha$  is a tangent slope to the singular peg-board representative. We may assume that  $c_0$  and  $c_1$  are not solid torus like components. If, for example,  $c_0$  were solid torus like then  $\alpha$  would be the rational longitude of  $M_0$  and every component of  $\gamma_0$  would have a tangent line of slope  $\alpha$ ; we could then replace  $c_0$  by another component, at least one of which is not solid torus like because  $M_0$  is not solid torus like. By reparametrizing  $\partial M_0$  and  $\partial M_1$ , we may assume that  $\alpha = 0$ .

Fixing a small peg radius  $\epsilon$ , consider transverse peg-board representatives of  $c_0$  and  $c_1$  with a chosen orientation on each curve. Since  $c_0$  and  $c_1$  are in minimal position, to show that  $M_0 \cup_h M_1$  is not an L-space it is enough to find two intersection points between  $c_0$  and  $c_1$  with the same  $\mathbb{Z}/2\mathbb{Z}$ -grading. It is easy to find two such generators if both curves have peg-wrapping. In this case the curves  $c_0$  and  $c_1$  contain complete circles of radius  $\epsilon_0$  and  $\epsilon_1$  around the puncture, with  $\epsilon_0 \neq \epsilon_1$ . Suppose, without loss of generality, that  $\epsilon_0 < \epsilon_1$ . Then  $c_0$  also contains two line segments tangent at their ends to the circle of radius  $\epsilon_0$ , one oriented toward the circle and one oriented away from it. These two segments clearly intersect the oriented circle of radius  $\epsilon_1$  with opposite sign, and the two corresponding generators of  $HF(\gamma_0, \gamma_1)$  have opposite  $\mathbb{Z}/2\mathbb{Z}$  grading. Thus we may assume that there is no peg-wrapping in  $c_0$ .

In the singular peg-board diagram for  $c_0$ , the line segments connecting corners can be classified as moving upwards, downwards, or horizontally (once we have fixed an orientation on  $c_0$ ). The segments can not be all upward or all downward, since then  $\alpha = 0$  would not be a tangent slope. If the slopes are not all horizontal, we can choose a corner so that the segments preceding and following the corner are up and down, up and horizontal, or horizontal and down. Note that the corresponding corner in a radius  $\epsilon$  peg-board diagram for  $c_0$  has a point of horizontal tangency on the top side of the peg, at the point  $(0, \epsilon)$ . If every line segment in  $c_0$  is horizontal, then every corner has horizontal tangency to the peg, and we can choose the corner so that this point of tangency is on the top side of the peg. Moving away from this point of tangency in either direction,  $c_0$  moves either horizontally or downwards. If it moves horizontally it wraps once around the torus and returns to the peg at another horizontal tangency on the top of the peg; after some number of horizontal segments like this,  $c_0$  must move downwards. Thus,  $c_0$  contains an upward moving piece  $c_0^I$  oriented toward the point  $(0, \epsilon)$  and a downward moving piece  $c_0^O$  oriented away from  $(0, \epsilon)$ , as in Figure 24(a). Note that  $c_0$  may traverse any number of horizontal segments between  $c_0^I$  and  $c_0^O$ ; we will ignore these horizontal segments. Similarly, we can choose a corner of  $c_1$  such that the preceding segment in a the singular peg-board diagram moves downward or horizontally and the following segment moves horizontally or upward, and such that in a radius  $\epsilon$  peg-board diagram there is a horizontal tangency to the peg

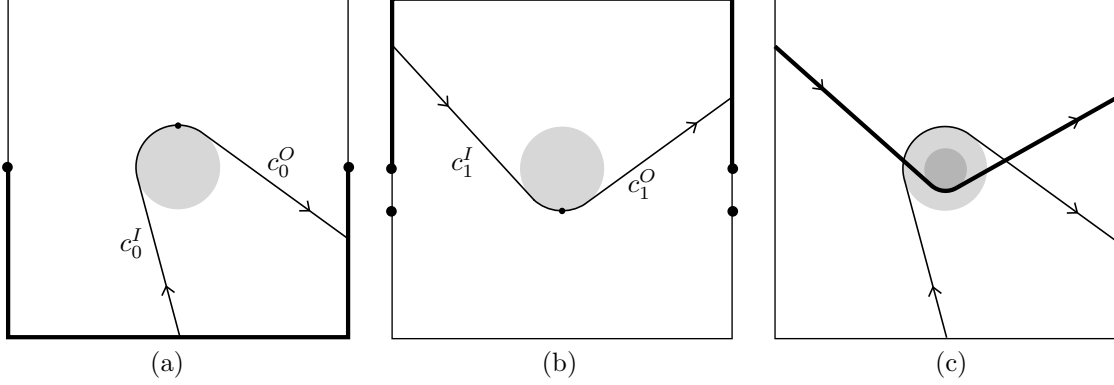


**Figure 24.** (a) The segments  $c_0^I$  and  $c_0^O$  in  $c_0$ ; these segments can enter/leave the square anywhere in the bottom half of its boundary. (b) The segments  $c_1^I$  and  $c_1^O$  in  $c_1$ ; these segments can enter/leave the square anywhere in the top half of its boundary or through the points  $(\pm\frac{1}{2}, -\epsilon)$ . (c) A transverse peg-board diagram for  $c_0^I \cup c_0^O$  and  $c_1^I \cup c_1^O$ .

at  $(0, -\epsilon)$ . Let  $c_1^I$  be the horizontal or downward piece of  $c_1$  oriented toward  $(0, -\epsilon)$  and let  $c_1^O$  be the horizontal or upward piece oriented away from  $(0, -\epsilon)$ , as in Figure 24(b). Note that we ignore any full wraps around the peg between  $c_1^I$  and  $c_1^O$ . We consider these curves in one fundamental domain of  $T$ , the square  $[-\frac{1}{2}, \frac{1}{2}] \times [-\frac{1}{2}, \frac{1}{2}]$ . The intersection of  $c_0^I$  and  $c_0^O$  with the boundary of this square can be any point with non-positive  $y$ -coordinate; the intersection of  $c_1^I$  and  $c_1^O$  with the boundary of this square can have any non-negative  $y$ -coordinate or  $y$ -coordinate  $-\epsilon$ .

We can overlay the portions of  $c_0$  and  $c_1$  described above in a transverse peg-board diagram. We may assume that the corner of  $c_0$  has larger peg radius; since the corner of  $c_1$  passes through  $(0, -\epsilon)$  and the corner of  $c_0$  does not, this is consistent with the partial order on corners. It is clear that if both  $c_0^I$  and  $c_0^O$  intersect the boundary of the square  $[-\frac{1}{2}, \frac{1}{2}] \times [-\frac{1}{2}, \frac{1}{2}]$  with strictly negative  $y$ -value or if both  $c_1^I$  and  $c_1^O$  intersect the boundary of the square with strictly positive  $y$ -value (equivalently, if the corresponding segments in the singular diagram are not horizontal), then there are two intersection points with opposite  $\mathbb{Z}/2\mathbb{Z}$  grading (see Figure 24(c)).

The remaining case is when one of the specified segments in both  $c_0$  and  $c_1$  correspond to horizontal segments in a singular diagram. We consider the case that  $c_0^O$  and  $c_1^O$  are both horizontal moving to the right (see Figure 25); cases when the incoming segments or both segments are horizontal are similar. In this case, we do not get two intersection points of  $c_0^I \cup c_0^O$  and  $c_1^I \cup c_1^O$  if we restrict to one fundamental domain of  $T$ . However,  $c_0^O$  and  $c_1^O$  both wrap once around  $T$  horizontally, leading to new corners of  $c_0$  and  $c_1$ , respectively. In the transverse peg-board diagram, let  $\epsilon_1$  and  $\epsilon_2$  be the peg radii associated with these two corners. If  $\epsilon_2 < \epsilon_1$ , then  $c_0^O$  intersects  $c_1^I$  before reaching the next corner (Figure 25(a)). If  $\epsilon_1 > \epsilon_2$ , then  $c_1$  must not have peg-wrapping at this corner. It follows that  $c_1$  must continue by leaving the peg horizontally or upwards. If it leaves the peg moving upwards, it will intersect with  $c_0^I \cup c_0^O$  (Figure 25(b)). If it leaves the peg horizontally, it wraps around  $T$  once more to a new corner with some radius  $\epsilon_3$ , and we repeat the argument using this corner in place of the corner with radius  $\epsilon_2$ . In either case, we find two intersection points between  $c_0$  and  $c_1$  with the opposite sign, as desired.  $\square$

**4.4. Toroidal integer homology spheres.** Theorem 5 allows us to generalize a result of Hedden and Levine subject to the loop-type assumption.

**Theorem 6.** *If  $Y \cong M_0 \cup M_1$  is a integer homology sphere  $L$ -space, and both  $M_0$  and  $M_1$  are loop-type manifolds, then at least one of  $M_0$  or  $M_1$  is boundary compressible.*

*Proof.* We will parametrize the slopes on  $\partial M_0$  and  $\partial M_1$  so that 0 is the slope of the rational longitude on each side, and such that the slope  $r$  glues to the slope  $1/r$ . Note that since  $Y$  is an

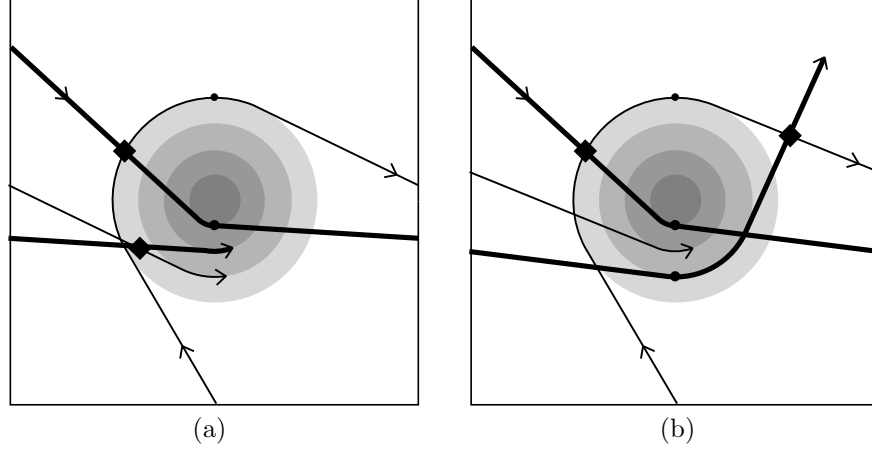


**Figure 25.** A transverse peg-board diagram for  $c_0^I \cup c_0^O$  and  $c_1^I \cup c_1^O$  when  $c_0^O$  and  $c_1^O$  both correspond to horizontal segments in singular diagrams for  $c_0$  and  $c_1$ . There are two cases, depending on the partial order on corners; in either case there are two intersection points between  $c_0$  and  $c_1$  with opposite sign.

integer homology sphere,  $M_0(\infty)$  and  $M_1(\infty)$  must be integer homology spheres. Hedden and Levine prove the conjecture in the case that  $M_0(\infty)$  and  $M_1(\infty)$  are L-space integer homology spheres [11]. As a simple corollary to Theorem 5, the conjecture holds without this assumption if  $M_0$  and  $M_1$  are loop type.

Since  $Y$  is an L-space and  $0 \notin \mathcal{L}^\circ(M_0)$ , Theorem 5 implies that  $\infty \in \mathcal{L}^\circ(M_1)$ . Similarly since  $0 \notin \mathcal{L}^\circ(M_1)$ ,  $\infty \in \mathcal{L}^\circ(M_0)$ . (Note that this reduces the problem immediately to the case treated by Hedden and Levine.) Now since  $M_0$  and  $M_1$  are complements of knots in integer homology sphere L-spaces, we can use that  $\mathcal{L}(M_i)$  is either  $\{\infty\}$ ,  $[2g_i - 1, \infty]$  or  $[-\infty, -2g_i + 1]$  if the knots are nontrivial, where  $g_i$  is the genus of the knot associated to  $M_i$  [18]. In particular,  $1 \notin \mathcal{L}^\circ(M_0)$  and  $1 \notin \mathcal{L}^\circ(M_1)$ , and thus by Theorem 5  $Y$  is not an L-space, unless  $M_0$  or  $M_1$  are boundary compressible.  $\square$

**4.5. A dimension inequality for pinches.** We now turn to another gluing result, which gives a rank inequality for gluing along torus boundary. Consider the following construction. Let  $Y$  be a rational homology sphere of the form  $M_0 \cup_h M_1$ , so that each  $M_i$  is a rational homology solid torus. Denote by  $\lambda_i$  the rational longitude in each  $\partial M_i$ ; recall that this slope is characterized by the property that some number of like oriented copies of  $\lambda_i$  bounds a properly embedded surface in  $M_i$ . The Dehn surgery  $Y' = M_0(h(\lambda_1))$  is the result of pinching  $M_1$  in  $Y$ . Note that  $h(\lambda_1)$  is a well defined slope in  $\partial M_1$ ; this operation is symmetric in  $i = 0, 1$ . In certain settings there is an associated degree  $n$  map  $Y \rightarrow Y'$ , where  $n$  is the order of  $i_*([\lambda_1])$  in  $H_1(M_1)$ . In particular, when both  $M_0$  and  $M_1$  are integer homology spheres, there is always a degree one map associated with the pinch.

**Theorem 7.** *Given a rational homology sphere  $Y = M_0 \cup_h M_1$ , where  $M_0$  and  $M_1$  are loop-type rational homology solid tori, there is an inequality*

$$\dim \widehat{HF}(Y) \geq nm \dim \widehat{HF}(Y')$$

where  $Y' = M_0(h(\lambda_1))$ ,  $n$  is the order of  $i_*([\lambda_1])$  in  $H_1(M_1)$ , and  $m = |\text{Spin}^c(M_1)| = |H_1(M_1, \partial M_1)|$ .

*Proof.* Let  $\gamma_0$  and  $\gamma_1$  denote the curves  $\gamma(M_0)$  and  $\bar{h}(\gamma(M_1))$ , respectively, in  $T = \partial M_1 \setminus z$ . By the gluing theorem,  $\widehat{HF}(Y)$  is equivalent to the Floer homology  $HF(\gamma_0, \gamma_1)$  and, in particular, the dimension is given by the intersection number  $i^a(\gamma_0, \gamma_1)$ .

Let  $\hat{\gamma}_1$  be the collection of curves obtained from  $\gamma_1$  by deleting any curve components that are nullhomotopic in  $T$  (ignoring the base point) and pulling the remaining curves tight (again, ignoring

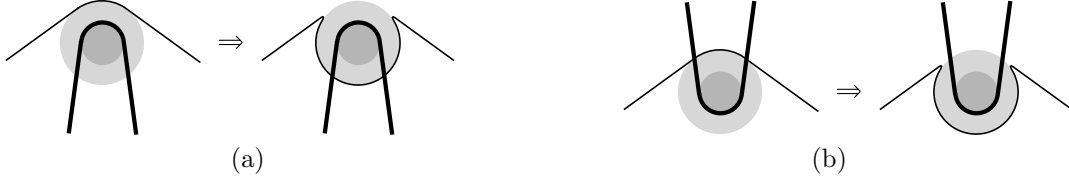


**Figure 26.** Sliding a component of  $\gamma_1$  over a basepoint in  $T$  to produce  $\hat{\gamma}_1$ , as in the proof of Theorem 7: Every instance of (a) adding intersection points is balanced by an instance of (b) removing intersection points.

the base point), that is, replacing them with minimal length representatives of their homotopy class, allowing homotopies that pass the basepoint. Let  $\frac{p}{q}$  be the slope of the curve in  $T$  determined by  $h(\lambda_1)$ , and let  $L_{p,q}$  be the corresponding simple closed curve  $p\alpha_0 + q\beta_0$ .

For each  $\text{spin}^c$ -structure of  $M_1$ ,  $\gamma_1$  contains at least one curve that is homotopic in  $T$  to  $\bar{h}(\lambda_1) = n \cdot L_{p,q}$  along with some number of nullhomotopic curves. It follows that  $\hat{\gamma}_1$  is a collection of at least  $m$  copies of  $n \cdot L_{p,q}$  so that

$$\dim HF(\gamma_0, \hat{\gamma}_1) \geq nm \dim HF(\gamma_0, L_{p,q}) = nm \widehat{HF}(Y').$$

It remains to show that  $\dim HF(\gamma_0, \gamma_1) \geq \dim HF(\gamma_0, \hat{\gamma}_1)$ .

Note that  $\hat{\gamma}_1$  can be obtained from  $\gamma_1$  by a sequence of the following moves: (i) deleting a component; (ii) resolving a self-intersection to split off a closed component; (iii) homotopy in  $T$  to put curves in transverse peg board position with  $\gamma_0$ ; and (iv) passing the curve through a peg at which it changes direction in a transverse peg board diagram. We claim that none of these moves increases the intersection number with  $\gamma_0$ . Indeed, (i) clearly does not increase intersection number, and (ii) does not change the number of intersections with  $\gamma_0$  at all. Further, (iii) does not increase intersection number, since transverse peg board position realizes the minimal intersection for homology classes in  $T$ . It only remains to check that (iv) does not increase intersection number.

Allowing a corner of  $\gamma_1$  to slide over the base point may add new intersection points with  $\gamma_0$ ; this happens exactly when there is a corner of  $\gamma_0$  such that the arc determined by the corner of  $\gamma_0$  is contained in the arc determined by the corner of  $\gamma_1$  (see Figure 26(a)). In this case, as  $\gamma_0$  passes through the relevant corner, it both approaches the peg and leaves the peg on the same side of  $\gamma_1$ , namely on the side that contains the peg. Sliding  $\gamma_1$  across the peg adds two intersections for each such corner. However, this is balanced by the fact that intersection points are removed for other corners of  $\gamma_0$ . If at a given corner  $\gamma_0$  approaches and leaves the peg from the side of  $\gamma_1$  not containing the peg, sliding  $\gamma_1$  over the peg removes two intersection points (see Figure 26(b)). For each corner of  $\gamma_0$  of the first type, there is a corner of the second type; this follows from the fact that if  $\gamma_0$  leaves a corner on one side of  $\gamma_1$ , it approaches the next corner on the opposite side of  $\gamma_1$ . Thus, overall, (iv) does not increase intersection number.  $\square$

**4.6. Satellite L-space knots.** Given a pattern knot  $P$  and a companion knot  $C$ , both in the three-sphere, denote by  $P(C)$  the result of forming a satellite knot (note that this depends on some additional choices). The following is a conjecture of Lidman, Hom, and Vafaee [14, Conjecture 1.7]:

**Conjecture 34.** *If  $P(C)$  is an L-space knot, then  $P$  and  $C$  are L-space knots as well.*

**Theorem 35.** *Restricting to loop-type manifolds, Conjecture 34 is true.*

Before proving this result, we make the restriction in the hypothesis precise. Suppose that  $K$  is an L-space knot with toroidal exterior  $M_K$ , and fix an L-space  $Y = M_K(\alpha)$ . Writing  $Y = M_0 \cup_h M_1$ , our hypothesis requires that  $M_0$  and  $M_1$  be loop-type manifolds. We continue with this notation below.



*Proof of Theorem 35.* Consider the L-space  $Y = M_0 \cup_h M_1$  resulting from surgery on a satellite knot  $K$ . By Theorem 5,  $\mathcal{L}_{M_0}^\circ \cup h(\mathcal{L}_{M_1}^\circ) = \hat{\mathcal{Q}}$  so that the loop-type manifolds  $M_0, M_1$  are, in fact, simple loop type. That is,  $M_0$  is a Floer simple manifold hence the complement of an L-space knot  $C$  in  $S^3$  (the companion knot). Since the Seifert longitude  $\lambda_C$  of  $C$  is not an L-space slope, it must be that  $\lambda_C \in h(\mathcal{L}_{M_1}^\circ)$  so that  $\alpha_P = h^{-1}(\lambda_C)$  gives an L-space  $M_1(\alpha_P)$ .

Now consider the pattern knot  $P$  in  $D^2 \times S^1$ , obtained from  $M_K \setminus M_0$ , where the boundary of  $D^2 \times S^1$  is framed so that  $\alpha_P \simeq \{\text{pt}\} \times S^1$ . Note that filling this manifold along  $\alpha_P$  gives a knot in  $S^3$  (the pattern knot), which we will also denote by  $P$ . Further,  $P$  must be an L-space knot since there is more than one choice  $\alpha$ , which existed by Floer simplicity of  $M_K$  (and was required for the construction of  $Y$ ).  $\square$

There is a converse to this statement which only requires results concerning simple loop-type manifolds from [9]; see Hom [12].

## 5. EXAMPLES

This section discusses various natural families of loop-type manifolds, in an attempt to illustrate just how wide spread the loop-type phenomenon is in practice.

**5.1. Loop-type graph manifolds.** By [9], any manifold with torus boundary and more than one L-space filling is loop type (in fact, it is *simple* loop type). Complements of knots in  $S^3$  provide another family of examples: we will show in Section 7 that the complement of  $K$  is loop type if  $CFK^-(K)$  admits a horizontally and vertically simplified basis. These examples all have at least one L-space filling (the  $S^3$  filling). We now describe a family of graph manifolds with torus boundary which are loop type, and within this family we will produce a loop type manifold with no L-space fillings.

Following [10, Section 6], a (bordered) graph manifold can be constructed from solid tori using three operations. The operations  $\mathcal{E}$  and  $\mathcal{T}$  amount to reparametrizing the boundary; the only topologically significant operation is the *merge* operation  $\mathcal{M}$ , which takes two manifolds with parametrized torus boundary  $M_1$  and  $M_2$  and produces a new manifold  $\mathcal{M}(M_1, M_2)$  by gluing  $M_1$  and  $M_2$  to two boundary components of  $\mathcal{P} \times S^1$ , where  $\mathcal{P}$  is  $S^2$  with three disks removed (the particular gluing is determined by boundary parametrizations on  $\partial M_1$  and  $\partial M_2$ ). The following is a slight reformulation of [10, Lemma 6.5]:

**Lemma 36.** *Suppose  $M_1$  and  $M_2$  are loop type manifolds equipped with boundary parametrizations. The manifold  $\mathcal{M}(M_1, M_2)$  is loop type if for at least one  $i \in \{1, 2\}$ ,  $M_i$  is simple loop type and the slope in  $\partial M_i$  which glues to the fiber slope of  $\mathcal{P} \times S^1$  is in  $\mathcal{L}_{M_i}^\circ$ . If this holds for both  $i$ , then  $\mathcal{M}(M_1, M_2)$  is in fact simple loop type.*

The following is an immediate consequence:

**Proposition 37.** *A graph manifold  $M$  with torus boundary is loop type if every component of the JSJ decomposition contains at most two boundary components.*

*Proof.* We induct on the number of JSJ components. If there is only one, then  $M$  is Seifert fibered with torus boundary and thus simple loop type. Otherwise, let  $N$  be the JSJ component containing  $\partial M$  and let  $M' = M \setminus N$ .  $N$  is Seifert fibered with two boundary components; it can be obtained by gluing a Seifert fibered manifold  $N'$  with one boundary component to  $\mathcal{P} \times S^1$ , gluing fiber slope to fiber slope. Thus  $M$  can be viewed as  $\mathcal{M}(M', N')$ .  $N'$  is simple loop type, the fiber slope is in  $\mathcal{L}_{N'}^\circ$ , and  $M'$  is loop type by induction, so by Lemma 36  $M$  is also loop type.  $\square$

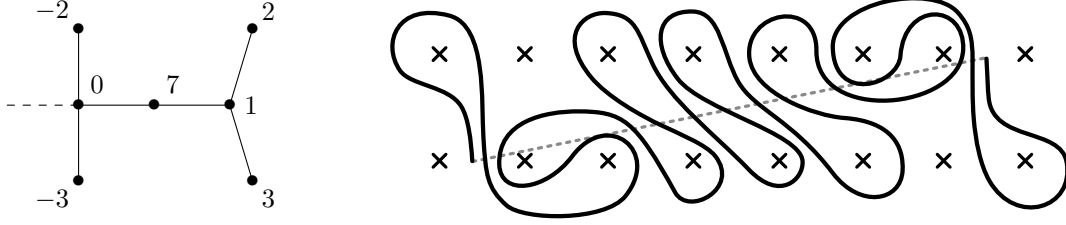


**Figure 27.** The curve  $\tilde{\gamma}(M)$ , where  $M$  is the graph manifold with plumbing tree shown. Note that, relative to the chosen basis, the longitude of  $M$  (dotted line) has slope  $1/6$ .

**5.2. Loop-type integer homology solid tori.** Proposition 37 provides a large family of loop type manifolds, many of which do not have multiple L-space fillings (that is, are not simple loop type). In fact, as the following example demonstrates, many do not have even a single L-space filling.

Let  $M$  be the graph manifold with boundary determined by the plumbing tree in Figure 27.  $M$  has two JSJ pieces, one with two boundary components (counting  $\partial M$ ) and the other with one boundary component. By Proposition 37,  $M$  is loop type. Using the algorithm described in [10], it is not difficult to compute  $\widehat{CFD}(M, \alpha, \beta)$  where  $\alpha$  and  $\beta$  are a fiber and a curve in the base surface, respectively, of the  $S^1$  corresponding to the boundary vertex; the result is a single loop. Using the loop notation of [10], this loop can be represented as follows:

$$(\bar{a}_1 d_2 \bar{e} b_1 c_1 \bar{a}_1 \bar{e} d_1 \bar{b}_1 \bar{e} \bar{a}_1 d_1 \bar{b}_1 \bar{e} \bar{a}_1 d_1 \bar{b}_1 \bar{e} \bar{a}_1 d_1 \bar{e} b_1 c_1 \bar{a}_1 \bar{e} d_2 \bar{b}_1 \bar{d}_1)$$

The corresponding curve  $\tilde{\gamma}(M)$  in the plane is shown in Figure 27. We see that there are no L-space fillings, since for any slope  $\frac{p}{q}$  there is a straight line of slope  $\frac{p}{q}$  which is in minimal position with  $\tilde{\gamma}(M)$  and intersects  $\tilde{\gamma}(M)$  multiple times. (Similar examples of such manifolds are also described in [31]). The fact that there is only one loop in  $\widehat{CFD}(M, \alpha, \beta)$  reflects the fact that in this example  $M$  is an integer homology solid torus. It is not difficult to produce more examples of loop type integer homology spheres with no L-space fillings. For example, an integer homology sphere graph manifold with at most two boundary tori on each JSJ component is loop type by Proposition 37 and if the plumbing tree has the tree in Figure 27 as a subtree it follows from Theorem 5 that there are no L-space fillings.

**5.3. Floer solid tori.** Another interesting class of manifolds are the Heegaard Floer solid tori defined in [32]. A rational homology sphere  $M$  is a Heegaard Floer solid torus if its bordered invariants are preserved by a Dehn twist about the longitude  $\lambda$ —that is, if  $\widehat{CFD}(M, \mu, \lambda) \cong \widehat{CFD}(M, \mu + \lambda, \lambda)$ , where  $\mu$  is any curve dual to  $\lambda$ . For loop type manifolds, this condition has a nice interpretation in terms of the curves  $\gamma(M)$ .

**Proposition 38.** *A loop type rational homology sphere  $M$  is a Heegaard Floer solid torus if and only if  $\gamma(M)$  can be homotoped to lie in a neighborhood of a curve in  $\partial M \setminus z$  representing the longitude  $\lambda$ .*

*Proof.*  $\widehat{CFD}(M, \alpha, \beta)$  is obtained from  $\gamma(M)$  by writing each closed curve in  $\gamma(M)$  in terms of the basis  $\{\alpha, \beta\}$  for  $\pi_1(\partial M \setminus z)$ . So  $\widehat{CFD}(M, \mu, \lambda) \cong \widehat{CFD}(M, \mu + \lambda, \lambda)$  means that  $\gamma(M)$  is the same when written in terms of the basis  $\{\mu, \lambda\}$  or in terms of the basis  $\{\mu + \lambda, \lambda\}$ . In other words,  $\gamma(M)$  is unchanged by a Dehn twist about  $\lambda$ . This happens if and only if  $\gamma(M)$  can be homotoped to be disjoint from a copy of  $\lambda$ . Equivalently, it can be homotoped to lie in small neighborhood of a (different) copy of  $\lambda$ .  $\square$

An example of a Floer homology solid torus is the twisted  $I$ -bundle over the Klein bottle, which we will denote  $N_2$ . The bordered invariants for  $N_2$  and the corresponding curves are shown in Figure

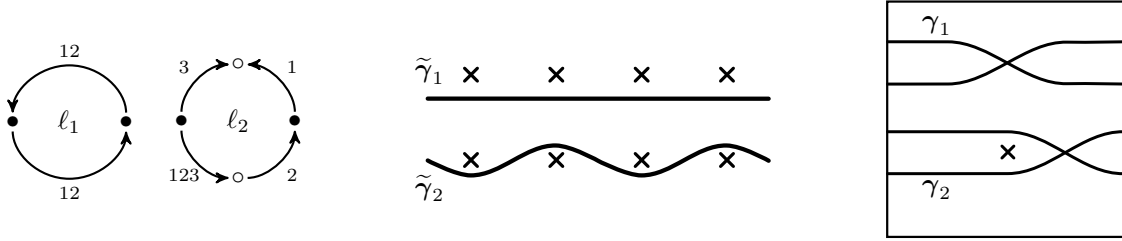


**Figure 28.**  $\widehat{CFD}(N_2, \mu, \lambda)$  consists of two loops,  $\ell_1$  and  $\ell_2$ . Corresponding to these two loops,  $\tilde{\gamma}(N_2)$  contains two curves  $\tilde{\gamma}_1$  and  $\tilde{\gamma}_2$  in  $\mathbb{R}^2 \setminus \mathbb{Z}^2$  and  $\gamma(N_2)$  contains two curves  $\gamma_1$  and  $\gamma_2$  in  $T$ .

28.  $\widehat{CFD}(N_2, \mu, \lambda)$  has two loops, so  $\gamma(N_2)$  has two components; the two components correspond to the two  $\text{spin}^c$  structures on  $N_2$ .

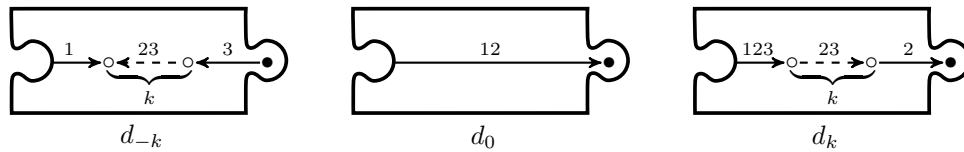
Note that the two components of  $\tilde{\gamma}(M)$  have slightly different behavior.  $\tilde{\gamma}_1$  is isotopic to a straight line in the complement of the lattice points; in contrast,  $\tilde{\gamma}_2$  can not be made straight but can be isotoped arbitrarily close to a straight line which passes through lattice points, weaving through the lattice points on this line. For any Floer homology solid torus  $M$ , the components of  $\tilde{\gamma}(M)$  have one of these two types. Components of the first type are solid torus like; the corresponding loops in  $\widehat{CFD}(M, \mu, \lambda)$  consist only of  $\rho_{12}$  arrows.

**Proposition 39.** *If  $M$  is a manifold with torus boundary and  $M$  has only one non L-space slope, then  $M$  is a Heegaard Floer solid torus. Conversely, for a Heegaard Floer solid torus either every slope but the rational longitude is an L-space slope or there are no L-space slopes.*

*Proof.* If  $M$  has only one non L-space slope, then  $M$  is simple loop type (in particular loop type). By Theorem 27 the set of tangent slopes  $S(M)$  contains the single slope  $\lambda$ ; it follows that  $\gamma$  can be isotoped arbitrarily close to a straight line representative for  $\lambda$  and  $M$  is a Heegaard Floer solid torus. On the other hand, if  $M$  is a Heegaard Floer solid torus with at least one L-space slope  $p\mu + q\lambda$ , the slope  $p\mu + (p+q)\lambda$  is also an L-space filling. Since there are at least two L-space fillings,  $M$  is (simple) loop type. Since each component of  $\tilde{\gamma}(M)$  weaves through the pegs on a straight line representing  $\lambda$  it is easy to see that  $S(M) = \{\lambda\}$  and  $\lambda$  is the only non L-space slope.  $\square$

**5.4. Surface bundles.** Other interesting examples of loop-type manifolds are given by products of once-punctured surfaces with  $S^1$ . Let  $S_{g,1}$  denote the surface of genus  $g$  with one boundary component, and let  $M_g$  denote  $S_{g,1} \times S^1$ . To parametrize the boundary  $\partial M_g = T^2$ , let  $\mu$  be a fiber  $\{p\} \times S^1$  for  $p \in \partial S_{g,1}$  and let  $\lambda$  be  $\partial S_{g,1} \times \{q\}$  for  $q \in S^1$ . We will compute  $\widehat{CFD}(M_g, \mu, \lambda)$ .

To state an explicit result, we briefly review some notation for loops from [10]. Breaking a loop along  $\bullet$ -vertices creates segments of certain types, and we record a loop as a cyclic word in letters representing these segments. For the present example, we only need the following types of segments:



Reading a loop with a fixed orientation, these segments may appear forward or backwards; we use a bar to denote backward oriented segments. For a loop with only type  $d$  segments, the orientations of each segment must agree, as indicated by the puzzle piece shapes above. For example, the cyclic words  $(d_1 d_2 d_3)$  and  $(\bar{d}_3 \bar{d}_2 \bar{d}_1)$  represent the same loop, read with different orientations. Either cyclic word suffices to define the loop, but recall that by the convention described in Section 2.4 fixing an orientation of the loop is equivalent to fixing the  $\mathbb{Z}/2\mathbb{Z}$  grading. To keep track of this grading

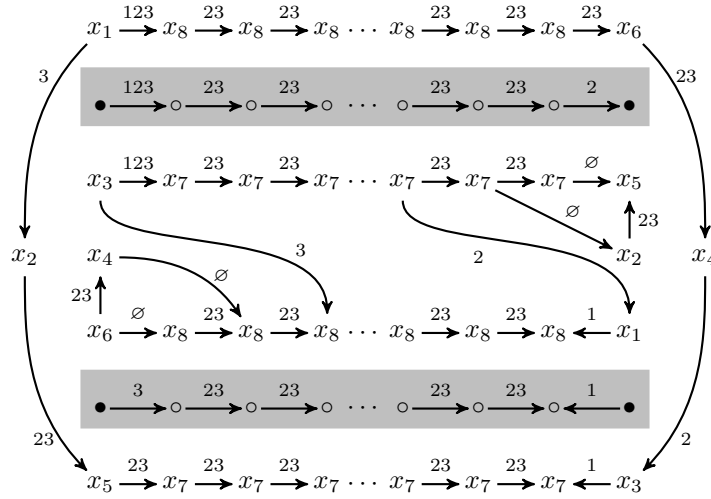
information, we will denote  $\widehat{CFD}$  by a collection of these cyclic words representing *oriented* loops. Recall that since the  $\mathbb{Z}/2\mathbb{Z}$  grading is only a relative grading in each  $\text{spin}^c$  structure, only the relative orientations among loops in the same  $\text{spin}^c$  structure are well defined. In the following example, all loops are in the same  $\text{spin}^c$  structure, so the relative orientations are meaningful.

**Theorem 40.** *For  $g \geq 0$ ,  $M_g$  is a loop-type manifold, with bordered invariants consisting of loop-components of the form  $d_0$  and  $d_{2i}d_{-2i}$  for  $0 \leq i \leq g$ . Specifically, when  $g = 0$ ,  $\widehat{CFD}(M_g, \mu, \lambda)$  consists of a single loop ( $d_0$ ) and, when  $g > 0$ , this invariant has  $2^g$  components of type  $(d_0)$ ,  $\frac{1}{2}\binom{2g}{g} - 2^{g-1}$  components of type  $(d_0d_0)$ , and  $\binom{2g}{g+i}$  components of type  $(d_{2i}d_{-2i})$  for  $1 \leq i \leq g$ , with the orientation of each  $(d_{2i}d_{-2i})$  component reversed if  $i$  is odd.*

*Proof.* The case when  $g = 0$  is immediate. To establish the result for positive genus we will induct on  $g$ , making use of the type DA bimodule  $\mathcal{G}$  described in [8, Section 5]. This has the property  $\widehat{CFD}(M_{g+1}, \mu, \lambda) \cong \mathcal{G} \boxtimes \widehat{CFD}(M_g, \mu, \lambda)$ , and can be explicitly calculated to show that  $\mathcal{G} \cong \mathcal{G}_1 \oplus \mathcal{G}_2 \oplus \mathcal{G}_3$  where both  $\mathcal{G}_2$  and  $\mathcal{G}_3$  are the identity bimodule. A list of operations describing  $\mathcal{G}_1$  is given in Table 3.

Write  $\mathcal{G}(\ell)$  to denote the result of box-tensoring the corresponding type D structure for  $\ell$  with  $\mathcal{G}$ . We fix the  $\mathbb{Z}/2\mathbb{Z}$  grading so that the identity components preserve orientation; that is, so that  $\mathcal{G}_2(\ell) = \ell$  and  $\mathcal{G}_3(\ell) = \ell$ . Using this choice, the generators  $x_1$  and  $x_3$  in  $\mathcal{G}_1$  have grading 1. Applying the bimodule  $\mathcal{G}_1$  to certain loops, we have that  $\mathcal{G}_1(d_0) = (\bar{d}_2\bar{d}_{-2})$ ,  $\mathcal{G}_1(d_0d_0) = (\bar{d}_2\bar{d}_{-2})(\bar{d}_2\bar{d}_{-2})$ , and  $\mathcal{G}_1(d_{2i}d_{-2i}) = (\bar{d}_{2(i-1)}\bar{d}_{-2(i-1)})(\bar{d}_{2(i+1)}\bar{d}_{-2(i+1)})$  for  $i > 0$ .

We compute  $\mathcal{G}_1(d_{2i}d_{-2i})$  for  $i > 1$  explicitly – leaving the remaining cases to the reader – as follows:



The shaded boxes contain  $d_{2i}$  (above) and  $d_{-2i}$  (below) for book-keeping purposes. Note that the  $\bullet$ -generators on the left of each shaded box are identified in the loop  $(d_{2i}d_{-2i})$ , as are the two rightmost  $\bullet$ -generators. The generators  $x_i$  correspond to those in Table 3, interpreted as tensored with the generator immediately above or below in the shaded box. Each  $\circ$ -generator in  $(d_{2i}d_{-2i})$  pairs with both  $x_7$  and  $x_8$  in the tensor product, while each  $\bullet$ -generator pairs with the six generators  $x_1, \dots, x_6$ . The inner loop gives  $d_{2(i-1)}d_{2(i-1)}$  (after reducing the loop by cancelling unlabelled edges) and the outer loop gives  $d_{2(i+1)}d_{2(i+1)}$ . Since the the generators  $x_1$  and  $x_3$  of  $\mathcal{G}_1$  have grading 1, the  $\bullet$ -generators of the resulting two loops have the opposite sign from the  $\bullet$ -generators of  $(d_{2i}d_{-2i})$ ; equivalently, the new loops have the opposite orientation.

$\delta_1^2(x_1, \rho_1) = \rho_1 \otimes x_8$	$\delta_1^1(x_1) = \rho_3 \otimes x_2$ ♣	$\delta_1^4(x_3, \rho_{123}, \rho_{23}, \rho_2) = \rho_{12} \otimes x_1$
$\delta_1^2(x_1, \rho_{12}) = \rho_{123} \otimes x_6$ ♣	$\delta_1^1(x_2) = \rho_{23} \otimes x_5$ ♣	$\delta_1^4(x_3, \rho_3, \rho_2, \rho_{12}) = \rho_{123} \otimes x_5$ ♣
$\delta_1^2(x_1, \rho_{123}) = \rho_{123} \otimes x_8$	$\delta_1^1(x_4) = \rho_2 \otimes x_3$ ♣	$\delta_1^4(x_3, \rho_3, \rho_{23}, \rho_2) = \rho_3 \otimes x_6$ ♣
$\delta_1^2(x_3, \rho_1) = \rho_1 \otimes x_7$	$\delta_1^1(x_6) = \rho_{23} \otimes x_4$ ♣	$\delta_1^4(x_3, \rho_3, \rho_{23}, \rho_{23}) = \rho_3 \otimes x_8$
$\delta_1^2(x_3, \rho_{12}) = \rho_1 \otimes x_5$ ♣	$\delta_1^3(x_2, \rho_3, \rho_2) = \rho_2 \otimes x_1$ ♣	$\delta_1^4(x_5, \rho_3, \rho_{23}, \rho_2) = \rho_2 \otimes x_1$ ♣
$\delta_1^2(x_3, \rho_{123}) = \rho_{123} \otimes x_7$	$\delta_1^3(x_3, \rho_{123}, \rho_2) = \rho_1 \otimes x_2$	$\delta_1^4(x_7, \rho_{23}, \rho_{23}, \rho_2) = \rho_2 \otimes x_1$
$\delta_1^2(x_5, \rho_3) = \rho_{23} \otimes x_7$	$\delta_1^3(x_3, \rho_3, \rho_2) = \rho_3 \otimes x_4$ ♣	$\delta_1^5(x_3, \rho_3, \rho_2, \rho_1, \rho_2) = \rho_1 \otimes x_2$ ♣
$\delta_1^2(x_6, \rho_3) = x_8$	$\delta_1^3(x_2, \rho_3, \rho_2) = x_6$ ♣	$\delta_1^5(x_3, \rho_3, \rho_2, \rho_{123}, \rho_2) = \rho_{123} \otimes x_2$ ♣
$\delta_1^2(x_7, \rho_2) = x_5$	$\delta_1^3(x_4, \rho_3, \rho_{23}) = x_8$	$\delta_1^6(x_3, \rho_3, \rho_2, \rho_1, \rho_{23}, \rho_2) = \rho_{12} \otimes x_1$ ♣
$\delta_1^2(x_7, \rho_{23}) = \rho_{23} \otimes x_7$	$\delta_1^3(x_5, \rho_3, \rho_2) = x_2$ ♣	$\delta_1^7(x_3, \rho_3, \rho_2, \rho_3, \rho_2, \rho_1, \rho_2) = \rho_{123} \otimes x_2$ ♣
$\delta_1^2(x_8, \rho_2) = \rho_{23} \otimes x_6$	$\delta_1^3(x_7, \rho_{23}, \rho_2) = x_2$	
$\delta_1^2(x_8, \rho_{23}) = \rho_{23} \otimes x_8$		

**Table 3.** The operations in the type DA bimodule  $\mathcal{G}_1$ . The flags ♣ single out those operations relevant to tensoring with loops ( $d_0$ ) or ( $d_0d_0$ ) while the flags ♠ highlight those operations that are *not* relevant to calculations involving loops of the form ( $d_{2i}d_{-2i}$ ).

As a result, incorporating the two identity bimodules in  $\mathcal{G}$ , we conclude that

$$\begin{aligned}\mathcal{G}(d_0) &= (\bar{d}_2\bar{d}_{-2})(d_0)(d_0) \\ \mathcal{G}(d_0d_0) &= (\bar{d}_2\bar{d}_{-2})(\bar{d}_2\bar{d}_{-2})(d_0d_0)(d_0d_0) \\ \mathcal{G}(d_{2i}d_{-2i}) &= (\bar{d}_{2(i-1)}\bar{d}_{-2(i-1)})(\bar{d}_{2(i+1)}\bar{d}_{-2(i+1)})(d_{2i}d_{-2i})(d_{2i}d_{-2i})\end{aligned}$$

where  $i > 0$ . From this it is immediate that the number of ( $d_0$ ) components in  $\widehat{CFD}(M_g, \mu, \lambda)$  must be  $2^g$ . Let  $m(g)$  denote the number of ( $d_0d_0$ ) components,  $n_0(g) = 2^g + 2m(g)$ , and  $n_i(g)$  be the number of ( $d_{2i}d_{-2i}$ ) components when  $1 \leq i \leq g$  (where the orientation is reversed if  $i$  is odd). By inspection,

$$n_i(g) = n_{i-1}(g) + 2n_i(g) + n_{i+1}(g)$$

for  $i > 0$ , which is precisely the recursion satisfied for  $\binom{2g}{g+i}$ . It remains to check that  $n_0(g) = \binom{2g}{g}$ , but as  $m(g) = 2m(g-1) + n_1(g-1)$  we have

$$n_0(g) = 2^g + 2m(g) = 2 \cdot 2^{g-1} + 2(2m(g-1) + n_1(g-1)) = 2n_0(g-1) + 2n_1(g-1)$$

as required.  $\square$

The curves associated with the loops ( $d_{2i}d_{-2i}$ ) are relatively simple. For example, Figure 29 shows a component of  $\gamma(M_g)$  (for  $g \geq 2$ ) corresponding to the loop ( $d_4d_{-4}$ ). The curves are easier to picture in the lift to  $\mathbb{R}^2$ ; see Figure 30.  $\tilde{\gamma}(M_g)$  consists of some number of copies of each curve  $\tilde{\gamma}_i$ . Recall that choosing a lift  $\tilde{\gamma}$  of a curve  $\gamma$  encodes additional grading information. Computing the  $\text{spin}^c$  gradings under the tensor product with the bimodule  $\mathcal{G}$  reveals that all components of  $\tilde{\gamma}(M_g)$  are centered vertically on the same horizontal line, as in the figure. The curves  $\tilde{\gamma}_{\pm i}$  correspond to loop ( $d_{2i}d_{-2i}$ ),  $\tilde{\gamma}_{-i}$  has a horizontal shift representing a difference in  $\text{spin}^c$  gradings. Note that the curve  $\tilde{\gamma}_i$  is obtained from  $\tilde{\gamma}_{i-1}$  by sliding one column of lattice points up one unit and sliding the other column down one unit. On the level of curves, the bimodule  $\mathcal{G}_1$  applied to  $\tilde{\gamma}_i$  produces two curves  $\gamma_{i-1}$  and  $\gamma_{i+1}$ .

As an immediate consequence of Theorem 40, we have the following result concerning the Floer homology of  $Y_g$ , the closed three-manifold resulting from the product of a closed, orientable surface of genus  $g$  with  $S^1$ .

**Corollary 41.** *For  $g \geq 0$ , the total dimension of  $\widehat{HF}(Y_g)$  is  $2^g + \binom{2g}{g} + 2 \sum_{i=1}^g (2i-1) \binom{2g}{g+i}$ .*

*Proof.* This follows from the minimal intersection of  $\gamma(M_g)$  with a horizontal line, which calculates  $\widehat{HF}(Y_g)$  via Theorem 2. The reader can verify that each of component ( $d_0$ ) or ( $d_0d_0$ ) contributes

two intersection points – in both cases admissibility forces the intersection. According to Theorem 40, the total resulting contribution for these curves must be  $2^g + \binom{2g}{g}$ . The contribution of curves  $(d_{2i}d_{-2i})$  when  $i > 0$  is summarized in Figure 29: Notice that the number of vertical lines is  $2(2i - 1)$ , hence the total contribution from  $(d_{2i}d_{-2i})$  components is  $2 \sum_{i=1}^g (2i - 1) \binom{2g}{g+i}$ .  $\square$

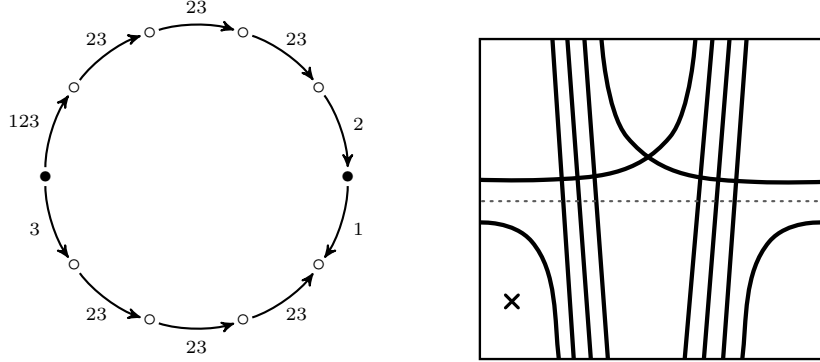


**Figure 29.** The loop  $(d_4d_{-4})$  (left) and the corresponding curve in  $T$  (right): Notice that the minimal intersection with a horizontal line is  $6 = 2(4 - 1)$ . More generally,  $(d_{2i}d_{-2i})$  gives rise to  $2(2i - 1)$  points of intersection, as in the proof of Corollary 41.

For comparison with earlier work, this sum may be split so that  $\sum_{\mathfrak{s} \neq \mathfrak{s}_0} \dim \widehat{HF}(Y_g, \mathfrak{s}) = 4 \sum_{i=1}^g (i - 1) \binom{2g}{2g+i}$  (compare Ozsváth and Szabó [26, Theorem 9.3]) and  $\dim \widehat{HF}(Y_g, \mathfrak{s}_0) = 2^g + 2^{2g}$  (compare Jabuka and Mark [17, Theorem 4.2]).

## 6. COMPARISON WITH SEIBERG-WITTEN THEORY

It is interesting to compare the invariant  $\bar{\gamma}(M)$  with the moduli space of finite energy solutions to the Seiberg-Witten equations on  $M$ . In this section, we briefly sketch the way this analogy should work, relying mainly on the work of Morgan, Mrowka, and Szabó [24] and Mrowka, Ozsváth and Yu [25].

**6.1. The Seiberg-Witten equations.** If  $M$  is a manifold with torus boundary, we let  $M' = M \cup_{\partial M} \partial M \times [0, \infty)$ . We fix a Riemannian metric  $g$  on  $M'$  which has the form  $g_E + dt^2$  on  $\partial M \times [0, \infty)$ , where  $g_E$  is a flat metric on  $\partial M \cong T^2$ .

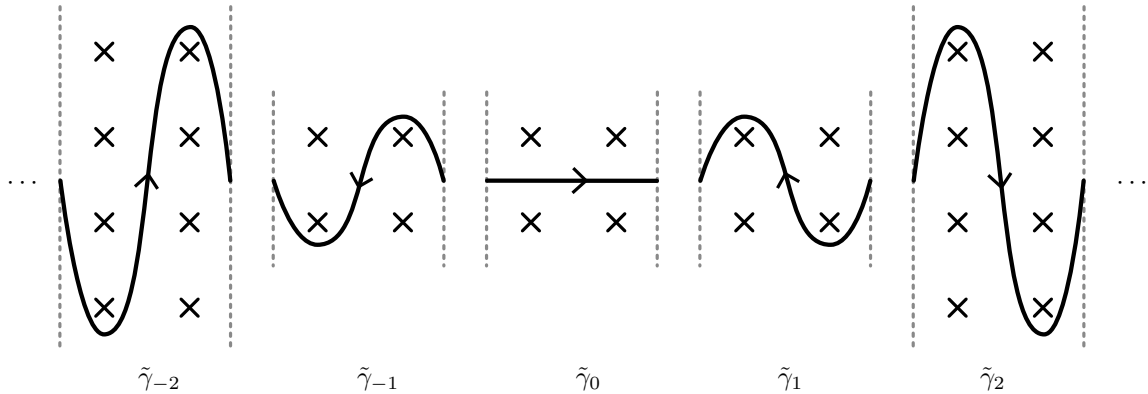


**Figure 30.** Components  $\tilde{\gamma}(M_g)$  in  $\mathbb{R}^2$ . The curves are invariant under translation by  $2\lambda$ , so each is pictured in  $\mathbb{R}^2/\langle 2\lambda \rangle$ . The curve  $\tilde{\gamma}_i$  corresponds to the loop  $(d_{2i}d_{-2i})$ .

Next, we choose  $\mathfrak{s} \in \text{Spin}^c(M')$ , and let  $E_{\mathfrak{s}}$  be the principal  $\text{Spin}^c(3)$  bundle over  $M'$  associated to  $\mathfrak{s}$ . A connection  $A$  on  $E_{\mathfrak{s}}$  induces a connection  $\widehat{A}$  on the determinant line bundle  $\det(\mathfrak{s})$ , as well as on the associated  $SO(3)$  bundle, which is the frame bundle of  $M'$ . We consider the space  $\mathcal{A}$  of connections on  $E_{\mathfrak{s}}$  which induce a fixed connection  $A_{\mathfrak{s}\sigma_3}$  on the frame bundle. (Usually  $A_{\mathfrak{s}\sigma_3}$  will be the Levi-Civita connection induced by  $g$ .)  $\mathcal{A}$  is an affine space modeled on  $\Omega^1(M'; i\mathbb{R})$ . Finally, we let  $W$  be the spinor bundle associated to  $E_{\mathfrak{s}}$ .

The Seiberg-Witten equations on  $M'$  are equations for a pair  $(A, \psi) \in \mathcal{C} = \mathcal{A} \times \Gamma(W)$ . They have the form

$$\begin{aligned}\not{D}_A \psi &= 0 \\ F_{\widehat{A}} &= q(\psi)\end{aligned}$$

where  $q(\psi)$  is a certain quadratic function of the spinor. The gauge group  $\mathcal{G} = \text{Map}(M', S^1)$  acts on  $\mathcal{C}$  by  $\gamma(A, \psi) = (A - \gamma^{-1}d\gamma, \gamma \cdot \psi)$ ; the equations are invariant under this action.

**6.2. The limit map.** The energy of a Seiberg-Witten solution  $(A, \psi)$  on  $M'$  is given by

$$E(A, \psi) = \frac{1}{4} \int_{M'} (\|F_{\widehat{A}}\|^2 + 4\|\nabla_A \phi\|^2 + \|\phi\|^4 + s\|\phi\|^2)$$

where  $s$  is the scalar curvature of  $M'$ . We let  $\mathcal{M}(M, \mathfrak{s})$  denote the quotient of the set of finite energy Seiberg-Witten solutions on  $M'$  by the action of  $\mathcal{G}$ .

Let  $\mathcal{M}(\partial M, \mathfrak{s}|_{\partial M})$  be the set of translation invariant solutions to the Seiberg-Witten equations on  $\partial M \times \mathbb{R}$  modulo the action of the group  $\text{Map}(\partial M, S^1)$  of translation invariant gauge transformations on  $M \times \mathbb{R}$ . A Seiberg-Witten solution on  $M'$  can be put in temporal gauge on the cylindrical end. Once this is done, the finite energy condition ensures that  $(A, \psi)|_{\partial M \times [T, \infty)}$  limits to an element of  $\mathcal{M}(\partial M, \mathfrak{s}|_{\partial M})$  as  $T \rightarrow \infty$ . We thus obtain a map

$$j: \mathcal{M}(M, \mathfrak{s}) \rightarrow \mathcal{M}(\partial M, \mathfrak{s}|_{\partial M})$$

which may be refined as follows. Let  $\overline{\mathcal{G}}_{\partial M} \subset \text{Map}(\partial M, S^1)$  be the subgroup of maps which extend to  $M$ , and let  $\overline{\mathcal{M}}(\partial M, \mathfrak{s}|_{\partial M})$  be the quotient of the set of translation invariant solutions by  $\overline{\mathcal{G}}_{\partial M}$ . Then there is a covering map  $\overline{\mathcal{M}}(\partial M, \mathfrak{s}|_{\partial M}) \rightarrow \mathcal{M}(\partial M, \mathfrak{s}|_{\partial M})$  and a well-defined map

$$\overline{j}: \mathcal{M}(M, \mathfrak{s}) \rightarrow \overline{\mathcal{M}}(\partial M, \mathfrak{s}|_{\partial M})$$

which is a lift of  $j$  to  $\overline{\mathcal{M}}(\partial M, \mathfrak{s}|_{\partial M})$ .

**6.3. Structure of  $\mathcal{M}(\partial M, \mathfrak{s}|_{\partial M})$ .** So far, everything we have said applies to an arbitrary manifold with a cylindrical end. We now use the fact that  $\partial M \cong T^2$ . Since the Riemannian metric  $g_E$  on  $\partial M$  has non-negative scalar curvature (in fact, it is flat), all Seiberg-Witten solutions on  $\partial M \times \mathbb{R}$  are *reducible*; that is they have  $\psi \equiv 0$ . It follows that  $\mathcal{M}(\partial M, \mathfrak{s}|_{\partial M}) = \emptyset$  unless  $c_1(\mathfrak{s}) = 0$ . Let  $\mathfrak{s}_0$  be the unique  $\text{Spin}^c$  structure on  $M$  with  $c_1(\mathfrak{s}_0) = 0$ .

Choose a connection  $A_0$  on  $E_{\mathfrak{s}}(\partial M \times \mathbb{R})$  such that  $F_{\widehat{A}_0} = 0$ . Then  $F_{\widehat{A_0+a}} = 2da$ , so  $(A_0 + a, 0)$  is a reducible solution to the Seiberg-Witten equations if and only if  $a$  is closed. Denote the identity component of  $\mathcal{G}_{\partial M}$  by  $\widetilde{\mathcal{G}}_{\partial M} = \{e^{if} \mid f: \partial M \times \mathbb{R} \rightarrow \mathbb{R}\}$ . We have  $e^{if} \cdot (A_0 + a, 0) = (A_0 + a - idf, 0)$ , so the quotient of the space of Seiberg-Witten solutions on  $\partial M \times \mathbb{R}$  by  $\widetilde{\mathcal{G}}_{\partial M}$  is naturally identified with  $H^1(\partial M, \mathbb{R})$ . The quotient  $\mathcal{G}_{\partial M}/\widetilde{\mathcal{G}}_{\partial M} = [\partial M, S^1] = H^1(\partial M, \mathbb{Z})$  acts on this space in the obvious way, so  $\mathcal{M}(\partial M, \mathfrak{s}_0) = H^1(\partial M, \mathbb{R})/H^1(\partial M, \mathbb{Z})$ . By Poincaré duality, this space can be identified with the torus  $H_1(\partial M, \mathbb{R})/H_1(\partial M, \mathbb{Z})$  which we have been using throughout the paper.

The quotient  $\overline{\mathcal{G}}_{\partial M}/\widetilde{\mathcal{G}}_{\partial M}$  consists of those elements of  $H^1(\partial M, \mathbb{Z})$  which pull back from  $H^1(M, \mathbb{Z})$ . Thus  $\overline{\mathcal{M}}(\partial M, \mathfrak{s}_0) = H^1(\partial M, \mathbb{R})/j^*(H^1(M, \mathbb{Z}))$ . By Poincaré duality, this can be identified with  $\overline{T} = H_1(\partial M, \mathbb{R})/\ker j_*$ .

An important feature of  $\mathcal{M}(\partial M, \mathfrak{s}_0)$  is that it contains a unique point  $z = (A_0, 0)$  for which  $\ker \not\partial_{A_0}$  is nontrivial. To understand this fact, we recall the structure of the Dirac operator on a Riemann surface  $\Sigma$  equipped with a  $\text{Spin}^c$  structure  $\mathfrak{s}$ . The spinor bundle  $W$  on  $\Sigma$  splits as  $W^+ \otimes W^-$  where  $W^\pm$  are complex line bundles. A connection  $A$  on  $E_{\mathfrak{s}}$  induces connections  $A^\pm$  on  $W^\pm$ . Since  $\Sigma$  is a Riemann surface, the curvature  $F_{A^\pm}$  is automatically of type  $(1, 1)$ , so the connections  $A^\pm$  induce holomorphic structures on  $W^\pm$ . As holomorphic line bundles,  $W^- = W^+ \otimes K_\Sigma^{-1}$ , where  $K_\Sigma$  is the canonical bundle, and the Dirac operator  $\not\partial_A: \Gamma(W^+) \rightarrow \Gamma(W^-)$  is given by  $\sqrt{2}\not\partial_A$ . Finally, we have  $\det(\mathfrak{s}) = W^+ \otimes W^- = (W^+)^2 \otimes K_\Sigma^{-1}$ .

When  $\Sigma = \partial M$  is a torus and  $\mathfrak{s} = \mathfrak{s}_0$ ,  $K_\Sigma$  is the trivial bundle and  $c_1(W^+) = 0$ . The moduli space  $\mathcal{M}(\partial M, \mathfrak{s}_0)$  can be identified with  $\text{Pic}^0(\Sigma)$  via the map which assigns to  $(A, 0)$  the line bundle  $W^+$  with the holomorphic structure induced by  $A$ . Then the Dirac operator  $\not\partial_A$  has nontrivial kernel precisely when  $W^+$  has a holomorphic section. There is a unique element of  $\text{Pic}^0(\Sigma)$  with a holomorphic section; namely, the trivial bundle. Let  $A_0$  be the corresponding flat connection.

**6.4. Conjugation symmetry.** A  $\text{Spin}^c$  structure  $\mathfrak{s}$  on  $M$  has a conjugate  $\text{Spin}^c$  structure  $-\mathfrak{s}$  whose transition functions are conjugate to the transition functions for  $\mathfrak{s}$ . We have  $W_{-\mathfrak{s}}^\pm = (W_{\mathfrak{s}}^\mp)^*$ . A connection  $A$  on  $\mathfrak{s}$  induces a connection  $\bar{A}$  on  $-\mathfrak{s}$ , and a spinor  $\psi$  for  $\mathfrak{s}$  induces a spinor  $\bar{\psi}$  for  $-\mathfrak{s}$ . The map  $c$  defined by  $(A, \psi) \mapsto (\bar{A}, \bar{\psi})$  identifies  $\mathcal{M}(M, \mathfrak{s})$  with  $\mathcal{M}(M, -\mathfrak{s})$ .

On  $\partial M$ ,  $-\mathfrak{s}_0 = \mathfrak{s}_0$ , so  $c$  induces an involution of  $\mathcal{M}(\partial M, \mathfrak{s}_0)$ . Under the identification  $\mathcal{M}(\partial M, \mathfrak{s}_0) = \text{Pic}^0(\partial M)$ , we have  $c(L) = L^*$ . The four fixed points of  $c$  correspond to the four spin structures on  $\partial M$ . The special point  $z$  is one of these points; to specify which one, we recall the following description of spin structures on  $S^1$ . Let  $V$  be a nonvanishing section of  $TS^1$ . The preimage of  $V$  in the spin bundle is a double cover of  $V$ ; if it is a trivial double cover, we say that the spin structure is the trivial spin structure on  $S^1$ , and if it is nontrivial, we say that the spin structure is nontrivial. If we write  $\partial M = S^1 \times S^1$ , then the spin structure corresponding to  $z$  is the product of the trivial spin structure with itself.

**6.5. Reducible solutions.** If  $\partial M = T^2$ , then  $j^*: H^2(M) \rightarrow H^2(\partial M)$  is the trivial map, so any  $\text{Spin}^c$  structure  $\mathfrak{s}$  on  $M$  restricts to  $\mathfrak{s}_0$ . Elements of  $\mathcal{M}(M, \mu, \mathfrak{s})$  may be divided into *reducibles* (solutions with  $\psi \equiv 0$ ) and *irreducibles* (all the rest). We let  $\mathcal{M}^{\text{red}}(M, \mathfrak{s})$  be the space of reducible solutions, and similarly for  $\mathcal{M}^{\text{irred}}$ . Arguing as we did for  $T^2$ , it is easy to see that  $\mathcal{M}^{\text{red}}(M, \mathfrak{s}) = H^1(M; \mathbb{R})/H^1(M; \mathbb{Z})$  if  $c_1(\mathfrak{s})$  is torsion, and is empty if it is not.

To describe the image of  $\mathcal{M}^{\text{red}}(M, \mathfrak{s})$  under  $j$ , we fix a basis  $(m, l)$  for  $H_1(\partial M)$ , where  $l$  is a rational homological longitude and  $m \cdot l = 1$ . We identify  $\mathcal{M}(\partial M, \mathfrak{s}_0)$  with  $S^1 \times S^1$  by the map which sends  $(A, 0)$  to  $(\text{hol}_m A^+, \text{hol}_l A^+)$ . Suppose that the order of  $l$  in  $H_1(M)$  is  $n$ . Then if  $S$  is a surface in  $M$  which bounds  $nl$ ,

$$2n \text{hol}_l A^+ = n \text{hol}_l \hat{A} = \int_S F_{\hat{A}} = 0 \in \mathbb{R}/(2\pi\mathbb{Z})$$

so  $j(\mathcal{M}^{\text{red}}(M, \mathfrak{s}))$  lies on a line of the form  $\text{hol}_l A^+ = k\pi/n$  for  $k \in \mathbb{Z}/(2p)$ .

To pin down the value of  $k$ , we fix a spin structure  $\mathfrak{t}$  on  $M$ , and let  $\mathfrak{s}$  be the associated  $\text{Spin}^c$  structure, so that  $c_1(\mathfrak{s}) = 0$ . The restriction of  $\mathfrak{t}$  to  $\partial M$  determines a 2-torsion point  $p_{\mathfrak{t}} \in \text{Pic}^0(\partial M)$ , and  $j(\mathcal{M}^{\text{red}}(M, \mathfrak{s}))$  is the horizontal line in  $\text{Pic}^0(\partial M)$  passing through  $p_{\mathfrak{t}}$ . More generally, for  $x \in H_1(M)$ , let  $l \cdot x = S \cdot x/p$ , which is a well-defined element of  $\mathbb{R}/\mathbb{Z}$ . Then it is not hard to show that  $j(\mathcal{M}^{\text{red}}(M, \mathfrak{s} + x))$  is the horizontal line given by the equation  $\text{hol}_l A^+ = \text{hol}_l p_{\mathfrak{t}} + 2\pi l \cdot x$ .

**6.6. First examples: Floer solid tori.** The solid torus  $M = S^1 \times D^2$  admits a metric of positive scalar curvature, so the Seiberg-Witten equations have only reducible solutions. Thus  $\mathcal{M}(M) = \mathcal{M}^{\text{red}}(M) \simeq S^1$ . Its image under  $j$  passes through the two points on  $\mathcal{M}(\partial M, \mathfrak{s}_0)$  corresponding to spin structures on  $\partial M$  which extend over  $S^1 \times D^2$ . The spin structure on  $S^1$  which extends to  $D^2$



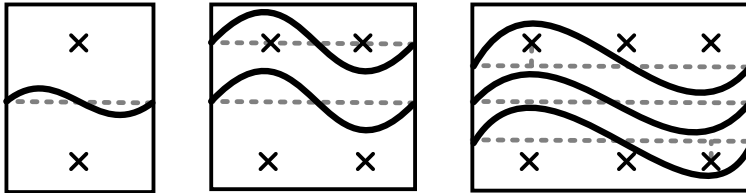


**Figure 31.** Moduli spaces of solutions for the solid torus, the twisted  $I$ -bundle over the Klein bottle, and the Seifert fibered Floer solid torus with base orbifold  $D^2(3, 3)$ . In each case, the cover  $\bar{T}$  is illustrated so that the left and right sides of each rectangle are identified. Here, and below, the moduli spaces of solutions is indicated with dashed lines while a representative of the invariant  $\bar{\gamma}(M)$  is illustrated with a solid line.

is the one corresponding to the non-trivial double cover of  $S^1$ , so  $j(\mathcal{M}(S^1 \times D^2))$  is disjoint from  $z$ .  $\bar{j}(\mathcal{M}(S^1 \times D^2)) = S^1 \times 0 \subset S^1 \times \mathbb{R}$ . It lies midway between two preimages of  $z$ , and coincides with  $\bar{\gamma}(S^1 \times D^2)$  (up to homotopy).

If  $M$  is the twisted  $I$ -bundle over the Klein bottle,  $M$  admits a metric of nonnegative scalar curvature, so we again have  $\mathcal{M}(M) = \mathcal{M}^{red}(M)$ .  $H^2(M) \simeq \mathbb{Z} \oplus \mathbb{Z}/2$ , so there are two torsion  $\text{Spin}^c$  structures  $\mathfrak{s}, \mathfrak{s}'$  on  $M$ , both of which are induced by spin structures. Their images under  $j$  are two parallel horizontal lines, each passing through 2 fixed points of  $c$ .

The kernel of the map  $H_1(\partial M) \rightarrow H_1(M)$  is a subgroup of the form  $2\mathbb{Z} \oplus 0 \subset \mathbb{Z} \oplus \mathbb{Z}$ , so the cover  $\bar{T} \simeq S^1 \times \mathbb{R}$ , where each circle of the firm  $S^1 \times n$  contains *two* preimages of  $z$ .  $\bar{j}(\mathcal{M}(M, \mathfrak{s}))$  has the same form as  $\bar{\gamma}(M, \mathfrak{s})$ , as shown in Figure 31.  $\bar{j}(\mathcal{M}(M, \mathfrak{s}'))$  is more interesting; it passes directly through two lifts of  $z$ . To understand what is going on, note that since the metric on  $M$  is flat rather than positively curved, reducible solutions need not be transversely cut out. Indeed, as we shall see in Section 6.8, the two reducible solutions passing through lifts of  $z$  are not transversely cut out. When we perturb to achieve transversality, we expect that the resulting curve will resemble  $\bar{\gamma}(M, \mathfrak{s}')$  as shown in Figure 31.

**6.7. Structure of  $\mathcal{M}(M, \mathfrak{s})$ .** The structure of  $\mathcal{M}(M, \mathfrak{s})$  was described by Morgan, Mrowka, and Szabó [24]. (In fact, [24] studies solutions to the four-dimensional solutions to the Seiberg-Witten equations on a manifold with an end of the form  $T^3 \times [0, \infty)$ , but their results can be made to apply in the 3-dimensional case by considering solutions on  $M' \times S^1$ .) It follows from their work that  $\mathcal{M}(M, \mathfrak{s})$  is compact. Moreover, they showed that the irreducible part of the moduli space has the following local structure.

The fact that  $\ker \partial_{A_0}$  is nontrivial implies that the moduli space  $\mathcal{M}(\partial M, \mathfrak{s}_0)$  is not transversely cut out at the point  $z = (A_0, 0)$ . This has important consequences for the structure of  $\mathcal{M}(M, \mathfrak{s})$ . If  $j(A, \psi) = z' \neq z$ , then it can be shown that the solution  $(A, \psi)$  decays exponentially to  $z$  as we go down the cylindrical end. In turn, this can be used to prove that for generic  $\mu$ , the moduli space  $\mathcal{M}(M, \mu, \mathfrak{s})$  is a 1-dimensional manifold near  $(A, \psi)$ .

In contrast, if  $j(A, \psi) = z$ , the solution decays more slowly as we go along the tube. A more delicate analysis using the center manifold technique shows that for generic  $\mu$ ,  $\mathcal{M}(M, \mu, \mathfrak{s})$  is locally homeomorphic to  $[0, 1)$ , where the point corresponding to 0 maps to  $z$  under  $j$ .

In summary,  $\mathcal{M}(M, \mu, \mathfrak{s})$  can be written as the union of  $\mathcal{M}^{red}$  and  $\mathcal{M}^{irred}$ . The unperturbed moduli space  $M^{red}$  is homeomorphic to the torus  $H^1(M; \mathbb{R})/H^1(M; \mathbb{Z})$ , while  $M^{irred}$  has the structure of a (possibly noncompact) 1-manifold with boundary. Boundary points of  $\mathcal{M}^{irred}$  map to  $z$  under  $j$ , while noncompact ends of  $\mathcal{M}^{irred}$  limit to  $\mathcal{M}^{red}$ .

**6.8. Seifert fibred spaces.** The Seiberg-Witten equations on closed Seifert fibred spaces were studied by Mrowka, Ozsváth and Yu [25]. Their results can be extended to Seifert fibred spaces with

boundary with little change. We sketch this process here. First, we equip  $TM'$  with a connection  $A_{\mathfrak{so}_3}$  compatible with the  $S^1$  action on  $M'$ , but which is not induced by a metric. Then it can be shown (as in [25, Theorem 4]) that any irreducible finite energy solution to the Seiberg-Witten equations on  $M'$  is invariant under the  $S^1$  action on  $M'$  induced by the Seifert fibration.

Next,  $S^1$ -invariant solutions to the Seiberg-Witten equations are shown to correspond to finite energy solutions of the vortex equations on the base orbifold  $\Sigma$  of  $M$ . These equations have the following form [25, equations (25)-(27)]

$$\begin{aligned} 2F_A - F_K &= i(|\alpha|^2 - |\beta|^2)\omega_\Sigma \\ \bar{\partial}_A\alpha &= 0 \quad \text{and} \quad \bar{\partial}_A^*\beta = 0 \\ \alpha &= 0 \quad \text{or} \quad \beta = 0 \end{aligned}$$

Here  $(\alpha, \beta)$  is a section of the spinor bundle  $W$  for  $\Sigma$ . As in Section 6.3,  $W$  can be decomposed as  $W = W^+ \oplus W^-$ , where  $W^- = W^+ \otimes K_\Sigma^{-1}$ , where  $K_\Sigma$  is the canonical bundle of  $\Sigma$ , endowed with the metric connection.  $A$  is a connection on  $W^+$ ; it induces a Hermitian metric on  $W^+$ , which we use to define both  $|\alpha|^2$  and  $\bar{\partial}_A$ . Finally,  $\omega_\Sigma$  is the area form on  $\Sigma$ .

Let  $\mathcal{M}_\alpha^{irred}(M)$  be the moduli space of solutions to these equations for which  $\alpha \neq 0$ , and similarly for  $\beta$ . Conjugation symmetry exchanges  $\mathcal{M}_\alpha^{irred}(M)$  and  $\mathcal{M}_\beta^{irred}(M)$ , so it is enough to understand  $\mathcal{M}_\alpha^{irred}(M)$ .

As we go down the tubular end, solutions to the vortex equations limit to flat  $S^1$  connections on the boundary  $S^1$ . The space of such solutions modulo gauge is naturally identified with  $S^1$ . If we only quotient by those gauge transformations which extend over  $\Sigma$ , the resulting moduli space can be identified with  $\mathbb{R}$ . As in the 3-dimensional case, we have a map  $j : \mathcal{M}_\alpha^{irred}(M) \rightarrow \mathbb{R}$  given by  $j(A, \alpha) = h_A := \frac{i}{2\pi} \int_\Sigma F_A$ .

Let  $\mathcal{D}(\Sigma)$  denote the set of effective orbifold divisors on  $\Sigma$ . In analogy with the results of [25], the moduli space  $j^{-1}(h) \cap \mathcal{M}_\alpha^{irred}(M)$  can be identified with the set

$$\mathcal{D}_h = \{D \in \mathcal{D}(\Sigma) \mid |D| \leq h\}$$

when  $h < -\chi(\Sigma)/2$ , and is empty for  $h \geq -\chi(\Sigma)/2$ . The correspondence between the two is established as follows. Suppose  $j(A, \alpha) = h$ . Then  $\alpha$  is a holomorphic section of  $W^+$  (with holomorphic structure induced by  $A$ ), so it determines an effective divisor  $D \in \mathcal{D}$ . We have  $h_A \geq |D|$ . By integrating the first vortex equation, we see that  $2h_A + \chi(\Sigma) < 0$ . It follows that  $|D| \leq h_A \leq -\chi(\Sigma)/2$ , so the condition above is certainly necessary. The converse follows from the fact that it is possible to solve the Kazdan-Warner equation on open surfaces, as established in [16].

When  $\chi(\Sigma) < -2$ , the divisor  $D$  can vary freely in  $\Sigma$ , and the spaces  $\mathcal{D}_h$  will be noncompact manifolds of positive dimension. In contrast, if  $\chi(\Sigma) > -2$ ,  $D$  must be supported at the orbifold points of  $\Sigma$ , and the moduli spaces  $\mathcal{D}_h$  will be discrete. If  $M$  is Seifert-fibred over  $D^2$  with two or three exceptional fibres, the latter condition holds, so  $\mathcal{M}_\alpha^{irred}(M)$  will consist of one arc  $X_D$  for each effective orbifold divisor  $D$  with  $|D| < -\chi(\Sigma)/2$ . Each arc starts at a point of  $\mathcal{M}^{red}$  (where  $h_A = \chi(\Sigma)/2$ ). Its other endpoint (where  $h_A = |D|$ ) maps to  $z$  under  $j$ . The moduli space  $\mathcal{M}_\beta^{irred}(M)$  is isomorphic to  $\mathcal{M}_\alpha^{irred}(M)$ ; the two are exchanged by the conjugation symmetry.

To determine the image of  $\mathcal{M}_\alpha^{irred}(M)$  under  $\bar{j}$  recall that the vertical coordinate of  $\bar{j}(A, \psi)$  is given by  $h_{\hat{A}} = \frac{i}{4\pi} \int_S F_{\hat{A}}$ , where  $\hat{A}$  is the induced connection on  $\det \mathfrak{s} = W^+ \otimes W^-$ , and  $S$  is a surface generating  $H_2(M, \partial M)$ . Since solutions to the Seiberg-Witten equations are invariant under the  $S^1$  action,  $F_{\hat{A}}$  pulls back from  $\Sigma$ . If the projection  $\pi : S \rightarrow \Sigma$  has degree  $d$ , then

$$h_{\hat{A}} = \frac{i}{4\pi} \int_S F_{\hat{A}} = d(h_A + \chi(\Sigma)/2).$$

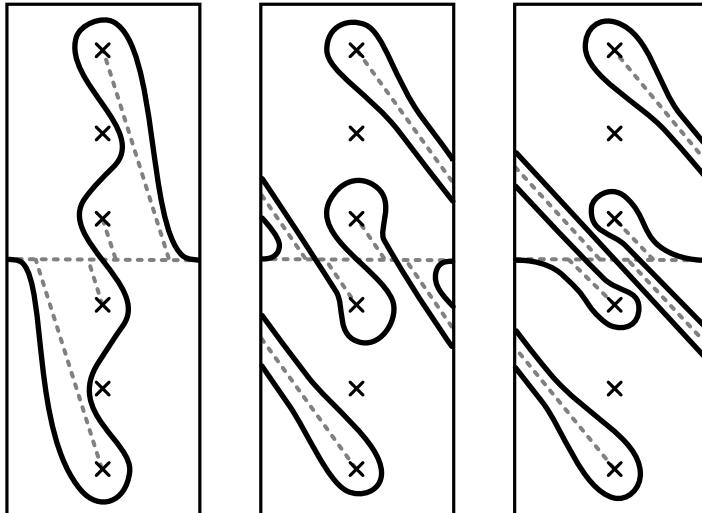


**Figure 32.** Further examples: moduli spaces of solutions for the three Seifert fibered spaces with base orbifold  $D^2(2, 7)$ , illustrated together with  $\bar{\gamma}(M)$  in each case. In terms of the basis shown the fiber slope in each example, from left to right, is  $-14$ ,  $-\frac{14}{5}$  and  $-\frac{14}{3}$ .

The value of  $h_{\hat{A}}$  on  $X_D$  will vary between 0 and  $d(|D| + \chi(\Sigma)/2) = d|D| + \chi(S)/2$ . Finally, let  $f \in H_1(\partial M)$  be the fibre slope. Since  $\hat{A}$  pulls back from  $\Sigma$ , it will have trivial holonomy along  $f$ . It follows that  $\bar{j}(X_D)$  lies on a line parallel to  $f$ .

**6.9. Further examples: Torus knots and other Seifert fibered spaces.** Seifert fibered spaces provide a family of examples on which to compare the curves arising from this point of view with those defined in terms of bordered Floer homology.

The complement of the right-handed trefoil fibres over  $D^2$  with exceptional fibres of multiplicities 2 and 3, so  $\chi(\Sigma) = -1 + (1/2) + (1/3) = -1/6$ . The only effective divisor with  $|D| < 1/12$  is the trivial divisor, so  $\mathcal{M}_\alpha^{irred}$  consists of a single arc, on which  $h_{\hat{A}} \in [-1/2, 0]$ . To determine its image under  $\bar{j}$ , note that  $f = l - 6m$ , where  $m$  and  $l$  are the standard meridian and longitude of the trefoil in  $S^3$ . Thus the arc maps to a line with slope 6. The full moduli space is shown in Figure 33.

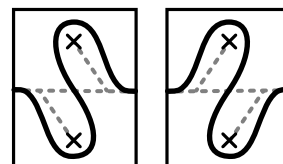


**Figure 33.** Curves for the left- and right-hand trefoil.

To pass from  $\mathcal{M}(M)$  to  $\bar{\gamma}(M)$  in this example, we employ the following heuristic: first, we consider the moduli space  $\widehat{\mathcal{M}}(M)$  obtained by dividing out by the group of maps  $f: S^1 \rightarrow M$  which satisfy  $f(p) = 1$  for some fixed point  $p \in M$ .  $\widehat{\mathcal{M}}(M)$  will contain one point for each reducible point of  $\mathcal{M}(M)$ , and an entire circle of points for each irreducible point. After an appropriate perturbation, this should reduce to a 1-dimensional space which contains roughly two points for each irreducible point of  $\widehat{\mathcal{M}}(M)$ . We expect that this moduli space should take the form of the curve shown in the figure, which is isotopic to  $\bar{\gamma}(M)$ .

Now suppose that instead of  $T(2, 3)$ , we consider  $T(2, 7)$ . The complement fibres over  $D^2$  with exceptional fibres of multiplicities 2 and 7, so  $\chi(\Sigma) = -5/14$ . Now there are two effective divisors with  $|D| < 5/28$ ; namely the trivial divisor and the divisor containing a single copy of the orbifold point of multiplicity 7.  $\mathcal{M}_\alpha^{irred}$  consists of two arcs, on which the maximum values of  $\text{hol}_\ell A$  are  $14 \cdot (5/28) = 5/2$  and  $14 \cdot (5/28 - 1/7) = 1/2$ . Both arcs map to lines of slope 14.

If instead of the complement of  $T(2, 7)$ , we considered another Seifert fibred space over  $D^2$  with exceptional fibres of multiplicities  $1/2$  and  $1/7$ , the general form of the Seiberg-Witten moduli space would be similar, but the slope of the relevant arcs with respect to a standard basis  $(m, l)$  for  $H_1(\partial M)$  would differ, as illustrated in Figure 32. (Note that the spaces in the figure are oriented so the fibre slopes are negative; *e.g.* the figure shows the moduli space for the complement of the left-hand  $(2, 7)$  torus knot.)

As a final, non-Seifert fibered, example, let  $M$  be the complement of the figure-8 knot in  $S^3$ . Here, we cannot determine the Seiberg-Witten moduli space explicitly, but we know from the Alexander polynomial that the signed number of ends of irreducible arcs at  $z_{\pm 1/2}$  (the preimages of  $z$  closest to the reducible line) should be  $\pm 1$ , respectively. We expect that with respect to an appropriate metric/deformation,  $\mathcal{M}(M)$  should consist of a single arc of irreducibles joining  $z_{1/2}$  to  $z_{-1/2}$ , together with the usual circle of reducibles. After passing to the unreduced moduli space and perturbing, the the arc should become the figure-8 component of  $\overline{\gamma}(M)$ .

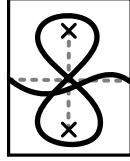


**Figure 34.** Curves for the figure eight.

## 7. KNOT FLOER HOMOLOGY AND FURTHER RELATIONSHIPS

It remains to prove Theorem 3 stated in in the introduction. Toward that end, we briefly review the essentials of knot Floer homology following the notation in [21, Chapter 11]; a more complete introduction can be found in [23].

**7.1. Background and notation.** Given a nullhomologous knot  $K$  in a three-manifold  $Y$ , the knot Floer chain complex  $CFK^-(Y, K)$  is a free,  $\mathbb{Z}$ -graded chain complex over  $\mathbb{F}[U]$ . As a complex it is quasi-isomorphic to  $CF^-(Y)$ , but it is also endowed with a filtration, the Alexander filtration,

$$\cdots \subset \mathcal{F}_i \subset \mathcal{F}_{i+1} \subset \cdots \subset CFK^-(Y, K)$$

with filtration level  $A(x) = \min\{i | x \in \mathcal{F}_i\}$ . Up to filtered chain homotopy equivalence,  $CFK^-(Y, K)$  is an invariant of the knot  $K$  in  $Y$ . When the ambient manifold  $Y$  is  $S^3$ , we will omit it from the notation.

Recall that  $CFK^-(Y, K)$  is defined using a doubly pointed Heegaard diagram for the pair  $(Y, K)$ . The differential is defined by counting certain pseudoholomorphic disks, which may be interpreted as domains in the Heegaard surface together with information about how these domains cover the two basepoints  $w$  and  $z$ . If a homotopy class of disks  $B$  from  $x$  to  $y$  covers the basepoints with multiplicities  $n_w(B)$  and  $n_z(B)$ , a differential corresponding to  $B$  connects  $x$  to  $U^{n_w(B)}y$  and lowers the filtration level by  $n_z(B)$ . By restricting the differential to disks which do not cover one or both basepoints, we can define several important quotient complexes. The associated graded object  $gCFK^-$  is obtained by considering only terms in the differential that do not change the Alexander grading (that is, by restricting to disks which do not cover  $z$ ). For both  $CFK^-$  and  $gCFK^-$ , further restricting to disks which do not cover  $w$  and generating the complex over  $\mathbb{F}$  instead of  $\mathbb{F}[U]$  produces the complexes  $\widehat{CFK}$  and  $g\widehat{CFK}$ ; note that this restriction is equivalent to setting  $U = 0$ . Knot Floer homology is the homology of  $gCFK^-(Y, K)$ , denoted  $HFK^-(Y, K)$ , or of  $g\widehat{CFK}(Y, K)$ , denoted  $\widehat{HFK}(Y, K)$ .

In order to construct  $\gamma(M)$  from knot Floer homology, we need to fix a particularly nice basis for  $CFK^-(Y, K)$ . Fix a representative for the filtered homotopy type of  $CFK^-(Y, K)$ , which as shorthand we will denote by  $C$ . Note that  $C$  has two filtrations, the Alexander filtration and the filtration by negative powers of  $U$ . We may choose  $C$  so that the differential  $\partial$  strictly drops one of these filtration levels; we say that such a filtered complex is reduced. The associated graded object is  $gC = \bigoplus_i \mathcal{F}_i / \mathcal{F}_{i-1}$ . Given  $x$  in  $C$ , let  $[x] \in gC$  denote the projection of  $x$  to  $\mathcal{F}_{A(x)} / \mathcal{F}_{A(x)-1}$ . A filtered basis for  $C$  is a basis  $\{v_1, \dots, v_n\}$  such that  $\{[v_1], \dots, [v_n]\}$  is a basis for the associated

graded  $gC$ . We say that a filtered basis is vertically simplified if for each basis vector  $v_i$ , either  $\partial v_i \in U \cdot C$  or  $\partial v_i \equiv v_j + x$  for some basis element  $v_j$  and  $x \in U \cdot C$ . In the latter case, we say there is a vertical arrow from  $v_i$  to  $v_j$ . Similarly, we say that a filtered basis is horizontally simplified if for each basis vector  $v_i$  with filtration level  $A(v_i) = k$ , either  $A(\partial v_i) < k$  or  $A(\partial v_i) = U^m \cdot v_j + x$  for some basis element  $v_j$  and integer  $m$  with  $A(U^m \cdot v_j) = k$  and some  $x$  with  $A(x) < k$ . The filtered complex  $CFK^-(Y, K)$  always admits a vertically simplified basis and a (possibly different) horizontally simplified basis [21].

**7.2. Curves from knot Floer homology.** The complements of knots in  $S^3$  provide many examples of loop type manifolds. Let  $K$  be a knot in  $S^3$ , and let  $M = S^3 \setminus \nu(K)$  be its complement. In [21], Lipshitz, Ozsváth, and Thurston describe an algorithm computing  $\widehat{CFD}(M, \mu, \lambda)$  from the knot Floer chain complex  $CFK^-(K)$ , making use of a horizontally simplified basis and a vertically simplified basis for  $CFK^-(K)$ . In the special case that the two bases coincide, i.e.,  $CFK^-$  admits a single basis which is both horizontally and vertically simplified, the construction of  $\widehat{CFD}(M, \mu, \lambda)$  from  $CFK^-(K)$  is simpler; in this case, we observe the following:

**Proposition 42.** *If  $CFK^-(K)$  admits a basis which is both horizontally and vertically simplified, then  $M = S^3 \setminus \nu(K)$  is a loop type manifold.*

*Proof.* According to the algorithm mentioned above, the generators of  $\iota_0 \widehat{CFD}(M, \mu, \lambda)$  are in one-to-one correspondence with the generators of  $CFK^-(K)$ . In the directed graph representing  $\widehat{CFD}(M, \mu, \lambda)$ , these generators are connected by chains of  $\iota_1$ -vertices referred to as horizontal chains, vertical chains, and unstable chains (these chains correspond to the segments denoted  $a_k, b_k, c_k, d_k$ , and  $e$  in [10]). Moreover, there are exactly two chains (or two ends of the same chain), at each  $\iota_0$ -vertex; that is, the graph representing  $\widehat{CFD}(M, \mu, \lambda)$  has valence two. It follows that  $M$  is a loop type manifold.  $\square$

**Remark 43.** It is not known whether  $CFK^-$  admits a horizontally and vertically simplified basis for all knots in  $S^3$ , so it is possible that all knot complements are loop type. Such a basis is known to exist of some families of knots, including L-space knots and thin knots.

It is clear that given  $CFK^-(K)$  along with a horizontally and vertically simplified basis, one can compute  $\widehat{CFD}(M, \mu, \lambda)$  using the algorithm in [21] and then convert this to  $\gamma(M)$  as described in Section 2. For convenience, we now describe an algorithm for recovering  $\gamma(M)$  directly from  $CFK^-$ . More precisely, we describe the lift  $\bar{\gamma}(M)$  in the covering space  $H_1(\partial M, \mathbb{R})/\langle \lambda \rangle$ . This space will be realized as the infinite strip  $[-1/2, 1/2] \times \mathbb{R}$  with  $(-1/2, t)$  and  $(1/2, t)$  identified, and  $\pi^{-1}(z)$  is the set of points  $(0, n + 1/2)$  for  $n \in \mathbb{Z}$ .

**Proposition 44.** *The collection of curves  $\bar{\gamma}(M)$  in the infinite strip described above can be obtained from  $CFK^-(K)$  by the following procedure:*

- (1) *For each basis element  $x$  of  $CFK^-$ , place a short horizontal segment  $[-1/4, 1/4] \times \{t\}$  at height  $t = A(x)$ , where  $A(x)$  denotes the Alexander grading of  $x$ .*
- (2) *If  $CFK^-(K)$  contains a vertical arrow from  $x$  to  $y$  (that is, if  $\partial x = y + Uz$  for some  $z \in CFK^-(K)$ ), then connect the left endpoints of the horizontal segments corresponding to  $x$  and  $y$  by a vertical segment.*
- (3) *If  $CFK^-(K)$  contains a horizontal arrow from  $x$  to  $y$  (that is, if  $\partial x = U^{A(y)-A(x)}y + z$  for some  $z \in CFK^-(k)$  with  $A(z) < A(x)$ ), then connect the right endpoints of the horizontal segments corresponding to  $x$  and  $y$  by a vertical segment.*
- (4) *There is a now unique horizontal segment with an unattached left endpoint, and a unique horizontal segment with an unattached right endpoint; connect these unattached endpoints to  $(-1/2, 0)$  and  $(1/2, 0)$ , respectively.*

*Proof.* By the algorithm in [21], the generators of  $CFK^-$  are in one-to-one correspondence with  $\iota_0$  generators of  $\widehat{CFD}(M, \mu, \lambda)$ , which correspond to horizontal segments in the construction of  $\bar{\gamma}(M)$ . A vertical arrow between  $x$  and  $y$  of length  $\ell = A(x) - A(y)$  corresponds to a chain

$$\bullet \xrightarrow{1} \circ \xleftarrow{23} \dots \xleftarrow{23} \circ \xleftarrow{123} \bullet$$

in  $\widehat{CFD}(M, \mu, \lambda)$  with  $\ell$  generators of idempotent  $\iota_1$ . In  $\bar{\gamma}(M)$  this corresponds to a (downward moving) vertical segment of length  $\ell$  connecting the left edge of the segment corresponding to  $x$  to the left edge of the segment corresponding to  $y$ . Similarly, a horizontal arrow between  $x$  and  $y$  of length  $\ell = A(y) - A(x)$  corresponds to a chain

$$\bullet \xrightarrow{3} \circ \xrightarrow{23} \dots \xrightarrow{23} \circ \xrightarrow{2} \bullet$$

in  $\widehat{CFD}(M, \mu, \lambda)$  with  $\ell$  generators of idempotent  $\iota_1$ . In  $\bar{\gamma}(M)$  this corresponds to an upward moving vertical segment of length  $\ell$  connecting the right edges of the segments corresponding to  $x$  and  $y$ . Finally, the unstable chain in the algorithm in [21] corresponds to a path from the unmatched right edge to the unmatched left edge (moving to the right and wrapping around the cylinder  $H_1(\partial M, \mathbb{R})/\langle \lambda \rangle$ ).  $\square$

We remark that when the curve  $\gamma(M)$  is pulled tight in a peg-board diagram, it is supported in a neighborhood of a meridian passing through the peg except for one segment which has slope  $2\tau(K) - \epsilon(K)$ , where  $\tau(K)$  is the Ozsváth-Szabó concordance invariant and  $\epsilon$  is the invariant defined by Hom [13].

In the other direction, it is also shown in [21] that  $HFK^-$  can be recovered from  $\widehat{CFD}$ ; we can ask if  $HFK^-$  can be recovered easily from  $\gamma(M)$  without passing through  $\widehat{CFD}$ .

**7.3. Knot Floer homology from curves.** Given a loop-type manifold  $M$  equipped with a meridian  $\mu$ , consider the curves  $\gamma(M)$  in  $T$ , avoiding a basepoint  $z$ . We now describe a method for recovering the knot Floer homology of  $K$  in  $Y = M(\mu)$ , where  $K$  is the core of the filling torus. Replace the basepoint  $z$  with a marked disk  $D$  (which  $\gamma(M)$  also avoids) containing two basepoints  $w$  and  $z$ , and consider a representative of  $\mu$  bisecting  $D$  and separating  $w$  and  $z$ . This setup is illustrated, for the right-handed trefoil, in Figure 35.

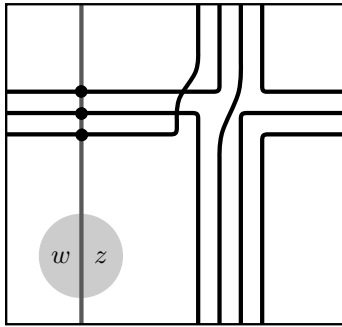


**Figure 35.** The curve associated with the right-hand trefoil, together with the meridian  $\mu$  passing through the marked disk and the basepoints  $w$  and  $z$ .

From this data, we define several variants of a filtered chain complex, which are refinements of the intersection Floer homology  $HF(\gamma(M), \mu)$ . As usual, the generators are intersection points between  $\gamma(M)$  and  $\mu$ .  $C^-(\gamma(M), \mu)$  is generated over  $\mathbb{F}[U]$  by these intersection points, where the differential counts immersed bigons and a bigon covering the basepoint  $w$  with multiplicity  $i$  contributes with

a factor of  $U^i$ . More precisely, the differential is defined by

$$d(x) = \sum_{i=0}^{\infty} \sum_{y \in \gamma_0 \cap \gamma_1} U^i N_i^w(x, y) \cdot y$$

where  $N_i^w(x, y)$  is the number of bigons from  $x$  to  $y$ , counted modulo 2, covering the  $w$  basepoint  $i$  times; compare Section 3.2. Given a bigon  $B$  connecting  $x$  to  $y$  (that is  $B \in \tilde{\pi}_2(x, y)$ , as in [21, Chapter 11]), let  $n_w(B)$  and  $n_z(B)$  be number of times  $B$  covers  $w$  and  $z$ , respectively. Then  $z$  induces a filtration  $A$  on  $C^-(\gamma(M), \mu)$  where  $A(x) - A(y) = n_z(B) - n_w(B)$  and  $A(U \cdot x) = A(x) - 1$ . The associated graded of this object, denoted  $gC^-(\gamma(M), \mu)$ , is obtained by disallowing bigons which cross the  $z$  basepoint in the differential. There are simpler versions,  $\widehat{C}(\gamma(M), \mu)$  and  $g\widehat{C}(\gamma(M), \mu)$ , which are obtained from  $C^-(\gamma(M), \mu)$  and  $gC^-(\gamma(M), \mu)$  by setting  $U = 0$ . Equivalently, these complexes are generated over  $\mathbb{F}$  for which bigons covering the basepoints  $w$  are disallowed in the differential.

We will not prove that  $C^-(\gamma(M), \mu)$  is well defined, in particular that  $d^2 = 0$  (though in practice it is for specific examples). However, the associated graded versions  $gC^-(\gamma(M), \mu)$  and  $g\widehat{C}(\gamma(M), \mu)$  are well defined and in fact agree with knot Floer homology.

**Theorem 45.** *If  $K$  is a knot in a 3-manifold  $Y$  and  $M = Y \setminus K$ , with  $\mu \subset \partial M$  the meridian and basepoints  $w$  and  $z$  as above, then the complex  $gC^-(\gamma(M), \mu)$  (resp.  $g\widehat{C}(\gamma(M), \mu)$ ) is filtered chain homotopy equivalent to  $gCFK^-(Y, K)$  (resp.  $g\widehat{CFK}(Y, K)$ ).*

*Proof.* This follows by construction from [21, Theorem 11.19], which produces  $gCFK^-$  and  $g\widehat{CFK}$  from  $\widehat{CFD}(M, \mu, \lambda)$ . The key observation is that intersections between  $\mu$  and  $\gamma(M)$  correspond precisely to  $\iota_0$  generators of  $\widehat{CFD}(M, \mu, \lambda)$ , and any bigon between intersection points not covering  $z$  must cover  $w$  with positive multiplicity  $i$  and correspond to a sequence

$$\bullet \xrightarrow{3} \circ \xrightarrow{23} \dots \xrightarrow{23} \circ \xrightarrow{2} \bullet$$

in  $\widehat{CFD}(M, \mu, \lambda)$  with  $i$  generators of idempotent  $\iota_1$ . □

The Alexander filtration is best illustrated by passing to  $\tilde{\gamma}(M)$ . The preimages of  $\lambda$  divide the plane into strips; reflecting our diagram across the line  $y = x$  so that these strips are vertical and numbering left-to-right, these strips encode the Alexander filtration  $A$ . This is illustrated for (the complement of) the  $(2, -1)$ -cable of the left-hand trefoil knot in Figure 36.

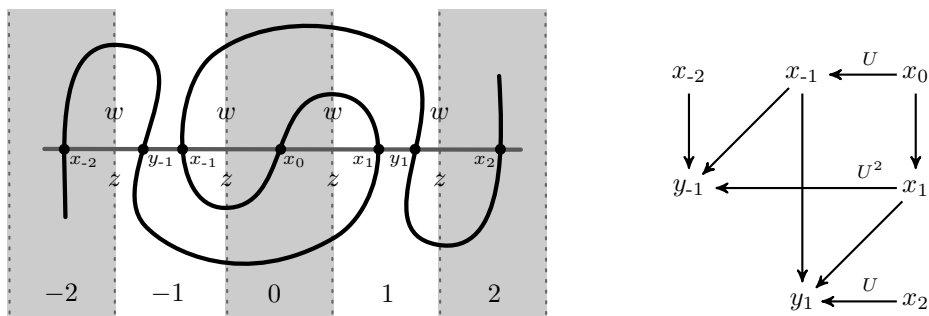


**Figure 36.** The  $(2, -1)$ -cable of the left-hand trefoil  $K$ ; compare [21, Figure 11.5]. We consider the relevant portion of  $\tilde{\gamma}(M)$ , where  $M = S^3 \setminus K$ , viewed reflected for comparison with the type D structure  $\widehat{CFD}(M, \mu, \lambda)$ . The intersection with the horizontal curve gives rise to  $CFK^-(S^3, K)$ , where rolling out the torus horizontally encodes the Alexander grading.

Given that  $\gamma(M)$  is extracted from  $\widehat{CFD}(M, \mu, \lambda)$  one might view the above result as tautological. The main thrust here is the nice interplay between the curves picture and knot Floer homology.

In particular, note the similarity between the usual construction of knot Floer homology with two basepoints on either side of a meridian. It is reasonable to view the data  $(T^2, \gamma(M), \mu, w, z)$  as a generalization of a doubly-pointed genus 1 Heegaard diagram.

$gCFK^-$  may be viewed as  $CFK^-$  with the differential restricted to only horizontal arrows. The vertical arrows in  $CFK^-$  may also be recovered from  $C^-(\gamma(M), \mu)$  by restricting the differential to bigons which do not cover the  $w$  basepoint. This follows from applying [21, Theorem 11.19] after reparametrizing  $\partial M$  by the elliptic involution, which has the effect of rotating  $\gamma(M)$  by 180 degrees and switching the roles of  $w$  and  $z$ . Note that in all examples known to the authors,  $\gamma(M)$  is unchanged by this rotation (see Remark 24); this corresponds to the typical diagonal symmetry in  $CFK^-$ .

The full filtered complex  $C^-(\gamma(M), \mu)$  also contains differentials coming from domains which cross both basepoints. Though this does not necessarily agree with  $CFK^-$ , we remark that it does in many examples, including the cable of the trefoil in Figure 36.  $C^-(\gamma(M), \mu)$  agrees with  $CFK^-(K)$  for thin knots and L-space knots in  $S^3$ , as in these cases  $CFK^-(K)$  is determined by  $gCFK^-(K)$ .

**7.4. The Thurston norm.** We can use the relationship between  $\bar{\gamma}(M)$  and knot Floer homology to prove the characterization of the Thurston norm stated in the introduction. We formulate a version which is applicable to arbitrary manifolds with  $b_1 = 1$ .

Let  $[\Sigma]$  generate  $H_2(M, \partial M)$ . For  $\mathfrak{s} \in \text{Spin}^c(M)$ , recall from Section 2.9 that the set  $p^{-1}(z) \subset \bar{T}_{\mathfrak{s}}$  can be identified with the set  $\text{Spin}^c(M, \partial M; \mathfrak{s})$  of relative  $\text{Spin}^c$  structures which induce  $\mathfrak{s}$ . If  $\bar{\gamma} \subset \bar{T}_{\mathfrak{s}}$  is a curve or collection of curves, we define

$$K^+(\bar{\gamma}) = \{\bar{\mathfrak{s}} \in \text{Spin}^c(M, \partial M, \mathfrak{s}) \mid z_{\bar{\mathfrak{s}}} \text{ is not connected to } +\infty \text{ in the complement of } \bar{\gamma}\}$$

and let  $k^+(\bar{\gamma}) = \max\{\langle c_1(\bar{\mathfrak{s}}), [\Sigma] \rangle \mid \bar{\mathfrak{s}} \in K^+(\bar{\gamma})\}$ .

**Proposition 46.** *Suppose  $b_1(M) = 1$  and that  $\Sigma$  is a norm-minimizing surface generating  $H_2(M, \partial M)$ . Then  $-\chi(\Sigma) = \max\{k^+(\bar{\gamma}(M, \mathfrak{s})) \mid \mathfrak{s} \in \text{Spin}^c(M)\}$ .*

*Proof.* If  $\bar{\gamma}$  is a curve in  $\bar{T}_{\mathfrak{s}}$ , let  $\mathcal{P}(\bar{\gamma})$  be the set of corners of the pegboard representative of  $\bar{\gamma}$ . We claim that if  $\mathcal{P}(\bar{\gamma}) \neq \emptyset$ , then

$$\max\{\langle c_1(\bar{\mathfrak{s}}), \Sigma \rangle \mid z_{\bar{\mathfrak{s}}} \in \mathcal{P}(\bar{\gamma})\} = k^+(\bar{\gamma}).$$

Indeed, if  $z_{\bar{\mathfrak{s}}}$  is a highest peg in  $\mathcal{P}(\bar{\gamma})$ , then it must lie below  $\bar{\gamma}$ , so  $\bar{\mathfrak{s}} \in K^+(\bar{\gamma})$ . Conversely, it is clear that every peg above  $z_{\bar{\mathfrak{s}}}$  is connected to  $+\infty$ .

Next, let  $l$  be the rational homological longitude of  $M$ , and let  $l_k \subset \bar{T}_{\mathfrak{s}}$  be the line parallel to  $l$  and passing through  $z_{\bar{\mathfrak{s}}}$  with  $\langle c_1(\bar{\mathfrak{s}}), [\Sigma] \rangle = k$ . Note that if  $\bar{\gamma} = \bar{\gamma}(M, \mathfrak{s})$ , Theorem 45 implies that

$$\widehat{HFK}(M(l), K_l, \mathfrak{s}_k) = HF(\bar{\gamma}, l_k).$$

Here  $\mathfrak{s}_k \in \text{Spin}^c(M, \partial M)$  is defined to be the relative  $\text{Spin}^c$  structure which restricts to  $\mathfrak{s}$  on  $M$  and satisfies  $\langle c_1(\mathfrak{s}_k), [\Sigma] \rangle = k$ .

If  $\mathcal{P}(\bar{\gamma}) \neq \emptyset$ , we claim that

$$\max\{k \mid HF(\bar{\gamma}, l_k) \neq 0\} = k^+(\bar{\gamma}).$$

To see this, pull  $\bar{\gamma}$  tight. If  $\langle c_1(\bar{\mathfrak{s}}), [\Sigma] \rangle > k^+$ , then the complex computing  $HF(\bar{\gamma}, l_k)$  has no generators. Conversely, since  $\bar{\gamma}$  hangs on a peg of height  $k^+$ , some arc of  $\bar{\gamma}$  must lie above  $l_{k^+}$ , and some arc of it must lie below. Since  $\bar{\gamma}$  is pulled tight,  $HF(\bar{\gamma}, l_{k^+}) \neq 0$ .

Now we consider the case where  $\mathcal{P}(\bar{\gamma}) = \emptyset$ . Then  $\bar{\gamma}$  is solid torus like. It is represented by a curve parallel to  $l$ , and is trapped between two rows of pegs at height  $n$  and  $n+1$ . We have  $HF(\bar{\gamma}, l_k) = 0$  for all  $k$ , but  $k^+(\bar{\gamma}) = n$ .



Now we consider  $\overline{\gamma}(M)$ . The case in which every component of  $\overline{\gamma}(M)$  is solid torus like has been studied by Gillespie [7], who showed that such an  $M$  must be boundary compressible. In this case, it is easy to see that the proposition holds. Thus we may assume that not every component of  $\overline{\gamma}(M)$  is solid torus-like. Taking the max of the relations above over all components of  $\overline{\gamma}(M)$ , we see that

$$\max\{\langle c_1(\overline{\mathfrak{s}}), [\Sigma] \rangle \mid z_{\overline{\mathfrak{s}}} \in \mathcal{P}(\overline{\gamma}(M))\} = \max\{k \mid \widehat{HFK}(M_\ell, K_\ell, \mathfrak{s}_k) \neq 0\} = -\chi(\Sigma)$$

where the last equality follows from the fact that the knot Floer homology determines the Thurston norm.

It remains to show that  $k^+(\overline{\gamma}(M)) = \max\{\langle c_1(\overline{\mathfrak{s}}), [\Sigma] \rangle \mid z_{\overline{\mathfrak{s}}} \in \mathcal{P}(\overline{\gamma}(M))\}$ . The only way this can fail to happen is if  $\overline{\gamma}(M)$  has a solid torus-like component at height  $n > k^+ + 1$ . Suppose that we have such a component. Then it pairs nontrivially with any curve  $\mu$  which satisfies  $\mu \cdot l = 1$ , so we have  $\widehat{HFK}(M(\mu), K_\mu, n) \neq 0$ . The fact that knot Floer homology determines the Thurston norm implies that  $-\chi(\Sigma) \geq n - 1 > k^+$ , which is a contradiction.  $\square$

**7.5. Plus and minus type invariants.** The definition  $C^-(\gamma(M), \mu)$  involves counting bigons in the whole torus  $T^2$ , in particular those covering the  $z$  basepoint. Expanding on this idea, we now discuss generalizations of the intersection Floer homology defined in Section 3 with coefficients in  $\mathbb{F}[U]$ -modules. In particular, we will be interested in coefficients in the ring of power series  $\mathcal{T}_- \cong \mathbb{F}[U]$  or in  $\mathcal{T}_+ \cong \mathbb{F}[U, U^{-1}]/U \cdot \mathbb{F}[U]$ . Let  $\gamma_0$  and  $\gamma_1$  be an admissible pair of (collections of) curves in  $T = T^2 \setminus z$ , and let  $CF^-(\gamma_0, \gamma_1)$  and  $CF^+(\gamma_0, \gamma_1)$  be generated over  $\mathcal{T}_-$  and  $\mathcal{T}_+$ , respectively, by intersection points of  $\gamma_0$  and  $\gamma_1$ . For points  $x, y \in \gamma_0 \cap \gamma_1$ ,  $N_i(x, y)$  denotes the number of Whitney disks in  $T^2$  (up to equivalence and counted modulo 2) connecting  $x$  to  $y$  and covering the basepoint  $z$  with (positive) multiplicity  $i$ . With this we define

$$d(x) = \sum_{i=0}^{\infty} \sum_{y \in \gamma_0 \cap \gamma_1} U^i N_i(x, y) \cdot y$$

If  $d$  is a differential (i.e.  $d^2 = 0$ ) on  $CF^-(\gamma_0, \gamma_1)$  and  $CF^+(\gamma_0, \gamma_1)$ , we define  $HF^-(\gamma_0, \gamma_1)$  and  $HF^+(\gamma_0, \gamma_1)$  to be the corresponding homologies. For arbitrary curves  $\gamma_0$  and  $\gamma_1$ ,  $d^2$  may not be zero. Problems arise when either curve has a cusp (i.e. a segment which bounds a disk in  $T^2$ ); however curves may have two cancelling cusps, as in the curve for the figure eight knot complement (see Figure 1), and  $d^2 = 0$  for curves of this form. It seems plausible that  $HF^-(\gamma_0, \gamma_1)$  and  $HF^+(\gamma_0, \gamma_1)$  are well defined for curves arising as  $\gamma(M)$  for a loop type manifold  $M$ . Note that  $HF(\gamma_0, \gamma_1)$  may be recovered from  $HF^+(\gamma_0, \gamma_1)$  by constructing the mapping cone of the map induced by the  $U$ -action.

We will consider the invariant  $HF^+(\gamma_0, \gamma_1)$  for a few examples. We will focus mainly on Dehn fillings of examples already computed above. That is, we consider  $Y = M_0 \cup_h M_1$  with  $M_0$  a loop type manifold and  $M_1$  a solid torus. We set  $\gamma_0 = \gamma(M_0)$  and  $\gamma_1 = h(\gamma(M_1))$ ; note that  $\gamma(M_1)$  is the meridian of the filling solid torus  $m$ , and  $h(m) = \bar{h}(m)$ . In each example,  $HF^+(\gamma_0, \gamma_1)$  agrees with the Heegaard Floer homology  $HF^+(M_0 \cup_h M_1)$ .

**7.6. Surgeries on knots.** As a first calculation, let  $K$  be the figure eight knot and consider the family of integer homology spheres obtained by  $S_{1/n}^3(K)$  where  $K$  is a non-negative integer; for negative integers, recall that  $S_{-r}^3(K) \cong S_r^3(K)$  since  $K$  is amphicheiral. We compute  $HF^+(\gamma_0, \gamma_1)$ , where  $\gamma_0$  is the pair of immersed curves associated with the figure eight knot exterior and  $\gamma_1$  is a simple closed curve of slope  $\frac{1}{n}$ .

The case  $n = 2$  is illustrated in Figure 37. Notice that there are 5 intersection points, each generating a copy of  $\mathcal{T}_+$ . However, in this case we have a non-trivial differential owing to the existence of two bigons covering the basepoint. As a result,  $HF^+(\gamma_0, \gamma_1) \cong \mathcal{T}_+ \oplus \mathbb{F}^2$ . More generally, one computes that the homology for general  $n$  is given by  $\mathcal{T}_+ \oplus \mathbb{F}^n$ , in agreement with  $HF^+(S_{1/n}^3(K))$ . Notice that if the figure eight curve is a component of  $\gamma(M)$ , then there is always a  $\mathbb{F}^n$  summand in  $HF^+(\gamma(M), \gamma_1)$  where  $\gamma_1$  is a line of slope  $\frac{1}{n}$  corresponding to  $\frac{1}{n}$ -surgery.

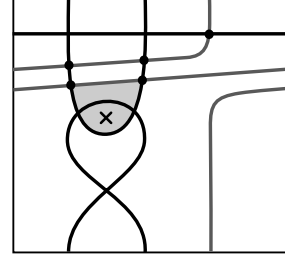


**Figure 37.** The intersection of curves associated with  $\frac{1}{2}$ -surgery on  $K$ .

We could also consider surgery on the right-hand trefoil knot  $T_{2,3}$  in a similar manner, though here it is simpler to calculate by considering  $\tilde{\gamma}(M)$ . In this case we calculate the  $+$ -version of the curves invariant to get  $\mathcal{T}_+$ , as expected, for  $+1$ -surgery. In general, by inspecting the diagram in Figure 38 (which illustrates the case  $n = 2$ ) it is immediate that  $HF^+(\gamma_0, h_n(m)) \cong \mathcal{T}_+ \oplus \mathbb{F}^{n-1}$  where  $h_n$  is the homeomorphism realising  $\frac{1}{n}$ -surgery and  $\gamma_0$  is the immersed curve associated with the exterior of the right-hand trefoil.

More generally, the result for  $S_1^3(T_{p,q})$  may be calculated, and compared with the observations of Borodzick and Némethi [3].

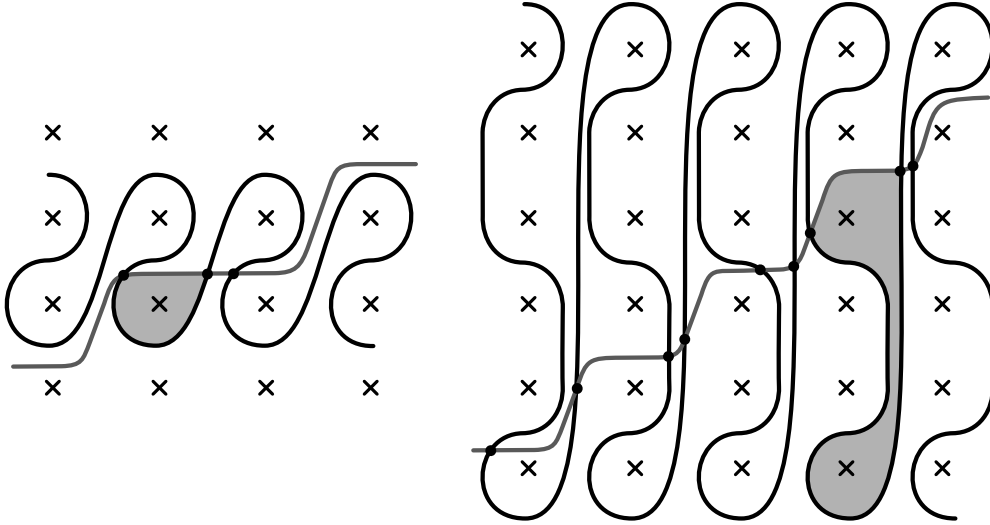


**Figure 38.** Computing  $+\frac{1}{2}$ -surgery on the trefoil (left) and  $+1$ -surgery on the  $(3,4)$ -torus knot (right).

We now consider large integer surgeries on an arbitrary nullhomologous knot  $K$  in a 3-manifold  $Y$ . Let  $M = Y \setminus \nu(K)$ ; as before  $\gamma_0 = \gamma(M)$  and  $\gamma_1$  is a simple closed curve of slope  $n > 0$ . Note that  $HF(\gamma_0, \gamma_1)$  has  $n$  spin<sup>c</sup> structures, which we index by integers  $s$  with  $|s| \leq \frac{n}{2}$ .

In analogy to the large integer surgery formula for Heegaard Floer homology, we relate  $HF^\pm(\gamma_0, \gamma_1)$  to the complex  $C^\infty(\gamma(M), \mu)$  (defined just as  $C^-(\gamma(M), \mu)$  but with  $\mathbb{F}[U, U^{-1}]$  coefficients). For  $s$  in  $\mathbb{Z}$ , let  $A_s^-(\gamma(M), \mu)$  denote the subcomplex of  $C^-(\gamma(M), \mu)$  obtained by restricting to Alexander grading less than or equal to  $s$  and let  $A_s^+(\gamma(M), \mu)$  be the corresponding quotient complex in  $C^\infty(\gamma(M), \mu)$ . We prove:

**Proposition 47.** *Assume  $n \geq 2g(K) + 1$ . For  $|s| < n/2$ ,  $HF^\pm(\gamma_0, \gamma_1; s) \cong H_*(A_s^\pm(\gamma(M), \mu))$ .*

Note that in the case that  $C^-(\gamma(M), \mu)$  agrees with  $CFK^-(Y, K)$ , this implies that  $HF^-(\gamma_0, \gamma_1) \cong HF^-(Y_n(K))$ .

*Proof.* We prove the statement for the minus invariants, the proof for plus is similar. It is convenient to work with the lifts of  $\gamma_0$  and  $\gamma_1$  in  $\mathbb{R}^2$ , where the marked point lifts to points of the form  $(a, b + \frac{1}{2})$  for  $a, b \in \mathbb{Z}$ . We work in a strip centered on the  $y$ -axis, which is a lift of the meridian  $\mu$ . Choose a homotopy representative for  $\tilde{\gamma}_0$  which lies between  $y = -g(K)$  and  $y = g(K)$  and which meets a neighborhood of the  $y$ -axis in horizontal segments.  $HF^-(\gamma_0, \gamma_1)$  has  $n$   $\text{spin}^c$  structures, so we choose  $n$  lifts of the line of slope  $n$ , crossing the  $y$ -axis at height  $s$  with  $|s| \leq \frac{n}{2}$  and homotoped to lie in a neighborhood of the  $y$ -axis between  $y = -g$  and  $y = g$ . See Figure 39 for the case of +5-surgery on the right-hand trefoil.

Consider the intersection homology with  $\mathbb{F}[U]$  coefficients of  $\gamma_0$  with the  $y$ -axis, with basepoints  $z$  and  $w$  to the left and right, respectively, of each marked point; this is simply  $C^-(\gamma(M), \mu)$ . Note that each line of slope  $n$  above is a slight perturbation of the vertical line in the relevant region; in particular, it has exactly the same intersection with  $\gamma_0$ . Clearly if  $s \geq g$ , the chain complex  $CF^-(\gamma_0, \gamma_1; s)$  is precisely the complex  $C^-(M, \mu, w, z)$  where the marked point corresponds to  $w$  and we ignore  $z$  (that is, we forget the filtration).

For the line corresponding to  $s = g - 1$ , note that the intersections with  $\gamma_0$  are unchanged, but one marked point has moved from the right of the left of the line. This has the effect that, for a generator  $x$  with Alexander grading  $g$ , any bigon starting at  $x$  covers an extra marked point, and any bigon connecting to  $x$  covers one less marked point. To see the effect on  $HF^-$ , we can replace the generator  $x$  with  $x' = Ux$  and keep the differential the same; indeed, if  $d(x) = y$  then  $d(x') = Uy$ , and if  $d(y) = Ux$  then  $d(y) = x'$ . More generally, considering the line corresponding to some integer  $s$ , we see that  $CF^-(\gamma_0, \gamma_1; s)$  is the same as  $CF^-(\gamma_0, \gamma_1; g)$  except that bigons from  $x$  to  $y$  cover one more marked point for each integer  $A(y) < m \leq A(x)$  with  $m > s$  and one fewer marked point for each integer  $A(x) < m \leq A(y)$  with  $m > s$ . It follows that if  $\{x_1, \dots, x_k\}$  is a basis for  $CF^-(\gamma_0, \gamma_1; g) \cong C^-(\gamma(M), \mu)$  over  $\mathbb{F}[U]$ , then  $\{U^{\ell_1}x_1, \dots, U^{\ell_k}x_k\}$  is a basis for  $CF^-(\gamma_0, \gamma_1; s)$  over  $\mathbb{F}[U]$ , where  $\ell_i = \max(0, A(x_i) - s)$ . But it is easy to see that this is a basis for  $A^-(\gamma(M), \mu)$  as well with the same differential.  $\square$

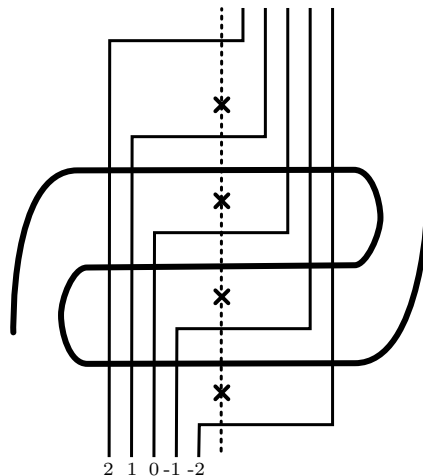


**Figure 39.** The intersection of curves, labelled by filtration level, associated with 5-surgery on the right handed trefoil.

**7.7. Surface bundles, revisited.** Let  $M_g$  be the product of a genus  $g$  surface with a single connected boundary component with  $S^1$ . Let  $\gamma_g = \gamma(M_g)$  be the associated invariant calculated in Section 5.4. We will compute  $HF^+(\gamma_g, L_0)$ , where  $L_0 = \bar{h}(\gamma(D^2 \times S^1))$  and  $h: \partial(D^2 \times S^1) \rightarrow \partial M_g$  realises the filling giving rise to the product  $Y_g = \Sigma_g \times S^1$ . As in Section 5.4, this is the result of intersection with a horizontal line; compare Figure 29.

The group  $HF^+(\gamma_g, L_0)$  will have a contribution from each connected component of  $\gamma_g$ . It is easy to calculate that the contribution of a  $(d_0)$  or a  $(d_0d_0)$  component is a summand of the form  $\mathcal{T}_+ \oplus \mathcal{T}_+$ . The same is true of the contribution of a  $(d_2d_{-2})$  component; in all three cases one observes that the map  $\mathcal{T}_+ \rightarrow \mathcal{T}_+$  is  $2U = 0$ . More generally, the contribution of any component of the form  $(d_{2k}d_{-2k})$ , for  $k > 0$ , can be seen from Figure 40. Each component of this form gives rise to a summand in the chain complex isomorphic (as a group) to  $\mathcal{T}_+^{2(2k-1)}$  with differential described by  $\bigoplus_{i=1}^{2k-1} (\mathcal{T}_+ \xrightarrow{D_i} \mathcal{T}_+)$  for  $D_i = U^i + U^{2k-i}$ . On homology, for each  $i < k$ , this gives rise to summands isomorphic

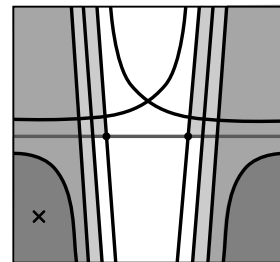


**Figure 40.** A bigon covering the basepoint in  $(d_4d_{-4})$ .

as modules to  $\mathcal{T}_i \cong H_*(\mathcal{T}_+ \xrightarrow{U^i} \mathcal{T}_+)$ . When  $i = k$  we again get  $\mathcal{T}_+ \oplus \mathcal{T}_+$ .

For ease of comparison with the calculation of  $HF^+(Y_g)$  [17, 26] we decompose according to spin<sup>c</sup> structures. For the torsion spin<sup>c</sup> structure  $\mathfrak{s}_0$  we have that

$$HF^+(\gamma_g, L_0; \mathfrak{s}_0) \cong HF(\gamma_g, L_0; \mathfrak{s}_0) \otimes \mathcal{T}_+ \otimes \mathbb{F} \cong \widehat{HF}(Y_g) \otimes \mathcal{T}_+ \otimes \mathbb{F}$$

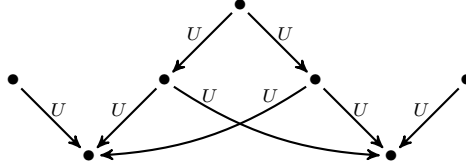
in agreement with Jabuka and Mark [17, Theorem 4.10] since  $\dim HF(\gamma_g, L_0; \mathfrak{s}_0)$  is given by twice the number of curve components of  $\gamma_g$ , that is,  $2^g + \sum_{i=0}^{2g} \binom{2g}{i} = 2^g + 2^{2g}$ .

For non-torsion spin<sup>c</sup> structures  $\mathfrak{s}_i$  we get non-trivial contributions for  $0 < i < k$  from each  $(d_{2k}d_{-2k})$  when  $k > 0$ . Namely, each  $(d_{2k}d_{-2k})$  curve component gives rise to a  $\mathcal{T}_{k-i}$  summand in spin<sup>c</sup> structure  $\mathfrak{s}_i$ . Thus

$$HF^+(\gamma_g, L_0; \mathfrak{s}_i) \cong \bigoplus_{j=i+1}^g \mathcal{T}_{j-i}^{\binom{2g}{j}}$$

for each  $0 < i < g + 1$ . This gives  $HF^+(\gamma_g, L_0; \mathfrak{s}_i) \cong HF^+(Y_g; \mathfrak{s}_i)$  comparing with Ozsváth and Szabó [26].

**7.8. Splicing trefoils, revisited.** As a final example, consider the result of splicing two right-hand trefoil complements  $Y$ ; see Figure 2 from the introduction. The chain group  $CF^+(\gamma_0, \gamma_1)$  has 7 generators and it is straightforward to check that there are 8 bigons contributing to the differential as follows:



The resulting homology is  $HF^+(\gamma_0, \gamma_1) \cong \mathcal{T}_+ \oplus \mathbb{F}^3$ , which is in agreement with the observation that  $\dim HF(\gamma_0, \gamma_1) = 7$ . Furthermore, one can apply the mapping cone formula to see that this agrees with  $HF^+(Y)$ .

**7.9. Plus invariants for curves vs Heegaard Floer homology.** It is certainly not true in general that  $HF^+(\gamma(M_0), \bar{h}(\gamma(M_1)))$  is isomorphic to  $HF^+(M_0 \cup_h M_1)$ , since  $HF^+(\gamma(M_0), \bar{h}(\gamma(M_1)))$  is determined completely by the bordered Floer invariants for  $M_0$  and  $M_1$  and these invariants do not carry any information about holomorphic disks covering the basepoint. In particular, let  $Y$  and  $Y'$  be closed 3-manifolds with isomorphic  $\widehat{HF}$  but different  $HF^+$ , and let  $M_0$  and  $M'_0$  be the connected sum of  $Y$  and  $Y'$ , respectively, with a fixed loop type manifold.  $M_0$  and  $M'_0$  are loop type and have the same bordered Heegaard Floer invariants; it follows that for any loop type  $M_1$  and gluing map  $h$ ,  $HF^+(\gamma(M_0), \bar{h}(\gamma(M_1))) \cong HF^+(\gamma(M'_0), \bar{h}(\gamma(M_1)))$ , but in general  $HF^+(M_0 \cup_h M_1)$  and  $HF^+(M'_0 \cup_h M_0)$  will be different.

Still, we have exhibited several examples for which  $HF^+(\gamma(M_0), \bar{h}(\gamma(M_1)))$  does recover  $HF^+(M_0 \cup_h M_1)$ . This is striking, and suggests that for manifolds obtained by gluing along a torus there are heavy constraints on the plus and minus invariants, to the extent that in many cases these stronger invariants can be recovered from the simpler hat version. We end by posing the following question:

**Question 48.** What conditions on loop-type manifolds  $M_0$  and  $M_1$  guarantee that  $HF^+(M_0 \cup_h M_1)$  and  $HF^+(\gamma(M_0), \bar{h}(\gamma(M_1)))$  are isomorphic?

If the conditions are sufficiently broad, using the intersection of immersed curves may make computing plus and minus invariants significantly easier for many toroidal manifolds.

## REFERENCES

- [1] Mohammed Abouzaid. On the Fukaya categories of higher genus surfaces. *Adv. Math.*, 217(3):1192–1235, 2008.
- [2] Manabu Akaho. Intersection theory for Lagrangian immersions. *Math. Res. Lett.*, 12(4):543–550, 2005.
- [3] Maciej Borodzik and András Némethi. Heegaard-Floer homologies of (+1) surgeries on torus knots. *Acta Math. Hungar.*, 139(4):303–319, 2013.
- [4] Steven Boyer and Adam Clay. Foliations, orders, representations, L-spaces and graph manifolds. Preprint, arXiv:1401.7726.
- [5] Eaman Eftekhary. Bordered Floer homology and existence of incompressible tori in homology spheres. Preprint, arXiv:1504.05329.
- [6] Benson Farb and Dan Margalit. *A primer on mapping class groups*, volume 49 of *Princeton Mathematical Series*. Princeton University Press, Princeton, NJ, 2012.
- [7] Thomas Gillespie. L-space fillings and generalized solid tori. Preprint, arXiv:1603.05016.
- [8] Jonathan Hanselman. Bordered Heegaard Floer homology and graph manifolds. Preprint, arXiv:1310.6696.
- [9] Jonathan Hanselman, Jacob Rasmussen, Sarah Dean Rasmussen, and Liam Watson. Taut foliations on graph manifolds. Preprint, arXiv:1508.05911.
- [10] Jonathan Hanselman and Liam Watson. A calculus for bordered Floer homology. Preprint, arXiv:1508.05445.
- [11] Matthew Hedden and Adam Simon Levine. Splicing knot complements and bordered Floer homology.
- [12] Jennifer Hom. Satellite knots and L-space surgeries. Preprint, arXiv:1601.05696.
- [13] Jennifer Hom. Bordered Heegaard Floer homology and the tau-invariant of cable knots. *J. Topol.*, 7(2):287–326, 2014.
- [14] Jennifer Hom, Tye Lidman, and Faramarz Vafaee. Berge-gabai knots and L-space satellite operations. *Algebr. Geom. Topol.*, 14(6):3745–3763, 2014.
- [15] Jennifer Hom, Tye Lidman, and Liam Watson. The Alexander module, Seifert forms, and categorification. Preprint, arXiv:1501.04866.
- [16] D. Hulin and M. Troyanov. Prescribing curvature on open surfaces. *Math. Ann.*, 293(2):277–315, 1992.
- [17] Stanislav Jabuka and Thomas E. Mark. On the Heegaard Floer homology of a surface times a circle. *Adv. Math.*, 218(3):728–761, 2008.
- [18] P. Kronheimer, T. Mrowka, P. Ozsváth, and Z. Szabó. Monopoles and lens space surgeries. *Ann. of Math. (2)*, 165(2):457–546, 2007.
- [19] Peter Kronheimer and Tomasz Mrowka. Knots, sutures, and excision. *J. Differential Geom.*, 84(2):301–364, 02 2010.
- [20] Yankı Lekili and Timothy Perutz. Fukaya categories of the torus and Dehn surgery. *Proc. Natl. Acad. Sci. USA*, 108(20):8106–8113, 2011.
- [21] Robert Lipshitz, Peter Ozsváth, and Dylan Thurston. Bordered Heegaard Floer homology: Invariance and pairing. Preprint, arXiv:0810.0687.
- [22] Robert Lipshitz, Peter S. Ozsváth, and Dylan P. Thurston. Bimodules in bordered Heegaard Floer homology. *Geom. Topol.*, 19(2):525–724, 2015.
- [23] Ciprian Manolescu. An introduction to knot Floer homology. Preprint, arXiv:1401.7107.
- [24] John W. Morgan, Tomasz S. Mrowka, and Zoltán Szabó. Product formulas along  $T^3$  for Seiberg-Witten invariants. *Math. Res. Lett.*, 4(6):915–929, 1997.
- [25] Tomasz Mrowka, Peter Ozsváth, and Baozhen Yu. Seiberg-Witten monopoles on Seifert fibered spaces. *Comm. Anal. Geom.*, 5(4):685–791, 1997.
- [26] Peter Ozsváth and Zoltán Szabó. Holomorphic disks and knot invariants. *Adv. Math.*, 186(1):58–116, 2004.
- [27] Peter Ozsváth and Zoltán Szabó. Holomorphic disks and three-manifold invariants: properties and applications. *Ann. of Math. (2)*, 159(3):1159–1245, 2004.
- [28] Ina Petkova. The decategorification of bordered Heegaard Floer homology. Preprint, arXiv:1212.4529.
- [29] Ina Petkova. Cables of thin knots and bordered Heegaard Floer homology. *Quantum Topol.*, 4(4):377–409, 2013.
- [30] Jacob Rasmussen and Sarah Dean Rasmussen. Floer simple manifolds and L-space intervals. Preprint, arXiv:1508.05900.
- [31] Sarah Rasmussen. L-space intervals for graph manifolds and cables. Preprint, arXiv:1511.04413.
- [32] Liam Watson. Heegaard Floer homology solid tori. AMS special session: Knots, links, and three-manifolds, San Diego, January 2013.
- [33] Yang Xiu. Elliptic involution on knot complements. Preprint, arXiv:1511.02298.

DEPARTMENT OF MATHEMATICS, UNIVERSITY OF TEXAS AT AUSTIN.

*E-mail address:* `Hanselman@math.utexas.edu`

DEPARTMENT OF PURE MATHEMATICS AND MATHEMATICAL STATISTICS, UNIVERSITY OF CAMBRIDGE.

*E-mail address:* `J.Rasmussen@dpms.cam.ac.uk`

SCHOOL OF MATHEMATICS AND STATISTICS, UNIVERSITY OF GLASGOW.

*E-mail address:* `Liam.Watson@glasgow.ac.uk`